Pyroglutamide-Based P2X7 Receptor Antagonists Targeting Inflammatory Bowel Disease

Germain Homerin, Davy Baudelet, Pierrick Dufrénoy, Benoît Rigo, Régis Millet, Xavier Dezitter, Christophe Furman, Guillaume Ragé, Emmanuelle Lipka, Amaury Farce, et al.

Pyroglutamide-Based P2RX7 Receptor Antagonists Targeting Inflammatory Bowel Disease

Germain Homerin[1,2], Davy Baudelet[1,2], Pierrick Dufrénoy[1,2], Benoît Rigo[1,2], Régis Millet[1,3], Xavier Dezitter[1,3], Christophe Furman[1,3], Guillaume Ragé[1,3], Emmanuelle Lipka[1,4], Amaury Farce[1,3], Nicolas Renault[1,3], Boualem Sendid[1], Samir Jawhara[1], Rogatien Charlet[1], Jordan Leroy[1], Melodie Phanithavong[5], Camille Richeval[5], Jean-François Wiart[5], Delphine Allorge[5], Sahil Adriouch[6,7], Valérie Vouret-Craviari[8,9], and Alina Ghinet[1,2,10,]*

[1] Inserm U995, LIRIC, Université de Lille, CHRU de Lille, Faculté de médecine – Pôle recherche, Place Verdun, F-59045 Lille Cedex, France

[2] Hautes Etudes d'Ingénieur (HEI), Groupe Yncréa Hauts-de-France, UCLille, Laboratoire de pharmacochimie, 13 rue de Toul, F-59046 Lille, France

[3] Institut de Chimie Pharmaceutique Albert Lespagnol, IFR114, 3 rue du Pr Laguesse, F-59006 Lille, France

[4] Faculté des Sciences Pharmaceutiques et Biologiques de Lille, Laboratoire de Chimie Analytique, F-59006 Lille Cedex, France

[5] CHRU de Lille, Centre de Biologie Pathologie, Laboratoire de Toxicologie & Génopathies, Bd du Pr J. Leclercq, CS 70001, F-59037 Lille, France

[6] INSERM U905, F-76183 Rouen, France

[7] Normandie University, Institute for Research and Innovation in Biomedicine, F-76183 Rouen, France

[8] Institute for Research on Cancer and aging (IRCAN), F-06100 Nice, France

[9] University of Nice Cote d'azur (UCA), F-06100 Nice, France

[10] 'Al. I. Cuza' University of Iasi, Faculty of Chemistry, Bd. Carol I, nr. 11, 700506 Iasi, Romania

KEYWORDS: Pyroglutamic acid, Pyroglutamides, Pyrroloimidazolediones, IBD, Inflammation, P2RX7, Purinergic receptors.

ABSTRACT.

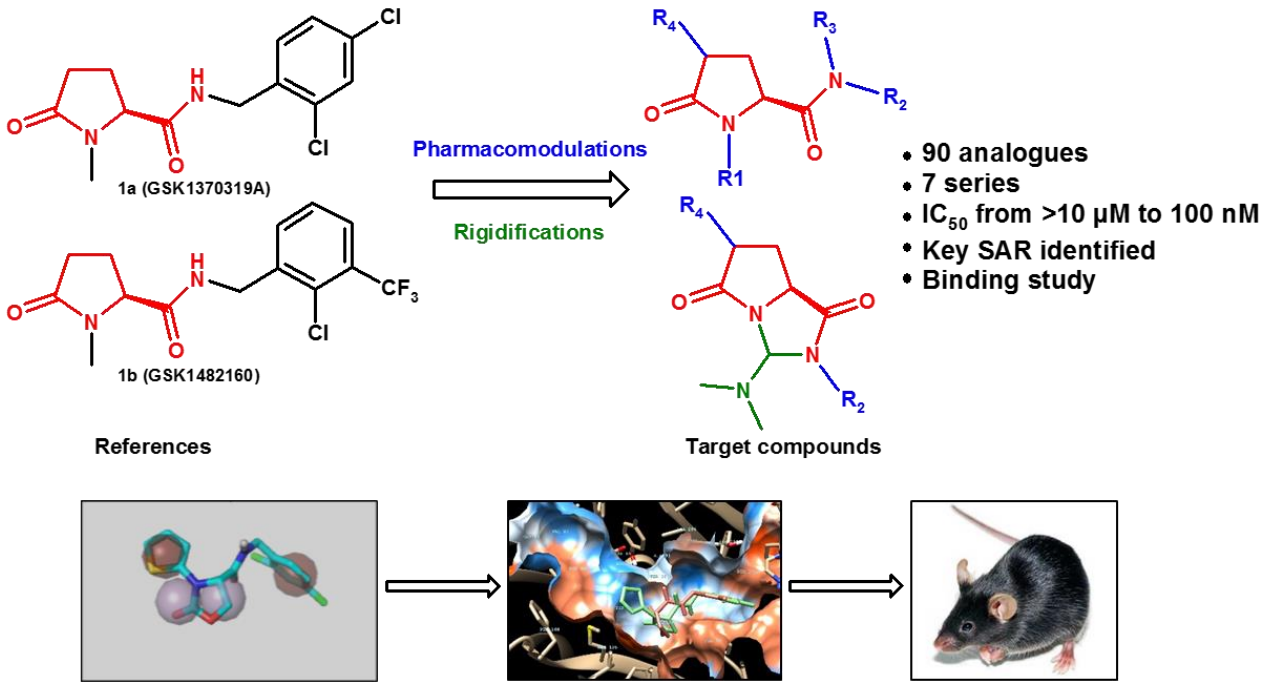

This report deals with the design, the synthesis and the pharmacological evaluation of pyroglutamide-based P2RX7 antagonists. A dozen were shown to possess improved properties, among which inhibition of YO-PRO-1/TO-PRO-3 uptake and IL1β release upon BzATP activation of the receptor and dampening signs of DSS-induced colitis on mice, in comparison with reference antagonist GSK1370319A. Docking study and biological evaluation of synthesized compounds has highlighted new SAR, and low toxicity profiles of pyroglutamides herein described are clues for the finding of a usable *h*-P2RX7 antagonist drug. Such a drug would raise the hope for a cure to many P2RX7-dependant pathologies, including inflammatory, neurological and immune diseases.

INTRODUCTION

The P2RX7 receptor (P2RX7) belongs to the purinergic receptor family. As all P2X receptors (P2XR), P2RX7 is a ligand-dependent ionic channel activated by ATP.[1] The target receptor possesses some particularities regarding the other P2XR of his sub-family. It has dissimilarities in terms of structure,[2] and sensitivity to P2X ligands. P2RX1-P2RX6 receptors have a structure with 379-472 amino acids, while P2RX7 contains 595 amino acids due to a longer COOH-terminal chain. P2RX7 is 100 to 1000 times less sensitive to ATP than the other P2XR.[3] Indeed, the different subtypes of P2XR are distinguished by their sensitivities to ATP. For example, millimolar concentrations are necessary to activate the P2RX7 receptor, whereas for the other sub-types these concentrations are in the micromolar range. The extracellular physiological concentrations of ATP being nanomolar, it is necessary that the ATP is released to reach sufficient concentrations to induce activation. Moreover, P2RX7 has two different behaviors, depending on the duration of its stimulation.[4] Over a brief time, the receptor acts as an ion channel permitting a K^+ efflux and a Ca^{2+} and Na^+ influx. These ions crossing the membrane are modifying the cell's potential, and activate different transduction mechanisms. In the case of a prolonged or repeated stimulation, or in presence of high concentrations of agonist, a large pore is formed. This pore enables molecules up to 900 Da to enter the cell, a process that eventually leads to apoptosis.

The main characteristic of P2RX7 is the opening of the channel that leads to a K^+ efflux, a key step in the inflammatory process. Studies have shown that macrophages pre-treated with KCl do not process or release cytokines when ATP is added, suggesting that channel opening precedes large pore opening that is mandatory for IL1β and IL18 maturation. The Ca^{2+} influx has been shown implicated in the release of these pro-inflammatory cytokines.[5] The natural circadian oscillation of

calcium is very important in the proper functioning of neurons, defects in Ca^{2+} homeostasis being involved in the pathogenesis of neurodegerative disorders.

IL1β is known to be a mediator of immunity and a cause of inflammation. Lipopolysaccharides (LPS) are the first inducer of IL1β. Nonetheless, their *stimulus* is not complete; it only induces an accumulation of pro-IL1β within the cell that must be cleaved into mature IL1β. Extracellular ATP was shown to be a strong inducer of pro-IL1β cleavage, *via* P2RX7 activation.[6] P2RX7 implication in the production and release of IL1β was reported in many studies.[7] The potassium efflux induces the formation of free radicals by the activation of Nicotinamide Adenine Dinucleotide Phosphate (NADPH) oxydase, which facilitate the inflammasome assembly. The inflammasome is a protein assembly where the activation of caspase-1 occurs. Then caspase-1 induces the cleavage of pro-IL1β into active IL1β.[7b] It is to be noted that NADPH oxydase also induces the death of T-regulatory cells.[8] Moreover, P2RX7 is implicated in the production of other IL1 family cytokins and chemokins (such as IL18),[7a,b] known for their role in many chronic inflammation diseases.[9] Besides its role in inflammation, P2RX7 has been shown to be involved in cell proliferation and cell death.[10]

Another well-known characteristic of P2RX7 is to form a large pore (like P2RX2 and P2RX4 do) when it is over-activated. This pore was the object of many studies.[11] After several seconds of activation, the large pore able molecules up to 900 Da to cross the membrane and to enter the cell.[12] It was reported that one or two ATP molecules binding to a "naïve" P2RX7 will induce a transition to desensitization, and a third ATP molecule binding will favor the transition to a dilated form of the receptor.[13] The pore formation generally leads to cell death *via* apoptosis, conferring to P2RX7 a cytolytic activity.[14] Many mechanisms were proposed to explain the pore formation but, to date, none of them was confirmed.[5a]

Following these observations, many studies were carried out to understand the P2RX7 physiological implications, and its potential uses in medicine. The potency of P2RX7 has been thus highlighted in numerous inflammation-related pathologies, among which neurodegenerative diseases (Parkinson's disease, Alzheimer's disease (AD), neurotrauma, multiple sclerosis, Huntington's disease, spinal cord injury and epilepsy), rheumatoid arthritis, and inflammatory bowel diseases (IBD).[15] As mentioned before, P2RX7 is implicated in the production and release of pro-inflammatory cytokines, such as IL1β and IL18.[16] In this context, ATP is a danger signal, secreted at high concentrations in inflammation *loci*.[17] The proof of concept regarding the reduction of inflammation by the inactivation of P2RX7 was given in rodent models,[18] and some P2RX7R antagonists were evaluated in clinical trials.[19] Unfortunately, none of the trialed drugs succeeded phase II so far, mostly due to a lack of efficiency. However, P2RX7 modulators (agonists or antagonists) are still of great interest for therapeutic applications.[20]

Our group is interested in pyroglutamic acid derivatives synthesis as drug-candidates.[21] The development of pyroglutamide-based P2RX7 antagonists by other groups,[22] attracted our attention (Figure 1). This report focuses on the design, the synthesis, and the pharmacological evaluation of analogues of GSK1370319A (compound **1a**) and GSK1482160 (compound **1b**) as P2RX7 potential antagonists.

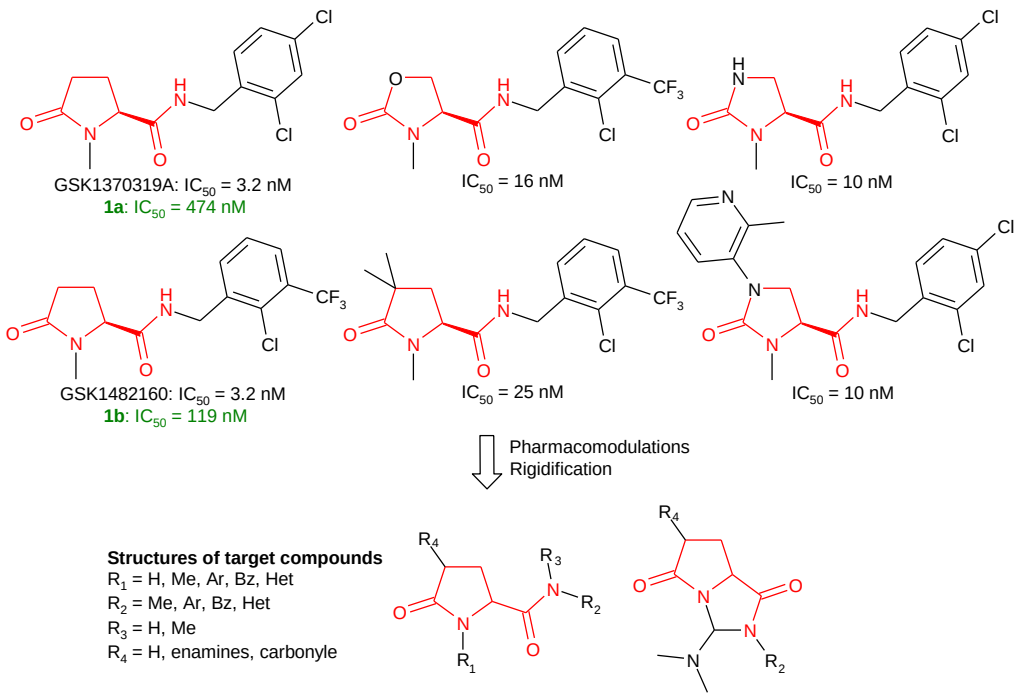

Figure 1. Structures and activities on *h*-P2RX7 *in vitro* reported in the literature (black) and activities observed in our biological assay (green) of reference P2RX7 antagonists GSK1370319A (compound **1a**) and GSK1482160 (compound **1b**), structures and activities reported in the literature of analog P2RX7 antagonists and general structures of target compounds.

RESULTS AND DISCUSSION

Pharmacophore perception of P2RX7 antagonists.

Since this study began previously to the recent crystallization of the panda (*pd*-) P2RX7,[23] a ligand-based approach was privileged. We first engineered a pharmacophore model based on 3D-structural similarities of published antagonists (see Supporting Information for the structure of selected antagonists of the literature).[24] The pharmacophore model was selected as fitting at best the 9 molecules of the reference dataset (Figure 2), which was the closest to the one described in the literature.[19b] Exhibiting two hydrogen bond acceptors and two lipophilic features, this pharmacophore query was used to filter a database of potential compounds; the best fitting ones being selected for synthesis (see Supporting Information for the structure and scores of designed compounds).

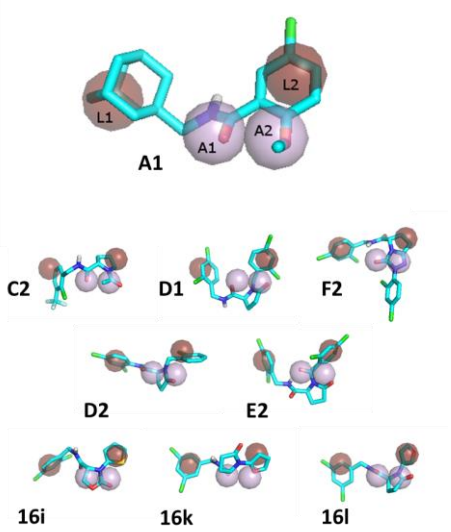

Figure 2. Representation of P2RX7 antagonists' pharmacophore (pink sphere: predicted hydrogen-bond acceptor location (A1 and A2); brown sphere: predicted lipophilic centers (L1 and L2)) and potentially active compounds **A1**, **C2**, **D1**, **D2**, **E2** and **F2** (see Supporting Information for structures and zooms) and further described *N*-heteroaryl-PGAm antagonists **16i**, **16k** and **16l**.

The investigations were firstly interested in the modulation of the positions 1 and 5 of the lactam ring. Three series were designed regarding the substitution on position 1 of the pyrrolidone scaffold: Series **I** (substitution by a methyl); Series **II** (introduction of (hetero-) aromatic units); Series **III** (*N*-benzyl and *N*-benzhydryl substituents). In these series, the amide in position 5 was substituted with various (hetero-)aryls, benzyls and alkyls groups.

In a second time, series **IV** was designed to explore the conformational space available in position 3 of the lactam. During the synthesis of this last series, we also unexpectedly observed the formation of pyrroloimidazolediones.[21j,k] These constrained analogues are gathered in series **V**.

Furthermore, other cycles replacing the pyroglutamide scaffold were investigated, such as oxazolidinone, pyridine and piperidone. The compounds bearing these moieties constitute series **VI**.

Chemistry.

The syntheses of pyroglutamides series **I-VI** are reported in Schemes 1 to 6. A large part was synthesized from natural amino-acids - *L*-pyroglutamic acid **2** (PGA), *L*-glutamic acid **3** (Glu), and *L*-serine **4** (Ser).

Esterification of PGA **2** was first conducted, leading to methyl pyroglutamate **5** (PGM) in quantitative yield.[21a] Synthesis of iminoether **6** and following rearrangement to methyl *N*-methyl pyroglutamate **7** was realized using dimethylsulfate.[21b] Aminolysis of ester **7** with corresponding amines furnished series **I** of *N*-methyl PGAm **1a-d** (Scheme 1).

Scheme 1. Synthesis of *N*-Methyl Pyroglutamide Derivatives **1a-d**[a] (Series **I**)

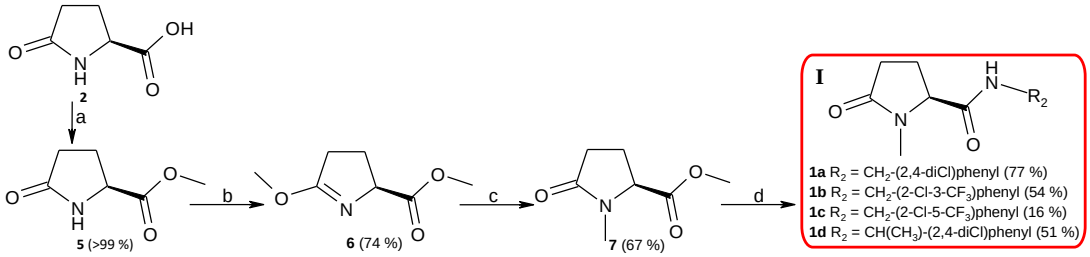

[a] Reagents and conditions. (a) CH_3SO_3H, MeOH/$CHCl_3$, MS 3Å, reflux, 24 h, quantitative yield; (b) (i) Me_2SO_4, 60°C, 12 h; (ii) Et_3N, 0°C–r.t., 1 h, 74%; (c) Me_2SO_4, THF, 80°C, 4 h, 67%; (d) amine, catalyst (PTSA or $ZrCl_4$), r.t.–120°C, 5–96 h, 16–77%.

N-aryl PGM **8a-l** were next obtained by a copper initiated method we recently developed.[21c] Aminolyses of esters **5**, **7** and **8a-l** furnished pyroglutamides **9-13**, **15**, **16a**, **16e**, **16g-o**, **18** and **22**.[21d] *N*-(hetero-)aryl derivatives **14**, **16a-d**, **16f**, **16p-q** , **17**, **19-21** and **23** were obtained by copper initiated coupling from pyroglutamides **10j**, **11e**, **11a**, **11g-h**, **12b** and **13** (Scheme 2).[21c]

Scheme 2. Synthesis of *N*-Aryl Pyroglutamide Derivatives **14** to **23**[a] (Series **II**)

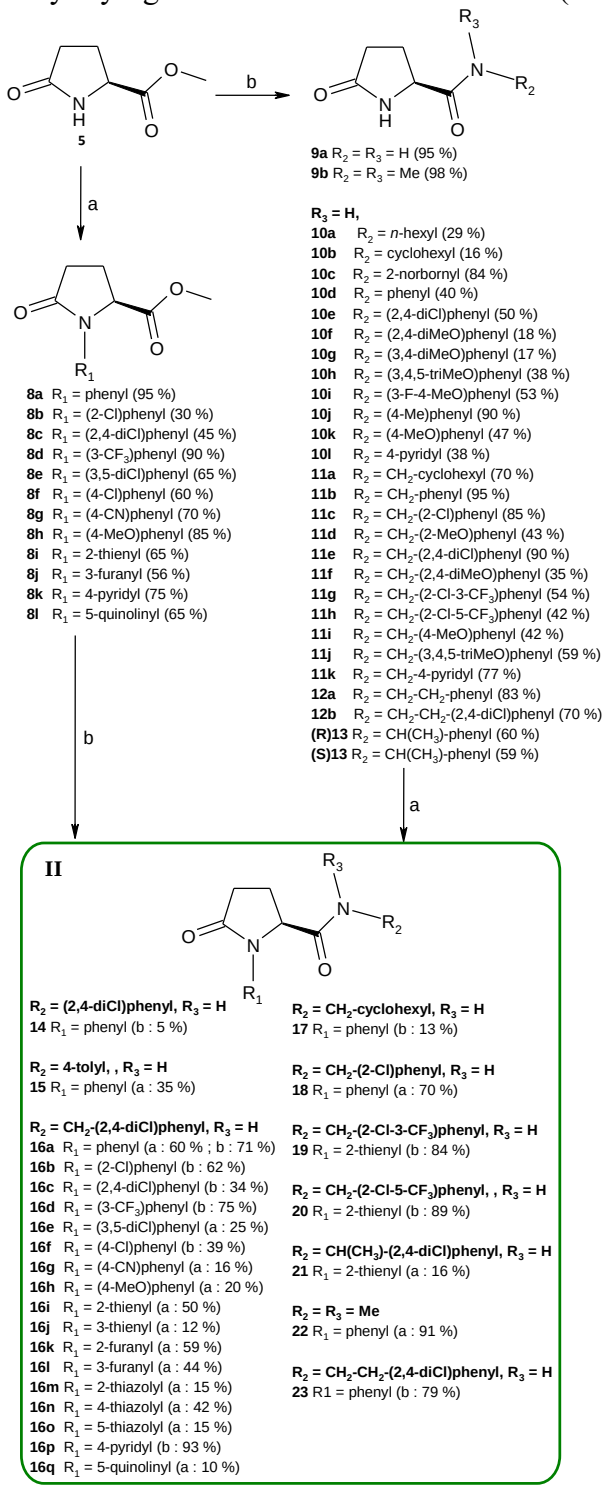

[a] Reagents and conditions. (a) R_1-X (X = Br, I), CuI, *N*,*N*'-DMEDA, Cs_2CO_3, dioxane, 60°C–reflux, 2–96 h, 12–95%; (b) amine, catalyst (PTSA or $ZrCl_4$), r.t.–120°C, 5–96 h, 5–98%.

PGM **5** was *N*-silylated to furnish compound **24**,[21f] then reacted on the one hand with silylated benzhydrols leading to *N*-benzhydryl PGM **25a** and **25b**[21g] and with 4-nitrobenzyl chloride at 150°C for 40 h to provide *N*-(4-nitrobenzyl) PGM **26**.[21f] Other *N*-benzyl PGM **27a**, **27b** and **27d-g** were synthesized from Glu **3** according to our reductive amination method.[21h] Ester **27c** was synthesized from PGM **5** using NaH and 2,4-dichlorobenzyl chloride.[21i] Amidation of esters **25-27** provided *N*-benzyl PGAm **28-43** (Scheme 3).[21d]

Scheme 3. Synthesis of *N*-Benzyl and *N*-Benzhydryl Pyroglutamide Derivatives **28** to **43**[a] (Series **III**)

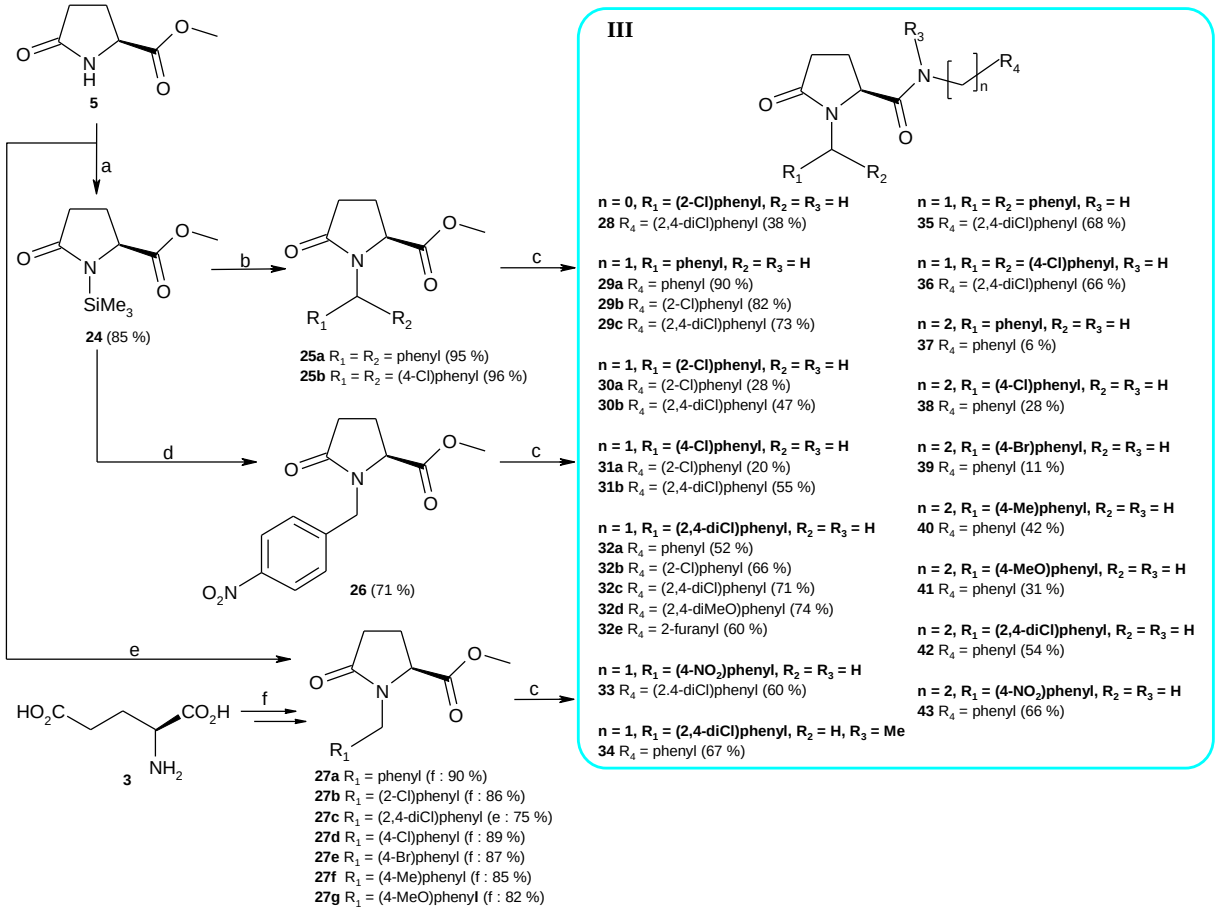

[a] Reagents and conditions. (a) Me_3SiCl, Et_3N, toluene, 80°C, 6 h, 85%; (b) $Me_3SiOCH(Ph)_2$, TfOH, 130°C, 2–5 h, 95–96%; (c) amine, catalyst (PTSA or $ZrCl_4$), r.t.–120°C, 24–72 h, 6–90%; (d) 4-nitrobenzyl chloride, 150°C, 40 h, 71%; (e) $ClCH_2$-(2,4-diCl)Ph, NaH, THF, 70°C, 24h, 75%; (f) (i) Et_3N, R_1-CHO, $NaBH_4$, MeOH, 2 h; (ii) EtOH, reflux, 5 h; (iii) MeOH, H^+, 81–90%.

The introduction of a dimethylenamine moiety in position 3 of the lactam ring can be realized using Bredereck's reagent (BR).[25] This transformation and further modifications of the obtained β-enaminones furnished compounds **44-48** constituting series **IV** (lactams modulated in position 3). Moreover, we have shown in two previous studies that BR was able to provide pyrroloimidazolediones **49** and **50** (compounds of series **V**), which can be next processed to synthesize β-enaminones **51-54** (series **IV**) and pyrroloimidazoletriones **55**.[21j,k] Thus, we enriched series **IV** with *NH*-free lactams, and we obtained series **V** of pyrroloimidazoles (Scheme 4).

Interestingly, the Vilsmeier-Haak reaction (equivalent to Bredereck's reaction) on the substrate **11e**, provided the *N*-formyl lactam **56**, which was attached to series **I** for its bulkiness, while the electronic properties are strongly different (Scheme 4).[21j]

Scheme 4. Synthesis of Pyroglutamide Derivatives **44** to **55** (Series **IV** and **V**) and Pyroglutamide Derivatives **56**[a] (Series **I**)

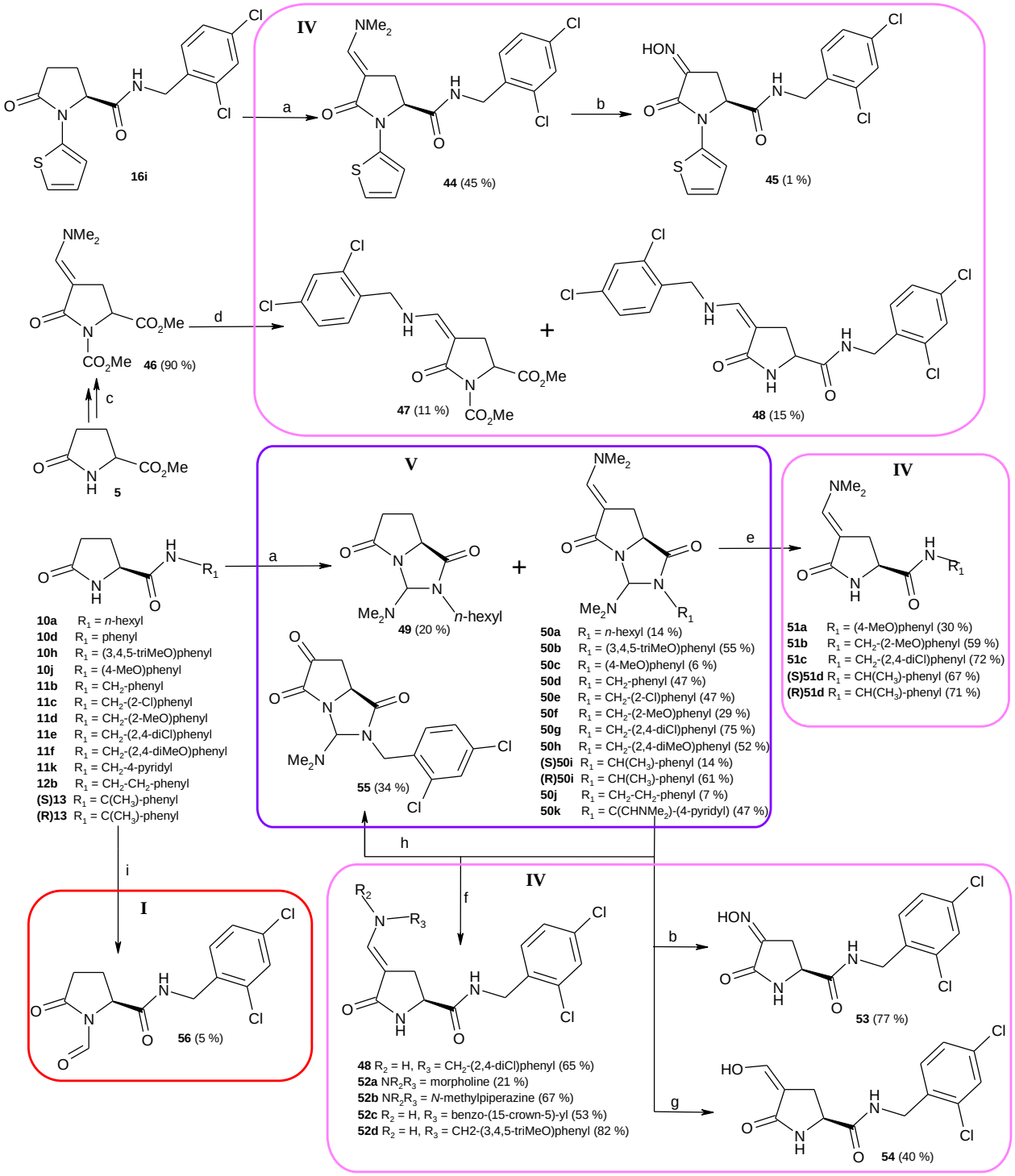

[a] Reagents and conditions. (a) *t*-BuOCH(NMe$_2$)$_2$, 120°C, 1–24 h, 7–75%; (b) NaNO$_2$, CH$_3$CO$_2$H, THF, 0°C, 3 h, 1-77%; (c) (1) ClCO$_2$Me, Et$_3$N, DMF, -10°C, 1 h, 33%; (2) *t*-BuOCH(NMe$_2$)$_2$, 120°C, 2 h, 90%; (d) amine, ZrCl$_4$, 60°C, 48 h, 11–15%; (e) MeOH, reflux, 24 h, 30–72%; (f) amine, toluene, reflux, 24 h, 21–82%; (g) CH$_3$SO$_3$H, H$_2$O, reflux, 24 h, 40%; (h) NaIO$_4$, EtOAc/CH$_3$CN/H$_2$O, r.t., 1 h, 34%; (i) (Me$_2$N$^+$=CHCl, Cl$^-$), DMF, r.t., 48 h, 5%.

Oxazolidinone **57** was synthesized from Ser **4** according the method reported in the literature.[26] Methyl ester **58** was further obtained upon esterification of oxazolidinone **57**,[21a] and then treated with 2,4-dichlorobenzylamine to provide the amide **59**.[21d] Afterward, the 2-iodothiophene was reacted with the resulting amide under copper-coupling conditions and provided *N*-(thienyl)oxazolidinone **60** and side products (Scheme 5).[21c]

To introduce the amide linker in position 4 of the lactam, a synthetic strategy starting from biosourced itaconic acid **61** was privileged. Further esterification to dimethyl itaconate **62** and cyclisation using ammonia provided lactam **63**.[27] Aminolysis and copper-coupling conditions were then applied to lactam **63** and provided PGAm **64** and **65**.

Some other analogues of the lactam moiety were investigated, such as pyridines **67** and **68**, synthesized through previously described route. The extension of the pyrrolidone ring to piperidone was also realized. Compound **70** was obtained by peptide coupling, and used as the substrate of BR to furnish β-enaminone **71**.

Scheme 5. Synthesis of Pyroglutamide Analogues **59**, **60**, **64**, **65**, **67**, **68**, **70** and **71**[a] (Series **VI**)

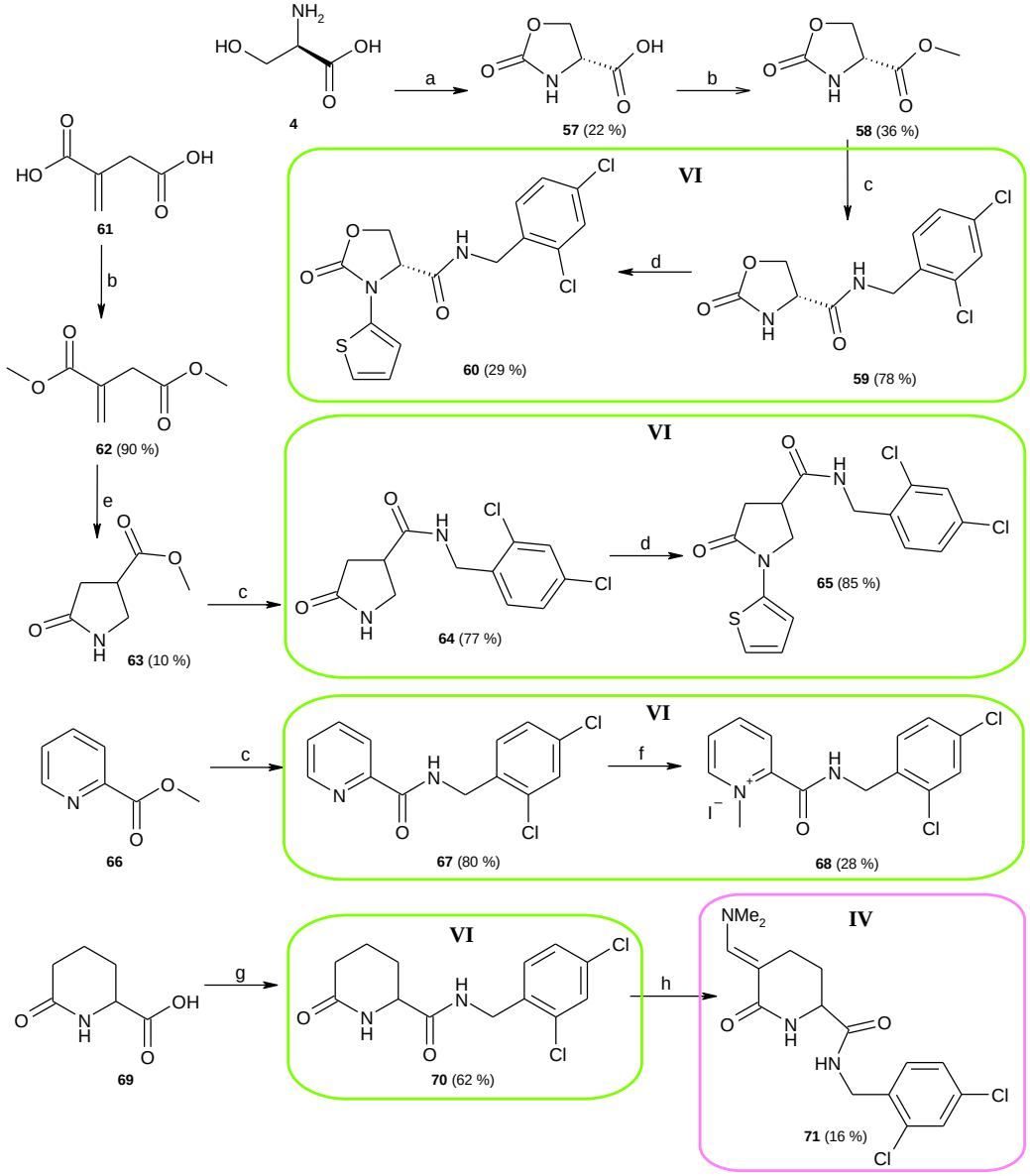

[a] Reagents and conditions. (a) $ClCO_2Ph$, NaOH, toluene/H_2O, <30°C, 3 h, 22%; (b) MeOH, $SOCl_2$, reflux, 48 h, 36–90%; (c) 2,4-dichlorobenzylamine, PTSA, r.t., 24 h, 77–80%; (d) 2-iodothiophene, CuI, *N*,*N*'-DMEDA, Cs_2CO_3, dioxane, r.t., 24 h, 25–85%; (e) NH_3, H_2O, rt, 10%; (f) MeI, reflux, 24 h, 28%; (g) 2,4-dichlorobenzylamine, EDCI, CH_2Cl_2, r.t., 24 h, 62%; (h) *t*-$BuOCH(NMe_2)_2$, 120°C, 3 h, 16%.

In order to evaluate the affinity of our antagonists with the receptor, a radioligand was synthesized from aminoquinoleine **72**. Thiocyanate **73** and aminoquinoleines **74** were synthesized according to a method of the literature (Scheme 6)[28]. The tritiation of compound **74b** was outsourced to provide

the radiolabeled P2RX7-ligand **75**, which was further used as the reference in the competitive binding assay further described.

Scheme 6. Synthesis of P2RX7 ligands **74** and **75**[a]

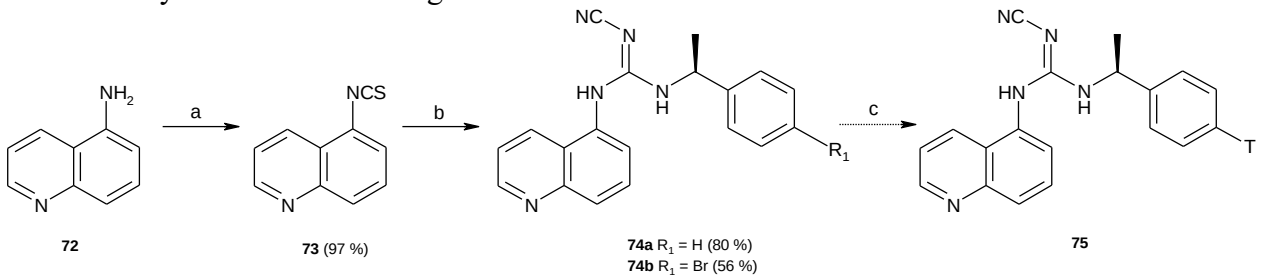

[a] Reagents and conditions. (a) $CSCl_2$, $NaHCO_3$, CH_2Cl_2, H_2O, N_2, 0°C, 2h, 97%; (b) (i) amine, THF, r.t., 1h, (ii) $Hg(OAc)_2$, (iii) NaNHCN, r.t., 15h, 56–80%; (c) ^3T labelling outsourced.[29]

Because harsh chemical conditions were used for aminolyses, compound **16i** was selected for supercritical fluid chiral chromatography (Figure S15 of the Supporting Information) to verify the retention of configuration. Only one isomer was identified, confirming the retention of configuration along the syntheses we previously described.[21c,d,j,k]

SAR of Pyroglutamide Derivatives as P2RX7 Antagonists.

Pyroglutamide derivatives and precursors were tested by flow cytometry using (4-benzoyl)benzoyl-adenosine-5'-triphosphate (BzATP) as activator of the P2RX7 and AZD11645373 as reference (see the Experimental Section for material and methods, see Table S1 to S6 in the Supporting Information file for detailed data of the flow cytometry study of series **I-VI**, see Table 1 for structure and activities of the most active compounds). Precursors (*NH*-free lactam **9-13**, and esters **5-8**, **24-27**, **46**, **57**, **58** and **63**) have shown no significant activity on the P2RX7 (data not shown). Thus, the amide in position 4 or 5 of the lactam, and the substitution of position 1 of the heterocycle seemed important for the activity.

Benzyl and benzhydryl substitution of series **III** provided no active compounds (Table S3). These substitutions may be too bulky for the receptor's binding site. This affirmation was sustained by some observations made in series **I** of *N*-methylated compounds (Table S1) and series **II** of *N*-

arylated compounds (Table S2). Indeed, a 5-member heterocycle is, most of the time, better than a methyl (compound **1a** *vs* compounds **16i-n**, and compound **1b** *vs* compound **19**), but 6- or more membered (hetero-)aromatic ring in position 1 provided less active compounds (compound **16a-h**, **16p** and **16q** *vs* compound **1a**, **1b** and **16i-n**). We thus hypothesized that the binding pocket size corresponding to position 1 is limited, but it needs to be occupied in order to obtain a P2RX7 antagonist. Interestingly, *N*-formyl lactam **56** was not active, either because the specific conformation issued from carbonyls repulsion, or due to an unfavorable charge distribution.

The substitution of the amide in position 5 was then studied. In series **I** of *N*-methylated compounds, only references **1a** and **1b** (respectively 2,4-dichlorobenzyl and 2-chloro-3-trifluorobenzyl substitution on the amine) were active. Changing the position of the trifluoromethyl group from position 3 to position 5 (in compound **1c**) was deleterious for the activity, such as the introduction of a methyl between the amide and the aromatic ring (compound **1d**). The same observations were made in series **II** of *N*-arylated PGAm, and the only acceptable substitutions for the amide seemed to be 2,4-dichlorobenzyl and 2-chloro-3-trifluoromethylbenzyl. Moreover, the 3-trifluoromethyl group provided a better activity than a 4-chloro modulation.

The activities of rigidified compounds of series **IV** and activities of compounds substituted in position 3 of series **V** are very low (Tables S4 and S5). We reported, in a previous work,[21k] that the substitution in position 3 of the lactam and the rigidification between the pyrrolidone nitrogen and amide nitrogen decreased the activity on P2RX7. This was once again confirmed with more compounds in the current study.

Finally, modulation of the pyrrolidin-2-one moiety of series **VI** was evaluated, with the hope of changing the lactam paradigm (Table S6). The introduction of an oxygen in position 3 (compounds **59** and **60**) and the modification of the amide position from 5 to 4 (compounds **64** and **65**)

diminished the biological activity. The modification of the pyrrolidone to a pyridine or to a piperidone (compounds **67** and **68**, and compounds **70** and **71**, respectively) was deleterious for the activity. Finally, the initial lactam seemed better than the other exemplified scaffolds.

Regarding their structures and activities (Table 1), 8 hits were selected for advanced biological studies and comparison with references **1a** and **1b** (Figure 3). Seven *N*-hetero-aryl pyroglutamides **16** and **19** (IC_{50} from 100 to 813 nM), were selected for their improved activities regarding **1a** and **1b** activities (respectively 474 nM and 119 nM). Oxazolidinone **60** was also chosen for further biological investigation as lactam closely related compound in spite of low antagonist activity P2RX7 is low (IC_{50} = 3168 nM). This choice was strategic for the comparison of pharmacokinetic parameters of oxazolidinone compared to active lactams. The antagonistic activity on P2RX7R of these compounds - first measured by flow cytometry - was assessed in a competitive binding study with radiolabeled [^{3}H]A-804598 **75** (Table 1). The results of the assay were concordant with flow cytometry results. Thus, the binding site of pyroglutamides should be the same as the binding site of A-804598 **74a**.

Table 1. Inhibition of P2RX7 Activity by References **1a** and **1b**, and Most Active Compounds.

compd	Structure	Series	Flow cytometry		Competitive radioligand binding study with **75**	
			Inhibition of *h*-P2RX7 at 10^{-5}M (%)[a]	IC_{50} ± SD[a]	K_i (nM)[a]	IC_{50} (nM)[a]
1a (ref)[c]	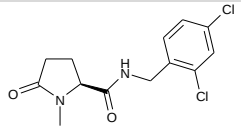	**I**	100	474.0 ± 12.0 nM	176	862
1b (ref)[d]	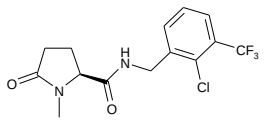	**I**	98	119.3 ± 7.0 nM	68	332

16a	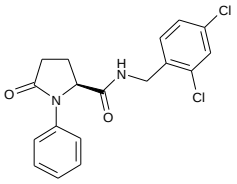	**I**	50	10.0 μM	—[b]	—[b]
16i	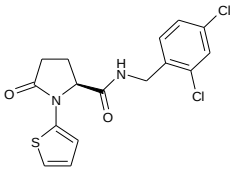	**II**	98	229.0 ± 4.5 nM	147	721
16j	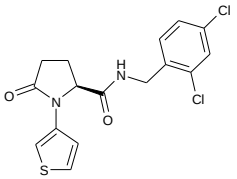	**II**	78	813.2 ± 56.7 nM	256	1252
16k	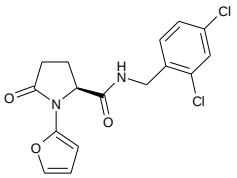	**II**	94	244.0 ± 105.0 nM	118	575
16l	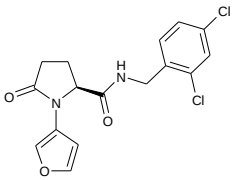	**II**	85	199.5 ± 15.5 nM	86	424
16m	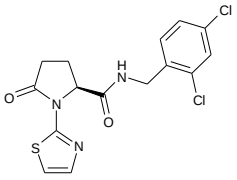	**II**	83	415.0 ± 85.0 nM	489	2386
16n	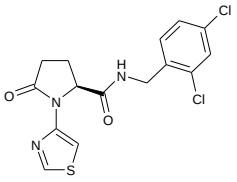	**II**	98	256.4 ± 1.0 nM	78	384
19	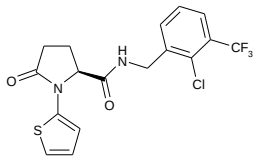	**II**	100	100.0 ± 10.1 nM	44	218

29c	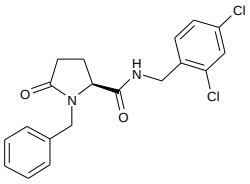	**III**	100	1.1 μM	—[b]	—[b]
30b	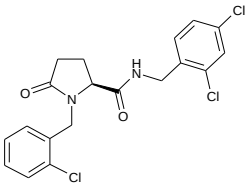	**III**	85	3.5 μM	—[b]	—[b]
45	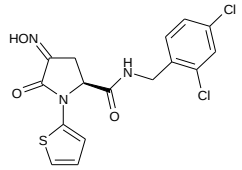	**IV**	76	3.7 μM	—[b]	—[b]
47	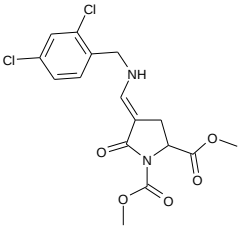	**IV**	99	4.3 μM	—[b]	—[b]
50g	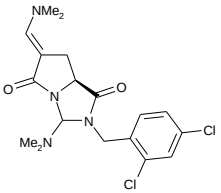	**V**	24	—[b]	—[b]	—[b]
51c	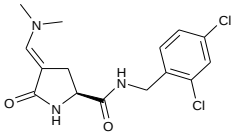	**IV**	53	—[b]	—[b]	—[b]
52a	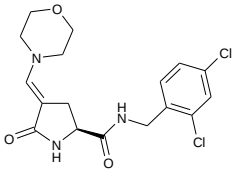	**IV**	56	9.6 nM	—[b]	—[b]

52b	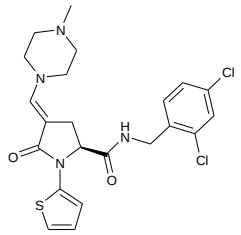	**IV**	49	6.9 nM	—[b]	—[b]
53	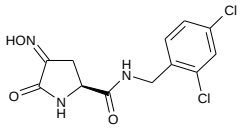	**IV**	52	—[b]	—[b]	—[b]
60	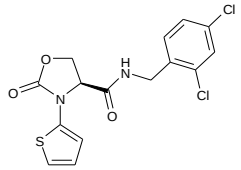	**VI**	80	3.2 μM	3110	15180
65	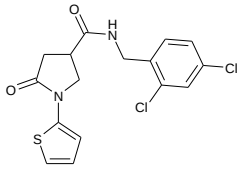	**VI**	92	2.4 μM	—[b]	—[b]
71	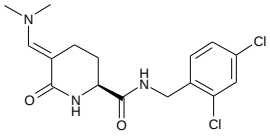	**IV**	6	—[b]	—[b]	—[b]

[a]Mean value of n ≥ 2 in the presence of a positive control. [b] Not determined. [c]GSK1370319A. [d]GSK1482160.

Figure 3. Structures of References **1a** and **1b** and of the Eight Selected Hits

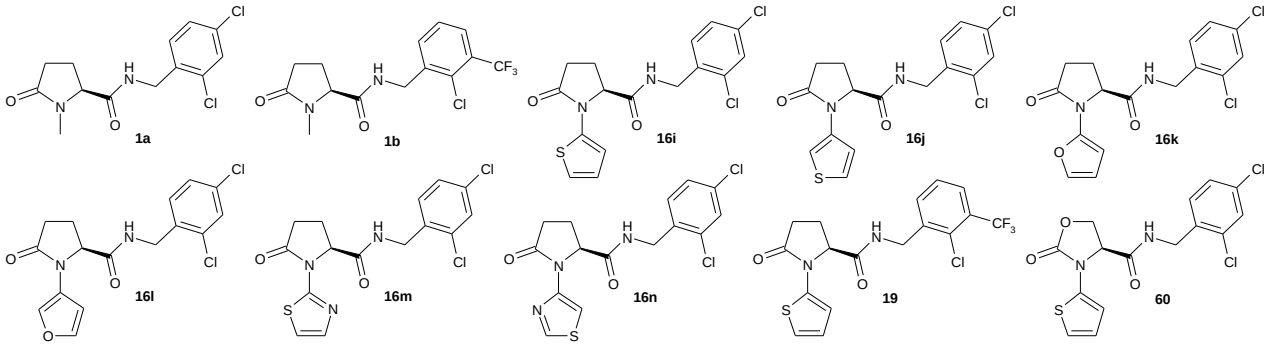

Structure-based insights for P2RX7 ligand binding

Thanks to the recent crystallization of *pd*-P2RX7,[23] the binding pocket of P2RX7-antagonists was shown to be allosteric, one of the best fitting compounds was JNJ47965567 (Figure 4).[30] Some P2RX7-ligands complex models were generated using docking experiments with the most suitable PDB template co-crystallized with JNJ47965567.

Figure 4. Structure of JNJ47965567

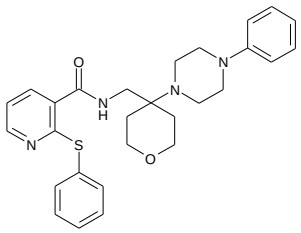

Some of the synthesized pyroglutamides and analogues were selected for a docking study in which pKd was estimated (Table 2) for the best predicted pose of each ligand (see Figure 5, see Figure S16 to Figure S27 of the Supporting Information for zooms).

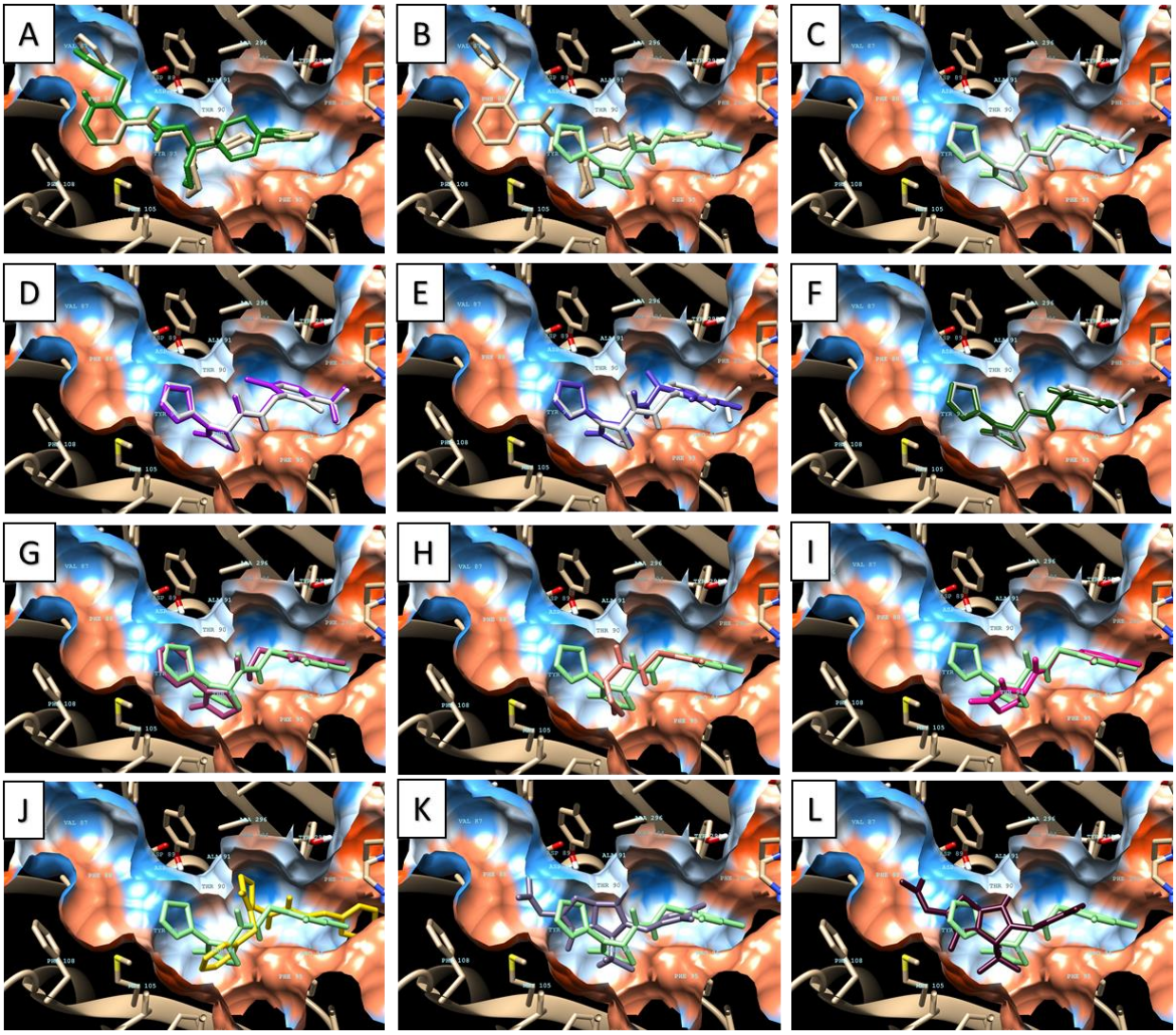

Figure 5. Docking poses predicted for selected compounds with JNJ47965567 as reference (A: JNJ47965567 experimental (grey) vs JNJ47965567 predicted (green); B: JNJ47965567 experimental (grey) vs **16i** (light green); C: **16i** (light green) vs **19** (white); D: **19** (white) vs **20** (pink); E: **19** (white) vs **(R)-21** (violet); F: **19** (white) vs **(S)-21** (green); G: **16i** (light green) vs **16a** (light pink); H: **16i** (light green) vs **1a** (orange); I: **16i** (light green) vs **11e** (pink); J: **16i** (light green) vs **37** (yellow); K: **16i** (light green) vs **50g** 1st best fitting pose (grey) ; L: **16i** (light green) vs **50g** 2nd best fitting pose (dark red)).

The docking protocol confirmed that the predicted pose of JNJ47965567 fitted with the experimental pose (Figure 5.A). The poses of compounds **1a**, **11e**, **16i**, **19**, **20**, **21** (**(R)-** and **(S)-** isomers), **37** and **50g** (**(R,R)-**, **(S,R)-**, **(R,S)-** and **(S,S)-** isomers) were calculated. All best poses fitted into the allosteric binding site of JNJ47965567. Antagonist **16i** (*N*-(2,4-dichlorobenzyl)-PGAm) pose was compared to JNJ47965567 experimental pose, with almost all positions fitting the pocket (Figure 5.B). *N*-(2-chloro-3-triofluorobenzyl)-PGAm **19** and *N*-(2-chloro-5-triofluorobenzyl)-PGAm **20** are in the same position as **16i** (Figure 5.C and Figure 5.D). Introduction of a methyl on the amide substituent in compounds **(R)-21** and **(S)-21** (*N*-[1-(2,4-dichlorophenyl)ethyl]-PGAm) seemed to change the position of the aromatic. These findings were in accordance with the results observed in the flow cytometry assay: i) the introduction of a methyl between the amide and the aromatic is deleterious foe the activity; ii) the 4-chlorine may be changed to a trifluoromethyl group. On this last point, our *in silico* model doesn't predict the loss of activity observed for compound **20** (*N*-(2-chloro-5-triofluorobenzyl)-PGAm).

Now substitution in position 1 of the lactam was studied (*NH*, *N*-methyl, *N*-(hetero-)aryl and *N*-benzyl lactams) and seemed to be of great importance for the position of this ring in the binding pocket: *N*-(hetero-)aryl-PGAm **16a**, **16i**, **19**, and **20** were not in a similar pose to the ones of *N*-methyl-PGAm **1a**, *NH*-free lactam **11e** and *N*-benzyl-PGAm **37** (Figure 5.C to Figure 5.J). We hypothesize that the interaction of (hetero-)aryl groups with the receptor is responsible of the positioning of the lactam ring and induces the better activity of *N*-thienyl-PGAm **16i** and **19** compared to *N*-methyl-PGAm **1a** and **1b**. For constrained analogs, the model showed a steric clash between the receptor and the pyrroloimidazoledione **50g** (Figure 5.K and Figure 5.L), as expected regarding the low activity of this compound.

Calculated pKd were in accordance with previous observations (Table 2).

Table 2. Calculated pKd of selected compounds for docking study.

compd	calc. pKd
JNJ47965567	9.03
1a	6.19
11e	5.83
16i	6.99
19	7.72
20	7.58
(R)-21	7.21
(S)-21	7.29
37	7.50
(R,R)-50g	6.27
(R,S)-50g	6.27
(S,R)-50g	6.41
(S,S)-50g	6.27

Impact of P2RX7 antagonists on IL1β production and ROS generation

IL1β is a major pro-inflammatory cytokine that is rapidly released *via* P2RX7 receptor activation. We analyzed the effect of ten P2RX7 antagonists on the modulation of IL1β production from human THP-1 macrophages. As expected, IL1β level gradually increased when macrophages were treated with LPS and BzATP, at 2, 4, and 6-hour post-incubation. The macrophages were pretreated with P2RX7 antagonist molecules, with GSK1370319A (compound **1a**) and GSK1482160 (compound **1b**) as references, at a concentration of 10^{-5} mol/L and 10^{-6} mol/L, and then stimulated with both LPS and BzATP.

IL1β production remained at a basal level at 2h, 4h and 6h and was like unstimulated macrophages ones. Besides, the pretreatment of the macrophages with the ten antagonists at a concentration of 10^{-5} mol/L, and following addition of LPS and BzATP showed a significantly lower level of IL1β when compared to that from unstimulated macrophages, whereas these antagonists at a concentration of 10^{-6} mol/L did not inhibit IL1β production after 6-hour incubation (Figure 6). In this test, *N*-heteroaryl-PGAm were as good as references **1a** and **1b** (*N*-methyl-PGAm). Compound **19**, bearing thiophene and 2-chloro-3-trifluoromethyl moiety was the best at 6h.

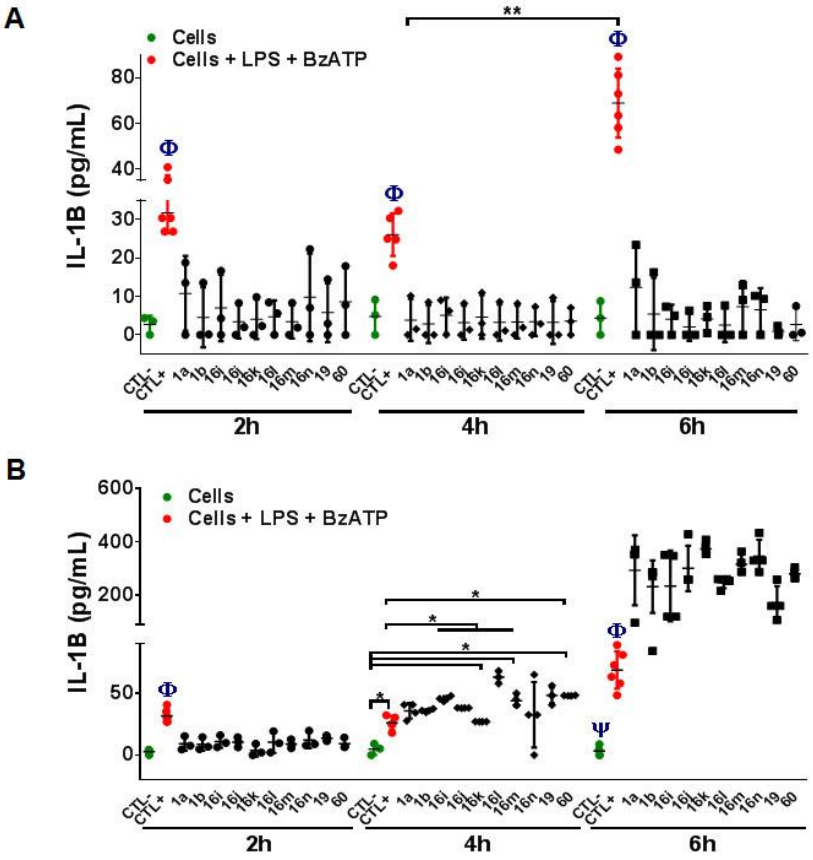

Figure 6. Effect of P2RX7 antagonists on IL1β production from macrophages. Analysis of IL1β level in the supernatant of macrophages pretreated with P2RX7 antagonist molecules at a decreasing concentration (A: 10^{-5} and B: 10^{-6} mol/L). CTL- corresponds to macrophages, CTL+ corresponds to macrophages + LPS + BzATP. $^{\Phi}P<0.05$ (CTL+ vs compounds). $^{\Psi}P<0.01$ (CTL- vs compounds).

The generation of reactive oxygen species (ROS) after activation of P2RX7 receptor by ATP is well known in macrophages. We observed that the percentage of ROS significantly increased in the macrophages incubated with LPS and BzATP whereas the pretreatment of macrophages with the ten molecules at a concentration of 10^{-5} mol/L significantly reduced the ROS production. We next used a decreasing concentration of antagonists and we found that PGAm **16m**, **16n** and **16k** at a concentration of 10^{-6} mol/L did not inhibit the ROS production when compared to other antagonist molecules (Figure 7). All tested PGAm were good inhibitors of the ROS production, and compounds **16i** and **19**, both bearing a thienyl moiety, were comparable to references **1a** and **1b**. 2,4-Dichlorobenzylamide **16i** being easier to afford in large quantity, the further assays described in this study were realized using it preferentially to 2-chloro-3-trifluoromethylbenzylamide **19** or other *N*-aryl-PGAm of formula **16**.

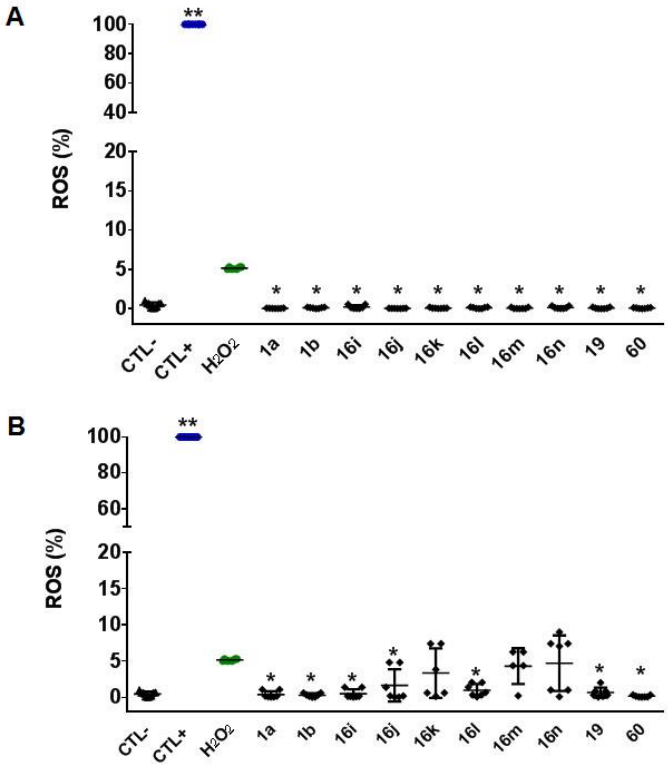

Figure 7. Effect of P2RX7 antagonists on the ROS generation from macrophages. Analysis of ROS generation in the supernatant of macrophages pretreated with P2RX7 antagonists at a decreasing

concentration (A: 10^{-5} and B: 10^{-6} mol/L). CTL- corresponds to macrophages. CTL+ corresponds to macrophages + LPS + BzATP. $^{**}P<0.01$ (CTL+ vs compounds). $^{*}P<0.05$ (Compounds vs CTL-, H_2O_2).

Selectivity and ADME-Tox evaluation.

Cytotoxicity was evaluated on wild-type HEK293 and P2RX7-transfected HEK293 cell lines for the 8 selected hits. No toxicity was found after 72 hours compared to control (data not shown).

Platelet aggregation assay was implemented to reveal an eventual interaction, notably with P2RX1, a receptor expressed on platelets membrane at a high concentration. No effect was observed (see Supporting Information), indicating the probable absence of interaction of these compounds with P2RX1 and influence on the platelets aggregation.

The pharmacokinetic (PK) profiles of the ten selected hits were investigated (Table 3). Lipophilicity was predicted to be low (calculated logP from 1.5 to 3.5)[31], and none of the tested compounds, but reference **1a**, was soluble in physiological saline at a concentration of 1 mg/mL. Moreover, while references **1a** and **1b** were very stable, *N*-aryl pyroglutamides were rapidly metabolized by *h*-hepatocytes. We determined that the main metabolite of *N*-aryl pyroglutamide **16i** using human hepatic microsomes was *NH*-free pyroglutamide **10e** (see Experimental Section for detailed protocol,[32] see Supporting Information for results). We hypothesize that the reduced activity of compound **16i** compared to **1a** – later described in the *in vivo* assays – comes from rapid metabolization of **16i** into inactive **10e**. Thus, modulations of *N*-aryl pyroglutamide P2RX7 antagonists to improve the PK profile and metabolic stability is to be investigated and will be reported in a further study.

Table 3. Pharmacokinetic Parameters for Selected Hits

Compd	logP	Solubility[a]	CL_{int} (μL/min/mg)	$t_{1/2}$ (min)	Mouse Metabolization at 40' (%)
1a (ref)[b]	1.61 ± 0.58	+	3.6	619	5.1
1b (ref)[c]	1.72 ± 0.66	-	2.8	800	4.4
16i	2.72 ± 0.93	-	1072	1.5	100.0
16j	2.72 ± 0.93	-	762	2.5	99.9
16k	2.20 ± 0.92	-	411	5.2	99.2
16l	2.20 ± 0.92	-	630	2.9	99.9
16m	1.31 ± 0.68	-	253	7.5	93.0
16n	1.26 ± 0.96	-	379	4.8	98.0
19	2.82 ± 0.98	-	530	3.8	99.7
60	3.37 ± 1.00	-	663	1.4	100.0

[a]The solubility was measured by a method as follows[33]: 1.0 mg of the appropriate compound dissolved in 1.0 mL of physiological saline (containing 2.5% ethanol and 2.5% Tween-80); + , completely dissolved; - , not all dissolved. [b]GSK1370319A. [c]GSK1482160.

Furthermore, 65 synthesized drug-candidates were selected by the National Cancer Institute (NCI) for evaluation of their antiproliferative activity against 60 cancer cell lines, including several multidrug-resistant (MDR) tumor cell lines (HCT-15: human colon Duke's type D, colorectal adenocarcinoma; UACC-62: human malignant melanoma; NCI/ADR-RES: human ovary adenocarcinoma; RXF 393: human kidney poorly differentiated hypernephroma; UO-31: human kidney carcinoma; MCF7: human breast adenocarcinoma; SF268: human CNS anaplastic astrocytoma and SF539: human CNS glioblastoma).

None of the tested compounds at a high single dose (10 μM) in the full NCI 60 cell panel has shown a cytotoxic profile (see Supporting Information for full evaluation report), indicating their

low toxicity on human cancer cells also. This result raises good hope for further development of pyroglutamide series as anti-inflammatory drugs.

The N-thienyl-PGAm 16i molecule ameliorates acute colitis

Having shown that the N-thienyl-PGAm **16i** molecule (need to explain, why 16i in particular) inhibits IL1β production from human THP-1 macrophages, we tested this molecule in mice, using the dextran sulfate sodium (DSS)-induced colitis protocol (Elson Charles O et al, 1995 Gastroenterology 109:1344-1367). Indeed, among experimental models of IBD, this model is one of the most popular for drug screening studies as reviewed by Valatas and colleagues (Valatas V. et al, European journal of pharmacology, 2015).

This model induces reproducible mucosal colonic inflammation manifested by bloody diarrhea, weight loss, mucosal ulceration and neutrophilic infiltration within colon. These features led to measurable clinical symptoms after 5 days of DSS treatment (Cooper HS et al, Lab Invest 1993).

Mice treated daily with compound **16i** lost 50% less weight than mice treated with placebo (figure 8.A) and showed milder signs of colitis, characterized by less diarrhea and less rectal bleeding. Indeed, the DAI score of mice treated with molecule **16i**, is decreased by 31% (figure 8.B). These clinical symptoms started at day 9 and were statistically significant between days 11 and 12, i.e. when re epithelization occurs. Of interest, compound **16i** is as efficient as the reference compound **1a** to dampen signs of colitis.

To evaluate the degree of inflammation, we performed histological analysis at day 14. Representative image of mice treated with placebo showed mucosal edema, transmural immune cell infiltration and the presence of large areas of erosion (Figure 8C, left panel). In mice treated with

compounds **16i** and **1a**, areas of normal colonic mucosa with crypts being straight, well defined and sitting on the muscularis mucosa are larger. Scoring of inflammation confirmed that both antagonists decreased by 42 to 50% the level of inflammation (Figure 8C, right panel).

The inhibition observed with 16i or the reference compound is within the range of what is classically observed with the DSS-colitis protocol (Greten F et al, Cell, 2004, Gong Z et al, 2018 Molecular Immunology, Melgar S. et al, International immunopharmacology, 2008). Of interest, analysis of clinical scores and inflammatory index, revealed that mice treated with the antagonist compounds recovered more rapidly from DSS-induced colitis than mice treated with placebo. Strikingly, a faster re-epithelization of the digestive mucosa was also observed in *P2rx7*$^{-/-}$ mice during the recovery phase (Hofman et al, Cancer Research, 2015). This observation suggests that **16i** compound phenocopies the loss of P2RX7 activity.

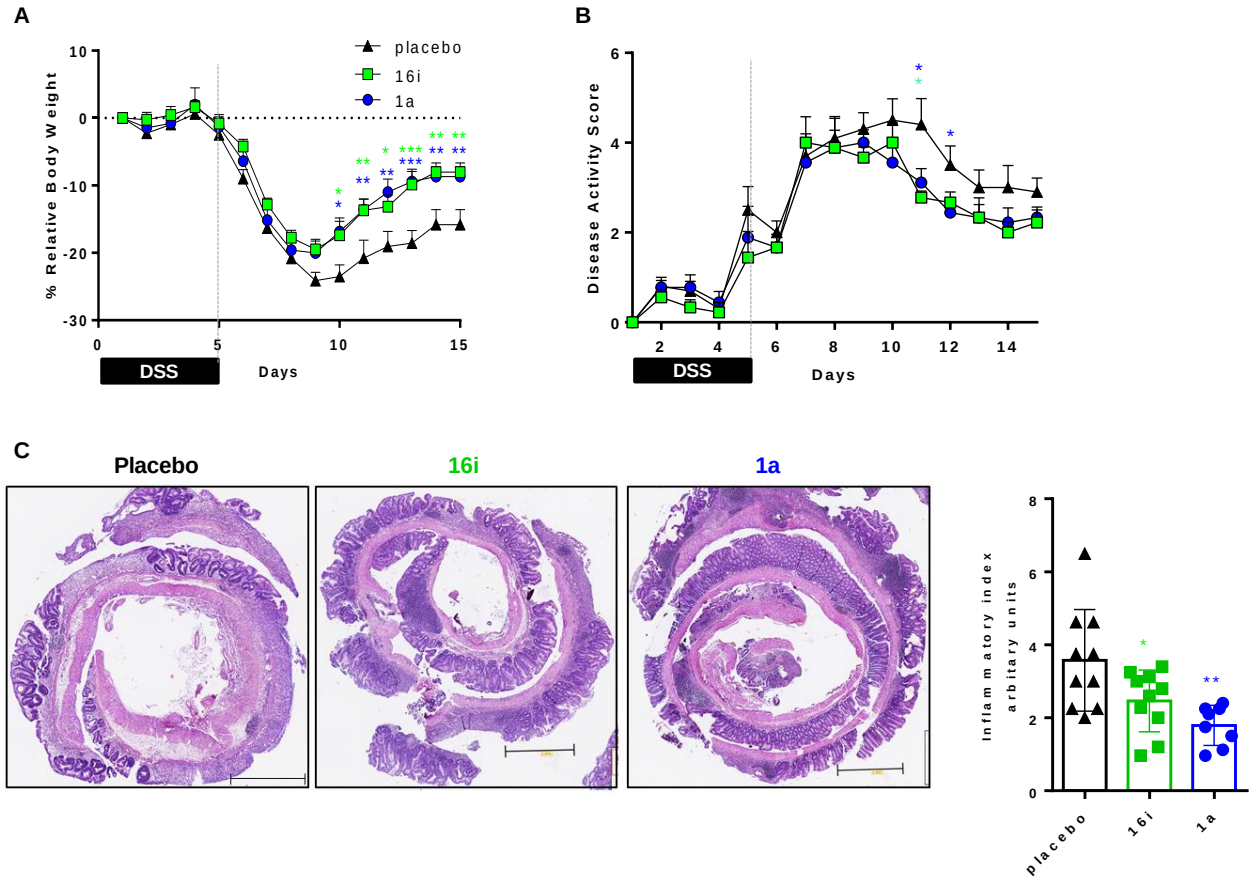

Figure 8. Compound **16i** ameliorates DSS-induced colitis. Analyses were performed from cohort of 10 WT mice treated with placebo, compound **16i** and **1a**. A. Body weight loss. B. Disease activity score. C. Tissue sections were stained with hematoxylin and eosin and analyzed microscopically (scale bar, 1 mm). Histologic scoring of colon tissue sections was calculated as indicated in Materials and Methods section. Data are presented as means ± SEM; *p<0.05, **p<0.01

CONCLUSION

Novel series of PGAm were designed following a ligand-based approach. They were synthesized using previously described methods and compared to references **1a** and **1b**. Improved properties were obtained regarding P2RX7 antagonism and decrease of IL1β and ROS production. New SAR have been proposed: 1) An hetero-aryl moiety in position 1 of the lactam was the best modulation for the antagonistic properties on P2RX7, but showed decreased metabolic stability compared to a methyl; 2) the amide substitution was limited to 2,4-dichlorobenzyle and 2-chloro-3-trifluoromethylbenzyle; 3) rigidification, such as modulation on position 3, of PGAm are deleterious to activity; 4) the lactam moiety can be replaced by an oxazolidinone, but resulted in diminished activity, and other analogues of the lactam, such as pyridine or piperidone had no antagonistic potential; 5) the amide can be transferred from position 5 to position 4 of the lactam ring, but slightly decreased the activity.

Ten hits were selected for further studies. They were effectively reducing IL1β and ROS production and were allosteric modulators of P2RX7 (binding site of A-804598). The ADME-Tox profile and selectivity for P2RX7 were encouraging for further development as low toxic drugs. Lastly, *in vivo* study in a rodent model of bowel inflammation showed a real potential of pyroglutamide P2RX7 antagonists to treat inflammation.

Finally, better understanding of P2RX7 antagonist interactions with P2RX7 have been provided, and PGAm have been shown as potential drug-candidates for inflammation-related diseases, such as IBD.

EXPERIMENTAL SECTION

Chemistry.

Starting materials were commercially available and were used without further purification. Melting points were measured on a MPA 100 OptiMelt® apparatus and are uncorrected. Nuclear magnetic resonance (NMR) spectra were acquired at 400 MHz for ^{1}H NMR, 100 MHz for ^{13}C NMR and 376 MHz for ^{19}F NMR on a Varian 400-MR spectrometer with tetramethylsilane (TMS) as internal standard, at room temperature. Chemical shifts (δ) are expressed in ppm relative to TMS. Splitting patterns are designed: s, singlet; d, doublet; dd, doublet of doublet; t, triplet; q, quadruplet; quint, quintuplet; m, multiplet; br s, broaden singlet; br t, broaden triplet. Coupling constants (J) are reported in Hertz (Hz). Thin layer chromatography (TLC) was realized on Macherey Nagel silica gel plates with fluorescent indicator and were visualized under a UV-lamp at 254 nm and 365 nm. Column chromatography was performed with a CombiFlash Rf Companion (Teledyne-Isco System) using RediSep packed columns. IR spectra were recorded on a Varian 640-IR FT-IR Spectrometer. Elemental analyses (C, H, N, S) of new compounds were determined on a Thermo Electron apparatus by 'Pôle Chimie Moléculaire-Welience', Faculté de Sciences Mirande, Université de Bourgogne, Dijon, France.

*(S)-N-[2-chloro-5-(trifluoromethyl)benzyl]-1-methyl-5-oxopyrrolidine-2-carboxamide (**1c**)*. A mixture of **7** (1.00 g, 6.4 mmol), 2-chloro-5-(trifluoromethyl)benzylamine (1.33 g, 6.4 mmol), and PTSA (0.05 g, 0.3 mmol) was stirred under a nitrogen atmosphere at 110°C for 24 hours. It was purified on a silica column (silica gel, CH_2Cl_2:MeOH = 95:5) to give **1c** (0.32 g, 15.6% yield) as a

white solid. mp 139-141°C (CH_2Cl_2); Rf (CH_2Cl_2:MeOH = 95:5) = 0.4; ^{1}H NMR ($CDCl_3$, 400 MHz) δ ppm 2.00-2.11 (m, 1H, CH_2CH_2CH), 2.21-2.32 (m, 1H, CH_2CH_2CH), 2.34-2.52 (m, 2H, CH_2CH_2CH), 2.80 (s, 3H, NCH_3), 4.04 (dd, *J* = 9.3, 3.9 Hz, 1H, CH_2CH_2CH), 4.59 (dd, *J* = 15.5, 6.1 Hz, 1H, $NHCH_2$), 4.64 (dd, *J* = 15.5, 6.1 Hz, 1H, $NHCH_2$), 7.28 (br t, *J* = 6.6 Hz, 1H, $NHCH_2$), 7.50 (s, 1H, ArH), 7.51 (s, 1H, ArH), 7.61 (s, 1H, ArH); ^{13}C NMR ($CDCl_3$, 100 MHz) δ ppm 23.4 (CH_2), 29.1 (CH_2), 29.4 (CH_3), 41.1 (CH_2), 64.0 (CH), 123.6 (q, *J* = 272.0 Hz, CF_3), 125.7 (q, *J* = 3.7 Hz, CH), 126.5 (q, *J* = 3.7 Hz, CH), 129.5 (q, *J* = 33.0 Hz, C), 130.2 (CH), 136.5 (C), 137.2 (C), 171.6 (C), 175.9 (C); ^{19}F NMR ($CDCl_3$, 376 MHz) δ (ppm) -62.7 (CF_3); IR ν (cm^{-1}): 3289, 1683, 1656, 1326, 1112, 1081, 845; Anal. Calcd for $C_{14}H_{14}ClF_3N_2O_2$: C, 50.24; H, 4.22; N, 8.37. Found: C, 50.02; H, 3.84; N 8.39%.

*(S)-N-(3,4-Dimethoxyphenyl)-5-oxopyrrolidine-2-carboxamide (**10g**)*. Amide **10g** was synthesized from **5** with $ZrCl_4$ as catalyst, following the procedure described for **1c**, and crystalized in CH_3CN. Yield 17.1%. Dark blue solid. mp 145-146°C (Et_2O); Rf (CH_2Cl_2:MeOH = 95:5) = 0.1; ^{1}H NMR ($CDCl_3$, 400 MHz) δ ppm 2.27-2.56 (m, 3H, CH_2CH_2CH), 2.60-2.72 (m, 1H, CH_2CH_2CH), 3.87 (s, 3H, OCH_3), 3.89 (s, 3H, OCH_3), 4.27-4.32 (m, 1H, CH_2CH_2CH), 6.08 (br s, 1H, NHCH), 6.82 (d, *J* = 8.6 Hz, 1H, ArH), 6.97 (dd, *J* = 2.3, 8.6 Hz, 1H, ArH), 7.33 (d, *J* = 2.3 Hz, 1H, ArH), 7.76 (br s, 1H, NHAr); ^{13}C NMR ($CDCl_3$, 100 MHz) δ ppm 26.3 (CH_2), 29.1 (CH_2), 56.0 (CH_3), 56.1 (CH_3), 57.4 (CH), 104.8 (CH), 111.3 (CH), 111.9 (CH), 130.4 (C), 146.4 (C), 149.1 (C), 169.7 (C), 179.1 (C); IR ν (cm^{-1}): 3358, 3244, 1669, 1513, 1237, 1131, 1020; Anal. Calcd for $C_{13}H_{16}N_2O_4$: C, 59.08; H, 6.10; N, 10.60. Found: C, 59.11; H, 6.13; N, 10.59%.

*(S)-N-(3-Fluoro-4-methoxyphenyl)-5-oxopyrrolidine-2-carboxamide (**10i**)*. Amide **10i** was synthesized from **5** following the procedure described for **1c**, and crystalized in CH_3CN. Yield 53.3%. White solid. mp 172-175°C (Et_2O); Rf (CH_2Cl_2:MeOH = 95:5) = 0.1; ^{1}H NMR ($CDCl_3$, 400

MHz) δ ppm 2.25-2.55 (m, 3H, C*H*$_2$C*H*$_2$CH), 2.60-2.71 (m, 1H, CH$_2$C*H*$_2$CH), 3.88 (s, 3H, OC*H*$_3$), 4.27-4.32 (m, 1H, CH$_2$CH$_2$C*H*), 6.36 (br s, 1H, N*H*CH), 6.91 (t, *J* = 9.0 Hz, 1H, Ar*H*), 7.19 (m, 1H, Ar*H*), 7.50 (dd, *J* = 12.6, 2.4 Hz, 1H, Ar*H*), 7.96 (br s, 1H, N*H*Ar); ^{13}C NMR (DMSO-*d*$_6$, 100 MHz) δ ppm 25.2 (CH$_2$), 29.1 (CH$_2$), 56.0 (CH), 56.3 (CH$_3$), 107.7 (d, *J* = 22.4 Hz, CH), 113.9 (d, *J* = 2.6 Hz, CH), 115.2 (d, *J* = 3.4 Hz, CH), 132.1 (d, *J* = 9.2 Hz, C), 143.0 (d, *J* = 11.1 Hz, C), 150.7 (d, *J* = 241.8 Hz, C), 171.0 (C), 177.3 (C); ^{19}F NMR (CDCl$_3$, 376 MHz) δ (ppm) -132.6 (ArF); IR ν (cm^{-1}): 3301, 3084, 2937, 1683, 1656, 1514, 1226, 1122, 1025; Anal. Calcd for $C_{12}H_{13}FN_2O_3$: C, 57.14; H, 5.19; N, 11.11. Found: C, 57.14; H, 5.18; N, 11.07%.

*(S)-N-(2-Chloro-3-(trifluoromethyl)benzyl)-5-oxopyrrolidine-2-carboxamide (**11g**)*. Amide **11g** was synthesized from **5** following the procedure described for **1c**, and crystalized in CH$_3$CN. Yield 62.4%. Yellow solid. mp 143-145°C (Et$_2$O); Rf (CH$_2$Cl$_2$:MeOH = 95:5) = 0.2; ^{1}H NMR (CDCl$_3$, 400 MHz) δ ppm 2.12-2.22 (m, 1H, CH$_2$C*H*$_2$CH), 2.26-2.41 (m, 2H, C*H*$_2$CH$_2$CH), 2.49-2.60 (m, 1H, CH$_2$C*H*$_2$CH), 4.19 (dd, *J* = 4.8, 9.1 Hz, 1H, CH$_2$CH$_2$C*H*), 4.57 (dd, *J* = 6.0, 14.6 Hz, 1H, NHC*H*$_2$), 4.63 (dd, *J* = 6.0, 14.6 Hz, 1H, NHC*H*$_2$), 6.65 (br s, 1H, N*H*CH$_2$), 6.81 (br t, *J* = 5.7 Hz, 1H, N*H*CH), 7.36 (t, *J* = 8.1 Hz, 1H, Ar*H*), 7.57 (d, *J* = 7.7 Hz, 1H, Ar*H*), 7.66 (d, *J* = 7.7 Hz, 1H, Ar*H*); ^{13}C NMR (CDCl$_3$, 100 MHz) δ ppm 26.0 (CH$_2$), 29.1 (CH$_2$), 41.6 (CH$_2$), 56.9 (CH), 125.5 (q, *J* = 273.5 Hz, CF$_3$), 126.9 (CH), 127.2 (q, *J* = 5.6 Hz, CH), 129.2 (q, *J* = 30.8 Hz, C), 131.7 (C), 133.7 (CH), 137.6 (C), 172.1 (C), 179.2 (C); ^{19}F NMR (CDCl$_3$, 376 MHz) δ (ppm) -62.5 (CF$_3$); IR ν (cm^{-1}): 3237, 2956, 1736, 1685, 1437, 1204, 1153, 1041; Anal. Calcd for $C_{13}H_{12}ClF_3N_2O_2$: C, 48.69; H, 3.77; N, 8.74. Found: C, 48.55; H, 3.74; N, 8.70%.

*(S)-N-(2-Chloro-5-(trifluoromethyl)benzyl)-5-oxopyrrolidine-2-carboxamide (**11h**)*. Amide **11h** was synthesized from **5** following the procedure described for **1c**, and crystalized in CH$_3$CN. Yield 45.5%. White solid. mp 157-158°C (Et$_2$O); Rf (CH$_2$Cl$_2$:MeOH = 95:5) = 0.3; ^{1}H NMR (CDCl$_3$, 400

MHz) δ ppm 2.14-2.24 (m, 1H, CH_2CH_2CH), 2.28-2.45 (m, 2H, CH_2CH_2CH), 2.53-2.64 (m, 1H, CH_2CH_2CH), 4.21 (dd, *J* = 5.0, 9.1 Hz, 1H, CH_2CH_2CH), 4.59 (d, *J* = 5.9 Hz, 2H, $NHCH_2$), 6.08 (br s, 1H, NHCH), 6.61 (br s, 1H, $NHCH_2$), 7.51-7.52 (m, 2H, ArH), 7.61 (s, 1H, ArH); ^{13}C NMR ($CDCl_3$, 100 MHz) δ ppm 26.0 (CH_2), 29.1 (CH_2), 41.2 (CH_2), 57.0 (CH), 125.9 (q, *J* = 3.9 Hz, CH), 126.3 (q, *J* = 272.0 Hz, CF_3), 126.7 (q, *J* = 3.8 Hz, CH), 129.6 (q, J = 33.1 Hz, C), 130.2 (CH), 136.2 (C), 137.3 (C), 172.2 (C), 179.4 (C); ^{19}F NMR ($CDCl_3$, 376 MHz) δ (ppm) -62.6 (CF_3); IR ν (cm^{-1}): 3279, 1690, 1665, 1551, 1326, 1264, 1170, 1112, 1083, 824; Anal. Calcd for $C_{13}H_{12}ClF_3N_2O_2$: C, 48.69; H, 3.77; N, 8.74. Found: C, 48.44; H, 3.61; N, 8.78%.

*(S)-N-(4-Methoxybenzyl)-5-oxopyrrolidine-2-carboxamide (**11i**)*. Amide **11i** was synthesized from **5** with PTSA as catalyst, following the procedure described for **1c**, and purified on a silica column (silica gel, CH_2Cl_2:MeOH = 95:5). Yield 42.1%. White solid. mp 122-123°C (Et_2O); Rf (CH_2Cl_2:MeOH = 95:5) = 0.1; ^{1}H NMR ($CDCl_3$, 400 MHz) δ ppm 2.07-2.17 (m, 1H, CH_2CH_2CH), 2.19-2.30 (m, 2H, CH_2CH_2CH), 2.38-2.49 (m, 1H, CH_2CH_2CH), 3.77 (s, 3H, OCH_3), 4.11 (dd, *J* = 4.5, 9.1 Hz, 1H, CH_2CH_2CH), 4.30 (dd, *J* = 14.5, 5.8 Hz, 1H, $NHCH_2$), 4.36 (dd, *J* = 14.5, 5.8 Hz, 1H, $NHCH_2$), 6.80-6.85 (m, 2H, ArH), 6.96 (br t, *J* = 6.1 Hz, 1H, $NHCH_2$), 7.14-7.19 (m, 3H, NHCH and ArH); ^{13}C NMR ($CDCl_3$, 100 MHz) δ ppm 25.8 (CH_2), 29.3 (CH_2), 43.0 (CH_2), 55.3 (CH_3), 57.1 (CH), 114.1 (2CH), 129.2 (2CH), 130.0 (C), 159.1 (C), 172.0 (C), 179.5 (C); IR ν (cm^{-1}): 3401, 3241, 1651, 1513, 1245; Anal. Calcd for $C_{13}H_{16}N_2O_3$: C, 62.89; H, 6.50; N, 11.28. Found: C, 62.91; H, 6.53; N, 11.27%.

*(S)-5-Oxo-N-(3,4,5-trimethoxybenzyl)pyrrolidine-2-carboxamide (**11j**)*. Amide **11j** was synthesized from **5** with PTSA as catalyst, following the procedure described for **1c**, and purified on a silica column (silica gel, CH_2Cl_2:MeOH = 95:5). Yield 58.6%. White solid. mp 181-183°C (Et_2O); Rf (CH_2Cl_2:MeOH = 95:5) = 0.1; ^{1}H NMR ($CDCl_3$, 400 MHz) δ ppm 2.14-2.24 (m, 1H,

CH_2CH_2CH), 2.25-2.41 (m, 2H, CH_2CH_2CH), 2.48-2.58 (m, 1H, CH_2CH_2CH), 3.82 (s, 3H, OCH_3), 3.83 (s, 6H, OCH_3), 4.18 (dd, *J* = 9.0, 4.9 Hz, 1H, CH_2CH_2CH), 4.30 (dd, *J* = 14.5, 5.6 Hz, 1H, $NHCH_2$), 4.41 (dd, *J* = 14.5, 5.6 Hz, 1H, $NHCH_2$), 6.48 (s, 2H, Ar*H*), 6.70 (br t, *J* = 5.7 Hz, 1H, $NHCH_2$), 6.77 (br s, 1H, N*H*CH); ^{13}C NMR ($CDCl_3$, 100 MHz) δ ppm 26.0 (CH_2), 29.2 (CH_2), 43.9 (CH_2), 56.2 ($2CH_3$), 57.0 (CH), 60.9 (CH_3), 105.1 (2CH), 133.4 (C), 137.5 (C), 153.4 (2C), 171.8 (C), 179.1 (C); IR ν (cm^{-1}): 3350, 3290, 1695, 1650, 1131; Anal. Calcd for $C_{15}H_{20}N_2O_5$: C, 58.43; H, 6.54; N, 9.09. Found: C, 58.40; H, 6.56; N, 9.07%.

(S)-N-(2,4-dichlorophenyl)-5-oxo-1-phenylpyrrolidine-2-carboxamide ***(14)***. Amide **14** was synthesized from **8a** with PTSA as catalyst and toluene as solvent, following the procedure described for **1c**, and crystalized in CH_3CN. Yield 7.9%. Dark-blue solid. mp 175-184°C (CH_3CN); Rf (CH_2Cl_2:MeOH = 95:5) = 0.8; ^{1}H NMR ($CDCl_3$, 400 MHz) δ ppm 2.28-2.38 (m, 1H, CH_2CH_2CH), 2.59-2.72 (m, 2H, CH_2CH_2CH), 2.73-2.88 (m, 1H, CH_2CH_2CH), 4.83-4.89 (m, 1H, CH_2CH_2CH), 7.18 (t, *J* = 1.3 Hz, 2H, Ar*H*), 7.21 (dd, *J* = 2.0, 9.0 Hz, 1H, Ar*H*), 7.39 (tt, *J* = 2.4, 7.4 Hz, 2H, Ar*H*), 7.53-7.59 (m, 2H, Ar*H*), 7.97 (br s, 1H, N*H*), 8.19 (d, *J* = 9.1 Hz, 1H, Ar*H*); ^{13}C NMR ($CDCl_3$ 100 MHz) δ ppm 23.9 (CH_2), 30.9 (CH_2), 63.5 (CH), 121.4 (2CH), 122.6 (CH), 124.1 (C), 126.1 (CH), 127.9 (CH), 128.8 (CH), 129.4 (2CH), 130.1 (C), 132.2 (C), 137.4 (C), 169.4 (C), 174.5 (C); IR ν (cm^{-1}): 3238, 1702, 1671, 1581, 1524, 1499; Anal. Calcd for $C_{17}H_{14}Cl_2N_2O_2$: C, 58.47; H, 4.04; N, 8.02. Found: C, 58.49; H, 4.06; N 8.22%.

(S)-N-(2,4-dichlorobenzyl)-5-oxo-1-(2,4-dichlorophenyl)pyrrolidine-2-carboxamide ***(16c)***. Amide **16c** was synthesized from **8c** with PTSA as catalyst and CH_3CN as solvent, following the procedure described for **1c**, and crystalized in CH_3CN. Yield 34.1%. Yellow solid. mp 123-155°C (CH_3CN); Rf (CH_2Cl_2:MeOH = 95:5) = 0.8; ^{1}H NMR ($CDCl_3$, 400 MHz) δ ppm 2.20-2.31 (m, 1H, CH_2CH_2CH), 2.44-2.58 (m, 2H, CH_2CH_2CH), 2.67-2.79 (m, 1H, CH_2CH_2CH), 4.30-4.45 (m, 2H,

NHC*H*$_2$), 4.53 (dd, *J* = 4.7, 8.3 Hz, 1H, CH_2CH_2CH), 6.23 (t, *J* = 5.5 Hz, 1H, Ar*H*), 7.03 (d, *J* = 8.2 Hz, 1H, Ar*H*), 7.13 (dd, *J* = 8.2, 2.0 Hz, 2H, Ar*H*), 7.18 (d, *J* = 2.0 Hz, 1H, Ar*H*), 7.34 (m, 1H, Ar*H*), 7.42 (m, 1H, Ar*H*); ^{13}C NMR ($CDCl_3$, 100 MHz) δ ppm 23.8 (CH_2), 29.7 (CH_2), 41.1 (CH_2), 63.0 (CH), 127.3 (CH), 128.2 (CH), 129.4 (CH), 130.1 (CH), 131.1 (C), 131.1 (CH), 132.6 (C), 133.2 (C), 133.3 (CH), 134.2 (C), 134.5 (C), 134.7 (C), 170.2 (C), 175.1 (C); IR ν (cm^{-1}): 3290, 3073, 2937, 1674, 1549, 1479, 1384, 1227, 1101, 1049, 813; Anal. Calcd for $C_{18}H_{14}Cl_4N_2O_2$: C, 50.03; H, 3.27; N, 6.48. Found: C, 49.60; H, 3.20; N, 6.42%.

*(S)-N-(2,4-dichlorobenzyl)-5-oxo-1-(4-chlorophenyl) pyrrolidine-2-carboxamide (**16f**)*. Amide **16f** was synthesized from **8f** with CH_3SO_3H as catalyst and CH_3CN as solvent, following the procedure described for **1c**, and crystalized in CH_3CN. Yield 38.7%. White solid. mp 165-168°C (CH_3CN); Rf (CH_2Cl_2:MeOH = 97:3) = 0.4; ^{1}H NMR ($CDCl_3$, 400 MHz) δ ppm 2.13-2.24 (m, 1H, CH_2CH_2CH), 2.47-2.61 (m, 2H, CH_2CH_2CH), 2.64-2.75 (m, 1H, CH_2CH_2CH), 4.34 (dd, *J* = 15.2, 5.6 Hz, 1H, NHC*H*$_2$), 4.46 (dd, *J* = 15.2, 5.6 Hz, 1H, NHC*H*$_2$), 4.61 (dd, *J* = 8.8, 4.4 Hz, 1H, CH_2CH_2CH), 6.35 (t, *J* = 5.6 Hz, 1H, $NHCH_2$), 6.97 (d, *J* = 8.0 Hz, 1H, Ar*H*), 7.12 (dd, *J* = 8.0, 2.4 Hz, 1H, Ar*H*), 7.23 (d, *J* = 9.2 Hz, 2H, Ar*H*), 7.31 (d, *J* = 2.4 Hz, 1H, Ar*H*), 7.35 (d, *J* = 9.2 Hz, 2H, Ar*H*); ^{13}C NMR ($CDCl_3$, 100 MHz) δ ppm 23.5 (CH_2), 31.0 (CH_2), 41.0 (CH_2), 63.1 (CH), 122.3 (2CH), 127.3 (CH), 129.2 (2CH), 129.4 (CH), 130.9 (CH), 131.0 (C), 133.3 (C), 134.0 (C), 134.4 (C), 136.2 (C), 170.8 (C), 174.5 (C); LC-MS (APCI$^+$) m/z: 397.0 (MH^+), tr 3.77 min; IR ν (cm^{-1}): 3278, 2923, 1698, 1661, 1557, 1493, 1354, 1229, 1098, 1053, 1011, 822; Anal. Calcd for $C_{18}H_{15}Cl_3N_2O_2$: C, 54.36; H, 3.80; N, 6.68. Found: C, 54.60; H, 4.08; N, 6.36%.

*(S)-N-(2,4-dichlorobenzyl)-5-oxo-1-(4-cyanophenyl)pyrrolidine-2-carboxamide (**16g**)*. Amide **16g** was synthesized from **8g** with CH_3SO_3H as catalyst and CH_3CN as solvent, following the procedure described for **1c**, and crystalized in CH_3CN. Yield 15.6%. White solid. mp 184-190°C

(CH_3CN); Rf (CH_2Cl_2:MeOH = 97:3) = 0.5; ^{1}H NMR ($CDCl_3$, 400 MHz) δ ppm 2.13-2.22 (m, 1H, CH_2CH_2CH), 2.45-2.64 (m, 2H, CH_2CH_2CH), 2.67-2.82 (m, 1H, CH_2CH_2CH), 4.37 (dd, *J* = 6.2, 14.9 Hz, 1H, $NHCH_2$), 4.45 (dd, *J* = 6.2, 14.9 Hz, 1H, $NHCH_2$), 4.62-4.68 (m, 1H, CH_2CH_2CH), 6.32 (br t, *J* = 6.3 Hz, 1H, $NHCH_2$), 7.15 (d, *J* = 8.4 Hz, 1H, Ar*H*), 7.16 (dd, *J* = 8.4, 2.0 Hz, 1H, Ar*H*), 7.33 (d, *J* = 2.0 Hz, 1H, Ar*H*), 7.56 (d, *J* = 9.0 Hz, 2H, Ar*H*), 7.59 (d, *J* = 9.0 Hz, 2H, Ar*H*); ^{13}C NMR ($CDCl_3$, 100 MHz) δ ppm 23.5 (CH_2), 31.1 (CH_2), 41.3 (CH_2), 62.5 (CH), 108.3 (CN), 118.3 (C), 120.2 (2CH), 127.4 (CH), 129.4 (CH), 131.4 (CH), 133.1 (C), 133.1 (2CH), 134.2 (C), 134.7 (C), 141.8 (C), 170.3 (C), 174.8 (C); LC-MS (APCI$^+$) m/z: 388.1 (MH^+), tr 3.50 min; IR ν (cm^{-1}): 3280, 2922, 2851, 1702, 1660, 1558, 1494, 1352, 1221, 821; Anal. Calcd for $C_{19}H_{15}Cl_2N_3O_2$: C, 58.78; H, 3.89; N, 10.82. Found: C, 59.06; H, 4.08; N, 10.66%.

*(S)-N-(2,4-dichlorobenzyl)-5-oxo-1-(4-methoxyphenyl)pyrrolidine-2-carboxamide (**16h**)*. Amide **16h** was synthesized from **8h** with PTSA as catalyst and CH_3CN as solvent, following the procedure described for **1c**, and crystalized in CH_3CN. Yield 19.9%. White solid. mp 153-158°C (CH_3CN); Rf (CH_2Cl_2:MeOH = 98:2) = 0.4; ^{1}H NMR ($CDCl_3$, 400 MHz) δ ppm 2.12-2.22 (m, 1H, CH_2CH_2CH), 2.43-2.58 (m, 2H, CH_2CH_2CH), 2.62-2.74 (m, 1H, CH_2CH_2CH), 3.79 (s, 3H, OCH_3), 4.31 (dd, *J* = 14.7, 5.7 Hz, 1H, $NHCH_2$), 4.43 (dd, *J* = 14.7, 5.7 Hz, 1H, $NHCH_2$), 4.56-4.61 (m, 1H, CH_2CH_2CH), 6.52 (br t, *J* = 5.7 Hz, 1H, Ar*H*), 6.77 (d, *J* = 6.6 Hz, 2H, Ar*H*), 6.85 (d, *J* = 8.2 Hz, 1H, Ar*H*), 7.04 (dd, *J* = 8.2, 2.0 Hz, 1H, Ar*H*), 7.27 (d, *J* = 2.0 Hz, 1H, Ar*H*), 7.29 (d, *J* = 6.6 Hz, 2H, Ar*H*); ^{13}C NMR ($CDCl_3$, 100 MHz) δ ppm 23.5 (CH_2), 30.9 (CH_2), 40.8 (CH_2), 55.4 (CH_3), 63.7 (CH), 114.3 (2CH), 123.4 (2CH), 127.1 (CH), 129.2 (CH), 130.5 (CH), 130.5 (C), 133.5 (2C), 134.0 (C), 157.5 (C), 171.3 (C), 174.6 (C); IR ν (cm^{-1}): 3270, 2924, 1696, 1647, 1514, 1249, 1228, 1027, 824; Anal. Calcd for $C_{19}H_{18}Cl_2N_2O_3$: C, 58.03; H, 4.61; N, 7.12. Found: C, 58.26; H, 4.62; N, 6.88%.

*(S)-N-(2,4-dichlorobenzyl)-5-oxo-1-(thiophen-3-yl)pyrrolidine-2-carboxamide (**16j**)*. A stirred mixture of **11e** (5.00 g, 17 mmol), 3-iodothiophene (3.66 g, 17 mmol), cuprous iodide (CuI) (1.66 g, 8 mmol), cesium carbonate (11.33 g, 34 mmol), and *N*,*N*'-dimethylethylene-1,2-diamine (1.53 g, 17 mmol) in dioxane was heated at reflux for 5 hours under a nitrogen atmosphere. The resulting solution was filtered, then the solvent was evaporated and the resulting crude was solved in CH_2Cl_2. It was washed two times with water and dried with $MgSO_4$. The organic phase is evaporated, resulting in a brown solid. The solid was purified on a silica column (silica gel, EtOAc:*n*-Heptane = 7:3) to give **16j** (0.73 g, 11.6% yield) as a pink solid. mp 156-159°C (Et_2O); Rf (CH_2Cl_2:MeOH = 95:5) = 0.6; ^{1}H NMR ($CDCl_3$, 400 MHz) δ ppm 2.18-2.27 (m, 1H, CH_2CH_2CH), 2.50-2.72 (m, 3H, CH_2CH_2CH), 4.34 (dd, *J* = 14.9, 5.5 Hz, 1H, $NHCH_2$), 4.51 (dd, *J* = 14.9, 6.8 Hz, 1H, $NHCH_2$), 4.60 (m, 1H, CH_2CH_2CH), 6.29 (br t, *J* = 6.7 Hz, 1H, $NHCH_2$), 7.02 (d, *J* = 8.1 Hz, 1H, Ar*H*), 7.13 (dd, *J* = 8.2, 2.0 Hz, 1H, Ar*H*), 7.24 (dd, *J* = 3.9, 1.2 Hz, 1H, Ar*H*), 7.26 (dd, *J* = 2.7, 2.0 Hz, 1H, Ar*H*), 7.29-7.31 (m, 2H, Ar*H*); ^{13}C NMR ($CDCl_3$, 100 MHz) δ ppm 23.7 (CH_2), 30.5 (CH_2), 41.1 (CH_2), 63.4 (CH), 110.9 (CH), 120.2 (C), 125.6 (CH), 127.3 (CH), 129.4 (CH), 130.7 (CH), 133.3 (CH), 134.1 (C), 134.3 (C), 136.1 (C), 171.2 (C), 173.5 (C); IR ν (cm^{-1}): 3278, 1687, 1647, 1537, 1455; Anal. Calcd for $C_{16}H_{14}Cl_2N_2O_2S$: C, 52.04; H, 3.82; N, 7.59; S, 8.68. Found: C, 51.31; H, 4.10; N, 7.70; S, 7.18%.

*(S)-N-(2,4-dichlorobenzyl)-1-(furan-2-yl)-5-oxopyrrolidine-2-carboxamide (**16k**)*. Amide **16k** was synthesized from **11e** following the procedure described for **16j**. Yield 58.6%. White solid. mp 189-191°C (Et_2O); Rf (CH_2Cl_2:MeOH = 95:5) = 0.4; ^{1}H NMR ($CDCl_3$, 400 MHz) δ ppm 2.22-2.35 (m, 1H, CH_2CH_2CH), 2.45-2.58 (m, 2H, CH_2CH_2CH), 2.62-2.75 (m, 1H, CH_2CH_2CH), 4.43 (dd, *J* = 15.4, 6.1 Hz, 1H, $NHCH_2$), 4.51 (dd, *J* = 15.4, 6.1 Hz, 1H, $NHCH_2$), 4.66 (dd, *J* = 9.3, 3.5 Hz, 1H, CH_2CH_2CH), 6.31 (br t, *J* = 6.0 Hz, 1H, $NHCH_2$), 6.39 (dd, *J* = 3.6, 1.6 Hz, 1H, Ar*H*), 6.41

(dd, *J* = 3.6, 1.2 Hz, 1H, Ar*H*), 7.03 (dd, *J* = 2.0, 1.2 Hz, 1H, Ar*H*), 7.13 (d, *J* = 8.2 Hz, 1H, Ar*H*), 7.15 (dd, *J* = 8.2, 1.9 Hz, 1H, Ar*H*), 7.36 (d, *J* = 1.9 Hz, 1H, Ar*H*); ^{13}C NMR ($CDCl_3$, 100 MHz) δ ppm 23.8 (CH_2), 30.0 (CH_2), 41.1 (CH_2), 61.3 (CH), 96.8 (CH), 111.8 (CH), 127.4 (CH), 129.4 (CH), 130.7 (CH), 133.5 (C), 134.1 (C), 134.2 (C), 136.5 (CH), 144.8 (C), 170.9 (C), 172.7 (C); IR ν (cm^{-1}): 3285, 1698, 1646, 1542, 1412, 710; Anal. Calcd for $C_{16}H_{14}Cl_2N_2O_3$: C, 54.41; H, 4.00; N, 7.93. Found: C, 54.06; H, 3.95; N, 7.95%.

*(S)-N-(2,4-dichlorobenzyl)-1-(furan-3-yl)-5-oxopyrrolidine-2-carboxamide (**16l**)*. Amide **16l** was synthesized from **11e** following the procedure described for **16j** and purified on a silica column (silica gel, EtOAc:*n*-Heptane = 8:2). Yield 44.5%. White solid. mp 174-178°C (Et_2O); Rf (CH_2Cl_2:MeOH = 95:5) = 0.5; ^{1}H NMR ($CDCl_3$, 400 MHz) δ ppm 2.20-2.31 (m, 1H, CH_2CH_2CH), 2.49-2.69 (m, 3H, CH_2CH_2CH), 4.38-4.45 (m, 2H, NHCH_2 and CH_2CH_2C*H*), 4.48 (dd, *J* = 14.8, 6.7 Hz, 1H, NHCH_2), 6.25 (br t, *J* = 6.3 Hz, 1H, N*H*CH_2), 6.43 (dd, *J* = 2.0, 0.8 Hz, 1H, Ar*H*), 7.14-7.21 (m, 2H, Ar*H*), 7.31 (t, *J* = 2.0 Hz, 1H, Ar*H*), 7.33 (t, *J* = 1.2 Hz, 1H, Ar*H*), 7.89 (q, *J* = 0.8 Hz, 1H, Ar*H*); ^{13}C NMR ($CDCl_3$, 100 MHz) δ ppm 24.2 (CH_2), 29.9 (CH_2), 41.2 (CH_2), 62.4 (CH), 103.6 (CH), 125.0 (C), 127.3 (CH), 129.4 (CH), 131.1 (CH), 132.1 (CH), 133.3 (C), 134.3 (C), 134.4 (C), 142.3 (CH), 171.0 (C), 173.4 (C); IR ν (cm^{-1}): 3278, 1689, 1645, 1542, 1229, 868, 770; Anal. Calcd for $C_{16}H_{14}Cl_2N_2O_3$: C, 54.41; H, 4.00; N, 7.93. Found: C, 54.04; H, 3.87; N, 7.94%.

*(S)-N-(2,4-dichlorobenzyl)-5-oxo-1-(1,3-thiazol-2-yl)pyrrolidine-2-carboxamide (**16m**)*. Amide **16m** was synthesized from **11e** following the procedure described for **16j** and purified on a silica column (silica gel, EtOAc:*n*-Heptane = 6:4). Yield 15.3%. White solid. mp 200-209°C (Et_2O); Rf (CH_2Cl_2:MeOH = 95:5) = 0.8; ^{1}H NMR ($CDCl_3$, 400 MHz) δ ppm 2.27-2.40 (m, 1H, CH_2CH_2CH), 2.55-2.67 (m, 2H, CH_2CH_2CH), 2.90-3.02 (m, 1H, CH_2CH_2CH), 4.46 (s, 1H, NHCH_2), 4.48 (s, 1H, NHCH_2), 5.03 (dd, *J* = 9.0, 1.6 Hz, 1H, CH_2CH_2C*H*), 7.02 (d, *J* = 3.5 Hz, 1H, Ar*H*), 7.14 (dd, *J* =

8.2, 2.0 Hz, 1H, Ar*H*), 7.21 (d, *J* = 8.1 Hz, 1H, Ar*H*), 7.33 (d, *J* = 2.1 Hz, 1H, Ar*H*), 7.37 (d, *J* = 3.5 Hz, 1H, Ar*H*), 7.48 (br s, 1H, N*H*CH_2); ^{13}C NMR ($CDCl_3$, 100 MHz) δ ppm 22.6 (CH_2), 30.9 (CH_2), 41.2 (CH_2), 61.3 (CH), 114.4 (CH), 127.3 (CH), 129.3 (CH), 130.7 (CH), 133.8 (C), 134.0 (C), 136.8 (CH), 150.7 (C), 157.9 (C), 169.5 (C), 173.6 (C); IR ν (cm^{-1}): 3281, 1696, 1645, 1542, 1508, 1467, 1330, 1237, 1172, 823, 703, 620; Anal. Calcd for $C_{15}H_{13}Cl_2N_3O_2S$: C, 48.66; H, 3.54; N, 11.35; S, 8.66. Found: C, 48.38; H, 3.73; N, 11.54; S, 7.65%.

*(S)-N-(2,4-dichlorobenzyl)-5-oxo-1-(1,3-thiazol-4-yl)pyrrolidine-2-carboxamide (**16n**)*. Amide **16n** was synthesized from **11e** following the procedure described for **16j**. Yield 38.1%. White solid. mp 227-228°C (Et_2O); Rf (CH_2Cl_2:MeOH = 96:4) = 0.5; ^{1}H NMR ($CDCl_3$, 400 MHz) δ ppm 2.37-2.45 (m, 2H, C*H*$_2$C*H*$_2$CH), 2.51-2.61 (m, 1H, C*H*$_2$CH$_2$CH), 2.82-2.93 (m, 1H, CH$_2$C*H*$_2$CH), 4.43 (dd, *J* = 15.3, 6.4 Hz, 1H, NHC*H*$_2$), 4.48 (dd, *J* = 15.0, 6.4 Hz, 1H, NHC*H*$_2$), 4.99 (dd, *J* = 6.1, 4.6 Hz, 1H, CH$_2$CH$_2$C*H*), 6.73 (br s, 1H, N*H*CH_2), 7.15 (dd, *J* = 8.4, 2.0 Hz, 1H, Ar*H*), 7.20 (d, *J* = 8.4 Hz, 1H, Ar*H*), 7.33 (d, *J* = 2.0 Hz, 1H, Ar*H*), 7.90 (d, *J* = 2.0 Hz, 1H, Ar*H*), 8.51 (d, *J* = 2.4 Hz, 1H, Ar*H*); ^{13}C NMR ($CDCl_3$, 100 MHz) δ ppm 23.1 (CH_2), 31.1 (CH_2), 41.1 (CH_2), 61.8 (CH), 102.9 (CH), 127.3 (CH), 129.2 (CH), 130.9 (CH), 133.8 (C), 134.0 (C), 134.1 (C), 148.1 (C), 149.9 (CH), 171.2 (C), 173.9 (C); IR ν (cm^{-1}): 3143, 3083, 2363, 1726, 1698, 1520, 1351, 1193, 858, 822, 725; Anal. Calcd for $C_{15}H_{13}Cl_2N_3O_2S$: C, 48.66; H, 3.54; N, 11.35; S, 8.66. Found: C, 48.40; H, 3.73; N, 11.35; S, 7.59%.

*(S)-N-(2,4-dichlorobenzyl)-5-oxo-1-(1,3-thiazol-5-yl)pyrrolidine-2-carboxamide (**16o**)*. Amide **16o** was synthesized from **11e** following the procedure described for **16j** and purified on a silica column (silica gel, EtOAc:*n*-Heptane = 1:1). Yield 15.1%. White solid. mp 183-185°C (Et_2O); Rf (CH_2Cl_2:MeOH = 95:5) = 0.5; ^{1}H NMR ($CDCl_3$, 400 MHz) δ ppm 2.25-2.34 (m, 1H, CH$_2$C*H*$_2$CH), 2.52-2.64 (m, 2H, C*H*$_2$CH$_2$CH), 2.68-2.82 (m, 1H, CH$_2$C*H*$_2$CH), 4.44 (dd, *J* = 14.9, 5.8 Hz, 1H,

NHC*H*$_2$), 4.46 (dd, *J* = 14.9, 6.3 Hz, 1H, NHC*H*$_2$), 4.58 (m, 1H, CH_2CH_2CH), 6.40 (br t, *J* = 5.5 Hz, 1H, N*H*CH_2), 7.18 (s, 1H, Ar*H*), 7.19 (s, 1H, Ar*H*), 7.34 (s, 1H, Ar*H*), 7.35 (s, 1H, Ar*H*), 8.47 (s, 1H, Ar*H*); ^{13}C NMR ($CDCl_3$, 100 MHz) δ ppm 24.2 (CH_2), 29.4 (CH_2), 41.4 (CH_2), 62.9 (CH), 127.5 (CH), 128.2 (C), 129.6 (CH), 131.3 (CH), 133.1 (CH), 134.2 (C), 134.6 (C), 147.5 (CH), 169.6 (C), 172.8 (C); IR ν (cm^{-1}): 3381, 3283, 2952, 2843, 1721, 1678, 1514, 1091, 1045, 833, 666; Anal. Calcd for $C_{15}H_{13}Cl_2N_3O_2S$: C, 48.66; H, 3.54; N, 11.35; S, 8.66. Found: Found: C, 48.49; H, 3.55; N, 11.30; S, 9.00%.

*(S)-N-(cyclohexylmethyl)-5-oxo-1-phenylpyrrolidine-2-carboxamide (**17**)*. Amide **17** was synthesized from **8a** with PTSA as catalyst and CH_3CN as solvent, following the procedure described for **1c**, and crystalized in CH_3CN. Yield 13.2%. Beige solid. mp 171-175°C (CH_3CN); R*f* (CH_2Cl_2:MeOH = 98:2) = 0.5; ^{1}H NMR ($CDCl_3$, 400 MHz) δ ppm 0.62-0.78 (m, 2H, cyclohex-*H*), 1.03-1.20 (m, 3H, cyclohex-*H*), 1.22-1.28 (m, 1H, cyclohex-*H*), 1.51-1.76 (m, 5H, cyclohex-*H*), 2.01-2.12 (m, 1H, CH_2CH_2CH), 2.17-2.24 (m, 2H, CH_2CH_2CH), 2.29-2.40 (m, 1H, CH_2CH_2CH), 2.44-2.53 (m, 1H, NHC*H*$_2$), 2.55-2.67 (m, 1H, NHC*H*$_2$), 4.42 (dd, *J* = 9.0, 2.7 Hz, 1H, CH_2CH_2CH), 7.00 (br s, 1H, N*H*CH_2), 7.09 (t, *J* = 7.4 Hz, 1H, Ar*H*), 7.28 (t, *J* = 7.4 Hz, 2H, Ar*H*), 7.57 (d, *J* = 7.4 Hz, 2H, Ar*H*); ^{13}C NMR ($CDCl_3$, 100 MHz) δ ppm 24.0 (CH_2), 25.3 (CH_2), 25.3 ($2CH_2$), 25.9 (CH_2), 30.1 ($2CH_2$), 35.9 (CH), 45.2 (CH_2), 64.0 (CH), 120.0 (2CH), 124.3 (CH), 128.8 (2CH), 139.3 (C), 175.1 (C), 177.8 (C); IR ν (cm^{-1}): 3277, 2920, 2848, 1694, 1660, 1558, 1494, 1380, 1222, 1040, 821; Anal. Calcd for $C_{18}H_{24}N_2O_2$: C, 71.97; H, 8.05; N, 9.33. Found: C, 72.26; H, 8.15; N, 9.18%.

*(S)-N-[2-chloro-3-(trifluoromethyl)benzyl]-5-oxo-1-(thiophen-2-yl)pyrrolidine-2-carboxamide (**19**)*. Amide **19** was synthesized from **11g** following the procedure described for **16j**. Yield 84.3%. Yellow solid. mp 160-161°C (Et_2O); Rf (CH_2Cl_2:MeOH = 95:5) = 0.7; ^{1}H NMR ($CDCl_3$, 400 MHz)

δ ppm 2.25-2.35 (m, 1H, CH_2CH_2CH), 2.56-2.82 (m, 3H, CH_2CH_2CH), 4.46 (dd, *J* = 15.3, 5.0 Hz, 1H, $NHCH_2$), 4.63 (m, 1H, CH_2CH_2CH), 4.64 (dd, *J* = 15.3, 6.7 Hz, 1H, $NHCH_2$), 6.40-6.48 (m, 2H, $NHCH_2$ and Ar*H*), 6.77 (dd, *J* = 7.9, 8.1 Hz, 1H, Ar*H)* 6.82 (dd, *J* = 5.4, 3.9 Hz, 1H, Ar*H*), 7.28 (dd, *J* = 5.4, 1.4 Hz, 1H, Ar*H*), 7.39 (d, *J* = 7.7 Hz, 1H, Ar*H*), 7.62 (d, *J* = 7.7 Hz, 1H, Ar*H*); ^{13}C NMR ($CDCl_3$, 100 MHz) δ ppm 23.9 (CH_2), 29.8 (CH_2), 41.7 (CH_2), 63.4 (CH), 112.2 (CH), 119.3 (CH), 124.0 (C), 125.4 (q, *J* = 272.0 Hz, CF_3), 126.8 (CH), 127.1 (q, *J* = 5.2 Hz, CH), 129.1 (q, *J* = 30.6 Hz, C), 133.4 (CH), 137.2 (C), 138.7 (C), 170.6 (C), 172.5 (C); ^{19}F NMR ($CDCl_3$, 376 MHz) δ ppm -62.5 (CF_3); IR ν (cm^{-1}): 3294, 1683, 1660, 1320, 1131, 1089, 801, 668.

*(S)-N-[2-chloro-5-(trifluoromethyl)benzyl]-5-oxo-1-(thiophen-2-yl)pyrrolidine-2-carboxamide **(20)***. It was synthesized from **11h** following the procedure described for **16j**. Yield 88.8%. Yellow solid. mp 210-213°C (Et_2O); Rf (CH_2Cl_2:MeOH = 95:5) = 0.7; ^{1}H NMR ($CDCl_3$, 400 MHz) δ ppm ppm 2.29-2.40 (m, 1H, CH_2CH_2CH), 2.53-2.82 (m, 3H, CH_2CH_2CH), 4.49 (dd, *J* = 15.8, 5.8 Hz, 1H, $NHCH_2$), 4.61-4.70 (m, 2H, CH_2CH_2CH and $NHCH_2$), 6.49 (d, *J* = 3.4 Hz, 1H, Ar*H*), 6.68 (br t, *J* = 5.8 Hz, 1H, $NHCH_2$), 6.80 (dd, *J* = 5.4, 3.8 Hz, 1H, Ar*H*), 6.86 (dd, *J* = 5.4, 0.8 Hz, 1H, Ar*H*), 7.41-7.50 (m, 3H, Ar*H*); ^{13}C NMR ($CDCl_3$, 100 MHz) δ ppm 24.1 (CH_2), 29.8 (CH_2), 41.2 (CH_2), 63.5 (CH), 111.9 (CH), 119.1 (CH), 123.5 (q, *J* = 272.0 Hz, CF_3), 124.0 (CH), 125.8 (q, *J* = 4.0 Hz, CH), 126.1 (q, *J* = 4.0 Hz, CH), 129.5 (q, *J* = 33.1 Hz, C), 130.1 (CH), 136.0 (C), 137.1 (C), 138.7 (C), 170.7 (C), 172.6 (C); ^{19}F NMR ($CDCl_3$, 376 MHz) δ ppm -62.5 (CF_3); IR ν (cm^{-1}): 3258, 1699, 1665, 1533, 1325, 1251, 1170, 1116, 1082, 822, 674; Anal. Calcd for $C_{17}H_{14}ClF_3N_2O_2S$: C, 50.69; H, 3.50; N, 6.95; S, 7.96. Found: C, 50.43; H, 3.59; N, 7.05; S, 7.07%.

*(S)-N-[(S)-1-(2,4-dichlorophenyl)ethyl]-5-oxo-1-(thiophen-2-yl)pyrrolidine-2-carboxamide **(21)***. Amide **21** was synthesized from **8i** following the procedure described for **1c**, and crystalized in CH_3CN. Yield 15.9%. White solid. mp 194-195°C (CH_3CN); Rf (CH_2Cl_2:MeOH = 75:25) = 0.3;

^{1}H NMR (DMSO-*d*$_6$, 400 MHz) δ ppm 1.36 (d, *J* = 6.6 Hz, 3H, CHC*H*$_3$), 1.95-2.04 (m, 1H, CH$_2$C*H*$_2$CH), 2.27-2.46 (m, 2H, C*H*$_2$CH$_2$CH), 2.50-2.59 (m, 1H, CH$_2$C*H*$_2$CH), 4.41 (d, *J* = 8.9 Hz, 1H, CH$_2$CH$_2$C*H*), 4.56 (q, *J* = 6.6 Hz, 1H, CH$_3$C*H*), 6.42 (dd, *J* = 3.5, 1.2 Hz, 1H, Ar*H*), 6.82 (dd, *J* = 5.5, 3.9 Hz, 1H, Ar*H*), 6.99 (dd, *J* = 5.6, 1.3 Hz, 1H, Ar*H*), 7.47 (dd, *J* = 8.6, 2.0 Hz, 1H, Ar*H*), 7.63 (d, *J* = 2.0 Hz, 1H, Ar*H*), 7.72 (d, *J* = 8.5 Hz, 1H Ar*H*), (N*H* not seen); ^{13}C NMR (DMSO-*d*$_6$, 100 MHz) δ ppm 20.9 (CH$_3$), 23.2 (CH$_2$), 29.9 (CH$_2$), 46.2 (CH), 63.2 (CH), 110.4 (CH), 117.1 (CH), 123.6 (CH), 127.7 (CH), 128.6 (CH), 128.7 (CH), 132.4 (C), 132.8 (C), 138.6 (C), 140.1 (C), 172.1 (C), 173.6 (C); IR ν (cm^{-1}): 3281, 2972, 2927, 1690, 1662, 1542, 1231, 1099, 815, 579; Anal. Calcd for $C_{17}H_{16}Cl_2N_2O_2S$: C, 53.24; H, 4.21; N, 7.31; S, 8.37. Found: C, 47.64; H, 4.70; N, 6.67; S, 6.97%.

*(S)-N-[2-(2,4-dichlorophenyl)ethyl]-5-oxo-1-phenylpyrrolidine-2-carboxamide (**23**)*. Amide **23** was synthesized from **11a** with PTSA as catalyst and CH$_3$CN as solvent, following the procedure described for **1c**, and crystalized in CH$_3$CN. Yield 79.5%. Beige solid. mp 174-182°C (CH$_3$CN); Rf (CH$_2$Cl$_2$:MeOH = 95:5) = 0.6; ^{1}H NMR (DMSO-*d*$_6$, 400 MHz) δ ppm 2.11-2.21 (m, 1H, CH$_2$C*H*$_2$CH), 2.45-2.89 (m, 5H, C*H*$_2$CH$_2$CH and CH$_2$C*H*$_2$CH and NHCH$_2$C*H*$_2$), 3.38-3.58 (m, 2H, NHC*H*$_2$CH$_2$), 4.60 (dd, *J* = 8.5, 3.6 Hz, 1H, CH$_2$CH$_2$C*H*), 5.83 (br t, *J* = 5.8 Hz, 1H, N*H*CH$_2$CH$_2$), 6.80 (d, *J* = 8.2 Hz, 1H, Ar*H*), 7.04 (dd, *J* = 8.2, 1.7 Hz, 1H, Ar*H*), 7.19 (t, *J* = 8.6 Hz, 1H, Ar*H*), 7.30 (d, *J* = 1.7 Hz, 1H, Ar*H*), 7.35 (t, *J* = 8.6 Hz, 2H, Ar*H*), 7.46 (d, *J* = 8.6 Hz, 2H, Ar*H*); ^{13}C NMR (DMSO-*d*$_6$, 100 MHz) δ ppm 23.7 (CH$_2$), 31.3 (CH$_2$), 32.6 (CH$_2$), 38.3 (CH$_2$), 61.8 (CH), 121.1 (2CH), 124.8 (CH), 127.6 (CH), 129.0 (2CH), 129.0 (CH), 132.2 (C), 132.8 (CH), 134.5 (C), 136.1 (C), 139.1 (C), 171.5 (C), 174.7 (C); IR ν (cm^{-1}): 3277, 2922, 1699, 1660, 1557, 1493, 1228, 1043, 1010, 821; Anal. Calcd for $C_{19}H_{18}Cl_2N_2O_2$: C, 60.49; H, 4.81; N, 7.43. Found: C, 60.52; H, 4.72; N, 7.42%.

*(S)-N,1-bis(2-chlorobenzyl)-5-oxopyrrolidine-2-carboxamide (**30a**)*. Amide **30a** was synthesized from **27b** with PTSA as catalyst following the procedure described for **1c**, and purified on a silica column (silica gel, CH_2Cl_2:MeOH = 99:1). Yield 27.8%. Yellow oil. Rf (CH_2Cl_2:MeOH = 97:3) = 0.4; ^{1}H NMR ($CDCl_3$, 400 MHz) δ ppm 2.02-2.09 (m, 1H, CH_2CH_2CH), 2.22-2.45 (m, 2H, CH_2CH_2CH), 2.52-2.31 (m, 1H, CH_2CH_2CH), 3.82-3.89 (m, 1H, CH_2CH_2CH), 4.19 (d, *J* = 15.2 Hz, 1H, NCH_2), 4.43 (dd, *J* = 14.8, 5.4 Hz, 1H, $NHCH_2$), 4.50 (dd, *J* = 14.8, 5.4 Hz, 1H, $NHCH_2$), 4.98 (d, *J* = 15.2 Hz, 1H, NCH_2), 6.73 (t, *J* = 5.4 Hz, 1H, $NHCH_2$), 7.12-7.16 (m, 2H, Ar*H*), 7.19-7.26 (m, 3H, Ar*H*), 7.28-7.41 (m, 3H, Ar*H*); ^{13}C NMR ($CDCl_3$, 100 MHz) δ ppm 23.7 (CH_2), 29.5 (CH_2), 41.8 (CH_2), 43.3 (CH_2), 60.8 (CH), 127.2 (CH), 127.3 (CH), 129.3 (CH), 129.4 (CH), 129.7 (CH), 129.7 (CH), 130.7 (CH), 130.7 (CH), 133.2 (C), 133.7 (C), 133.9 (C), 134.9 (C), 171.0 (C), 175.7 (C); LC-MS (APCI$^+$) m/z: 378.1 (MH^+), tr 3.47 min; Anal. Calcd for $C_{19}H_{18}Cl_2N_2O_2$: C, 60.49; H, 4.81; N, 7.43. Found: C, 60.50; H, 4.79; N, 7.79%.

*(S)-N-(2-chlorobenzyl)-1-(4-chlorobenzyl)-5-oxopyrrolidine-2-carboxamide (**31a**)*. Amide **31a** was synthesized from **27d** with PTSA as catalyst following the procedure described for **1c**, and crystalized in CH_3CN. Yield 20.1%. White solid. mp 86-89°C (CH_3CN); Rf (CH_2Cl_2:MeOH = 97:3) = 0.6; ^{1}H NMR ($CDCl_3$, 400 MHz) δ ppm 1.99-2.08 (m, 1H, CH_2CH_2CH), 2.17-2.30 (m, 1H, CH_2CH_2CH), 2.34-2.42 (m, 1H, CH_2CH_2CH), 2.51-2.62 (m, 1H, CH_2CH_2CH), 3.77-3.81 (m, 1H, CH_2CH_2CH), 3.82 (d, *J* = 14.9 Hz, 1H, NCH_2), 4.42 (dd, *J* = 14.4, 6.1 Hz, 1H, $NHCH_2$), 4.54 (dd, *J* = 14.4, 6.1 Hz, 1H, $NHCH_2$), 4.93 (d, *J* = 14.9 Hz, 1H, NCH_2), 6.00 (br t, *J* = 6.1 Hz, 1H, $NHCH_2$), 7.04 (d, *J* = 8.3 Hz, 2H, Ar*H*), 7.22 (d, *J* = 8.3 Hz, 2H, Ar*H*), 7.26-7.30 (m, 2H, Ar*H*), 7.32-7.36 (m, 1H, Ar*H*), 7.39-7.42 (m, 1H, Ar*H*); ^{13}C NMR ($CDCl_3$, 100 MHz) δ ppm 23.5 (CH_2), 29.6 (CH_2), 41.9 (CH_2), 45.1 (CH_2), 60.7 (CH), 127.3 (CH), 129.0 (2CH), 129.6 (CH), 129.8 (CH), 129.8 (2CH), 130.9 (CH), 133.7 (C), 133.8 (C), 134.2 (C), 134.8 (C), 170.7 (C), 175.7 (C); LC-MS (APCI$^+$) m/z:

378.0 (MH^+), tr 3.58 min; IR ν (cm^{-1}): 3266, 2935, 1683, 1651, 1544, 1404, 1243, 1034, 841; Anal. Calcd for $C_{19}H_{18}Cl_2N_2O_2$: C, 60.49; H, 4.81; N, 7.43. Found: C, 60.17; H, 4.86; N, 7.50%.

*(S)-1-(4-chlorobenzyl)-N-(2,4-dichlorobenzyl)-5-oxopyrrolidine-2-carboxamide (**31b**)*. Amide **31b**was synthesized from **27d** with PTSA as catalyst following the procedure described for **1c**, and purified on a silica column (silica gel, CH_2Cl_2:MeOH = 99:1). Yield 55.3%. White solid. mp 146-147°C (CH_3CN); Rf (CH_2Cl_2:MeOH = 97:3) = 0.4; ^1H NMR ($CDCl_3$, 400 MHz) δ ppm 1.95-2.08 (m, 1H, CH_2CH_2CH), 2.21-2.43 (m, 2H, CH_2CH_2CH), 2.50-2.60 (m, 1H, CH_2CH_2CH), 3.78-3.82 (m, 1H, CH_2CH_2CH), 3.83 (d, *J* = 14.7 Hz, 1H, NCH_2), 4.38 (dd, *J* = 14.7, 6.0 Hz, 1H, $NHCH_2$), 4.48 (dd, *J* = 14.7, 6.0 Hz, 1H, $NHCH_2$), 4.91 (d, *J* = 14.7 Hz, 1H, NCH_2), 6.23 (t, *J* = 6.0 Hz, 1H, $NHCH_2$), 7.05 (d, *J* = 8.7 Hz, 2H, Ar*H*), 7.24 (d, *J* = 8.7 Hz, 2H, Ar*H*), 7.25-7.32 (m, 2H, Ar*H*), 7.41 (d, *J* = 1.7 Hz, 1H, Ar*H*); ^{13}C NMR ($CDCl_3$, 100 MHz) δ ppm 23.5 (CH_2), 29.6 (CH_2), 41.2 (CH_2), 45.2 (CH_2), 60.6 (CH), 127.5 (CH), 129.0 (2CH), 129.5 (CH), 129.7 (2CH), 131.6 (CH), 133.5 (C), 133.9 (C), 134.2 (C), 134.3 (C), 134.6 (C), 170.9 (C), 175.7 (C); LC-MS ($APCI^+$) m/z: 412.7 (MH^+), tr 3.81 min; IR ν (cm^{-1}): 3275, 1684, 1655, 1557, 1473, 1385, 1244, 1103, 1044, 818; Anal. Calcd for $C_{19}H_{17}Cl_3N_2O_2$: C, 55.43; H, 4.16; N, 6.80. Found: C, 55.33; H, 3.73; N, 7.30%.

*(S)-N-benzyl-1-(2,4-dichlorobenzyl)-5-oxopyrrolidine-2-carboxamide (**32a**)*. Amide **32a** was synthesized from **27c** with PTSA as catalyst and CH_3CN as solvent following the procedure described for **1c**, and crystalized in CH_3CN. Yield 34.8%. White solid. mp 133-135°C (CH_3CN); Rf (CH_2Cl_2:MeOH = 97:3) = 0.4; ^1H NMR ($CDCl_3$, 400 MHz) δ ppm 2.00-2.11 (m, 1H, CH_2CH_2CH), 2.21-2.40 (m, 2H, CH_2CH_2CH), 2.45-2.61 (m, 1H, CH_2CH_2CH), 3.82-3.89 (m, 1H, CH_2CH_2CH), 4.15 (d, *J* = 15.2 Hz, 1H, NCH_2), 4.37 (dd, *J* = 12.8, 5.5 Hz, 1H, $NHCH_2$), 4.44 (dd, *J* = 12.8, 5.5 Hz, 1H, $NHCH_2$), 4.89 (d, *J* = 15.2 Hz, 1H, NCH_2), 6.33 (t, *J* = 5.5 Hz, 1H, $NHCH_2$), 7.13-7.16 (m, 2H, Ar*H*), 7.22 (dd, *J* = 7.8, 1.8 Hz, 2H, Ar*H*), 7.26-7.38 (m, 4H, Ar*H*); ^{13}C NMR

($CDCl_3$, 100 MHz) δ ppm 23.7 (CH_2), 29.4 (CH_2), 42.8 (CH_2), 43.7 (CH_2), 60.9 (CH), 127.6 (CH), 127.8 (CH), 127.9 (2CH), 128.8 (2CH), 129.4 (CH), 131.5 (CH), 132.0 (CH), 134.5 (C), 134.5 (C), 137.6 (C), 170.7 (C), 175.8 (C); LC-MS ($APCI^+$) m/z: 378.3 (MH^+), tr 3.56 min; Anal. Calcd for $C_{19}H_{18}Cl_2N_2O_2$: C, 60.49; H, 4.81; N, 7.43. Found: C, 60.14; H, 4.76; N, 7.79%.

*(S)-N-(2-chlorobenzyl)-1-(2,4-dichlorobenzyl)-5-oxopyrrolidine-2-carboxamide (**32b**)*. Amide **32b** was synthesized from **27c** with PTSA as catalyst and CH_3CN as solvent following the procedure described for **1c**, and crystalized in CH_3CN. Yield 66.2%. White solid. mp 94-97°C (CH_3CN); Rf (CH_2Cl_2:MeOH = 97:3) = 0.5; ^1H NMR ($CDCl_3$, 400 MHz) δ ppm 2.00-2.10 (m, 1H, CH_2CH_2CH), 2.23-2.42 (m, 2H, CH_2CH_2CH), 2.51-2.62 (m, 1H, CH_2CH_2CH), 3.85 (m, 1H, CH_2CH_2CH), 4.16 (d, *J* = 15.0 Hz, 1H, NCH_2), 4.44 (dd, *J* = 14.7, 5.7 Hz, 1H, $NHCH_2$), 4.52 (dd, *J* = 14.7, 5.7 Hz, 1H, $NHCH_2$), 4.90 (d, *J* = 15.0 Hz, 1H, NCH_2), 6.15 (t, *J* = 5.7 Hz, 1H, $NHCH_2$), 7.10-7.11 (m, 2H, Ar*H*), 7.22-7.31 (m, 3H, Ar*H*), 7.32-7.40 (m, 2H, Ar*H*); ^{13}C NMR ($CDCl_3$, 100 MHz) δ ppm 23.7 (CH_2), 29.4 (CH_2), 41.8 (CH_2), 42.8 (CH_2), 60.9 (CH), 127.2 (CH), 127.6 (CH), 129.4 (CH), 129.5 (CH), 129.7 (CH), 130.9 (C), 131.6 (CH), 132.0 (CH), 133.7 (C), 134.5 (C), 134.5 (C), 134.8 (C), 170.7 (C), 175.8 (C); LC-MS ($APCI^+$) m/z: 412.7 (MH^+), tr 3.73 min; IR ν (cm^{-1}): 3258, 1659, 1550, 1474, 1452, 1245, 1034, 757; Anal. Calcd for $C_{19}H_{17}Cl_3N_2O_2$: C, 55.43; H, 4.16; N, 6.80. Found: C, 55.11; H, 4.45; N, 7.18%.

*(S)-N,1-bis(2,4-dichlorobenzyl)-5-oxopyrrolidine-2-carboxamide (**32c**)*. Amide **32c** was synthesized from **27c** with PTSA as catalyst and CH_3CN as solvent following the procedure described for **1c**, and purified on a silica column (silica gel, CH_2Cl_2:MeOH = 99:1). Yield 71.3%. Yellow solid. mp 93-96°C (CH_3CN); Rf (CH_2Cl_2:MeOH = 97:3) = 0.4; ^1H NMR ($CDCl_3$, 400 MHz) δ ppm 2.00-2.09 (m, 1H, CH_2CH_2CH), 2.23-2.43 (m, 2H, CH_2CH_2CH), 2.52-2.62 (m, 1H, CH_2CH_2CH), 3.86 (dd, *J* = 3.8, 9.1 Hz, 1H, CH_2CH_2CH), 4.18 (d, *J* = 15.3 Hz, 1H, NCH_2), 4.42

(dd, *J* = 14.8, 5.7 Hz, 1H, NHC*H*$_2$), 4.47 (dd, *J* = 14.8, 5.7 Hz, 1H, NHC*H*$_2$), 4.88 (d, *J* = 15.3 Hz, 1H, NC*H*$_2$), 6.17 (br t, *J* = 6.2 Hz, 1H, N*H*CH$_2$), 7.15-7.16 (m, 2H, Ar*H*), 7.23 (dd, *J* = 8.2, 1.9 Hz, 1H, Ar*H*), 7.28-7.31 (m, 2H, Ar*H*), 7.40 (d, *J* = 1.9 Hz, 1H, Ar*H*); ^{13}C NMR ($CDCl_3$, 100 MHz) δ ppm 23.7 (CH_2), 29.4 (CH_2), 41.2 (CH_2), 42.8 (CH_2), 60.8 (CH), 127.4 (CH), 127.6 (CH), 129.4 (CH), 129.4 (CH), 131.4 (CH), 131.5 (CH), 131.9 (C), 133.6 (C), 134.3 (C), 134.4 (C), 134.5 (C), 134.5 (C), 171.0 (C), 175.8 (C); LC-MS (APCI$^+$) m/z: 447.0 (MH^+), tr 3.96 min; IR ν (cm^{-1}): 3276, 1683, 1652, 1554, 1473, 1242, 1101, 1047, 824; Anal. Calcd for $C_{19}H_{16}Cl_4N_2O_2$: C, 51.15; H, 3.61; N, 6.28. Found: C, 51.05; H, 3.54; N, 6.64%.

(S)-1-(2,4-dichlorobenzyl)-N-(2,4-dimethoxybenzyl)-5-oxopyrrolidine-2-carboxamide ***(32d)***. Amide **32d** was synthesized from **27c** with PTSA as catalyst and CH_3CN as solvent following the procedure described for **1c**, and crystalized in CH_3CN. Yield 73.8%. White solid. mp 194-196°C (CH_3CN); Rf (CH_2Cl_2:MeOH = 97:3) = 0.5; ^{1}H NMR ($CDCl_3$, 400 MHz) δ ppm 1.98-2.09 (m, 1H, CH_2CH_2CH), 2.19-2.29 (m, 1H, CH_2CH_2CH), 2.32-2.42 (m, 1H, CH_2CH_2CH), 2.51-2.62 (m, 1H, CH_2CH_2CH), 3.75-3.78 (m, 1H, CH_2CH_2CH), 3.82 (s, 3H, OC*H*$_3$), 3.83 (s, 3H, OC*H*$_3$), 4.12 (d, *J* = 15.4 Hz, 1H, NC*H*$_2$), 4.30 (dd, *J* = 13.5, 5.4 Hz, 1H, NHC*H*$_2$), 4.36 (dd, *J* = 13.5, 5.4 Hz, 1H, NHC*H*$_2$), 4.92 (d, *J* = 15.4 Hz, 1H, NC*H*$_2$), 6.08 (t, *J* = 5.4 Hz, 1H, N*H*CH$_2$), 6.42-6.49 (m, 2H, Ar*H*), 7.08-7.12 (m, 2H, Ar*H*), 7.15 (d, *J* = 8.0 Hz, 1H, Ar*H*), 7.29 (d, *J* = 1.3 Hz, 1H, Ar*H*); ^{13}C NMR ($CDCl_3$, 100 MHz) δ ppm 23.6 (CH_2), 29.4 (CH_2), 39.4 (CH_2), 42.7 (CH_2), 55.4 (CH_3), 55.4 (CH_3), 61.0 (CH), 98.7 (CH), 104.0 (CH), 117.9 (CH), 127.5 (CH), 129.3 (CH), 130.8 (CH), 131.6 (C), 132.0 (C), 134.3 (C), 134.5 (C), 158.5 (C), 160.8 (C), 170.2 (C), 175.7 (C); LC-MS (APCI$^+$) m/z: 438.4 (MH^+), tr 3.61 min; Anal. Calcd for $C_{21}H_{22}Cl_2N_2O_4$: C, 57.68; H, 5.07; N, 6.41. Found: C, 57.51; H, 5.21; N, 6.26%.

*(S)-1-(2,4-dichlorobenzyl)-N-(furan-2-ylmethyl)-5-oxopyrrolidine-2-carboxamide (**32e**)*. Amide **32e** was synthesized from **27c** with PTSA as catalyst and CH_3CN as solvent following the procedure described for **1c**, and crystalized in CH_3CN. Yield 60.5%. Black solid. mp 138-140°C (CH_3CN); Rf (CH_2Cl_2:MeOH = 97:3) = 0.4; ^{1}H NMR ($CDCl_3$, 400 MHz) δ ppm 1.99-2.11 (m, 1H, CH_2CH_2CH), 2.22-2.42 (m, 2H, CH_2CH_2CH), 2.51-2.62 (m, 1H, CH_2CH_2CH), 3.81-3.88 (m, 1H, CH_2CH_2CH), 4.16 (d, *J* = 15.0 Hz, 1H, NCH_2), 4.37 (dd, *J* = 13.5, 3.5 Hz, 1H, $NHCH_2$), 4.42 (dd, *J* = 13.5, 3.5 Hz, 1H, $NHCH_2$), 4.93 (d, *J* = 15.0 Hz, 1H, NCH_2), 6.15-6.25 (m, 2H, Ar*H*), 6.33 (d, *J* = 3.1 Hz, 1H, $NHCH_2$), 7.16-7.18 (m, 2H, Ar*H*), 7.32-7.36 (m, 2H, Ar*H*); ^{13}C NMR ($CDCl_3$, 100 MHz) δ ppm 23.6 (CH_2), 29.4 (CH_2), 36.4 (CH_2), 42.8 (CH_2), 60.8 (CH), 107.9 (CH), 110.5 (CH), 127.6 (CH), 129.4 (CH), 131.7 (CH), 131.9 (CH), 134.5 (C), 134.6 (C), 142.4 (C), 150.4 (C), 170.7 (C), 175.8 (C); LC-MS (APCI$^+$) m/z: 368.2 (MH^+), tr 3.36 min; IR ν (cm^{-1}): 3278, 2925, 1685, 1651, 1548, 1472, 1236, 1101, 817; Anal. Calcd for $C_{17}H_{16}Cl_2N_2O_3$: C, 55.60; H, 4.39; N, 7.63. Found: C, 55.60; H, 4.46; N, 8.17%.

*(S)-N-benzyl-1-(2,4-dichlorobenzyl)-N-methyl-5-oxopyrrolidine-2-carboxamide (**34**)*. Amide **34** was synthesized from **27c** with PTSA as catalyst and CH_3CN as solvent following the procedure described for **1c**, and crystalized in CH_3CN. Yield 67.0%. White solid. mp 131-134°C (CH_3CN); Rf (CH_2Cl_2:MeOH = 95:5) = 0.1; ^{1}H NMR ($CDCl_3$, 400 MHz) δ ppm 1.97-2.07 (m, 1H, CH_2CH_2CH), 2.19-2.32 (m, 1H, CH_2CH_2CH), 2.38-2.40 (m, 2H, CH_2CH_2CH), 2.41 (s, 3H, NCH_3), 3.86 (dd, *J* = 9.6, 3.2 Hz, 1H, CH_2CH_2CH), 3.89 (s, 2H, $N(CH_3)CH_2$), 4.16 (d, *J* = 15.6 Hz, 1H, $N(CH)CH_2$), 5.00 (d, *J* = 15.6 Hz, 1H, $N(CH)CH_2$), 7.17-7.21 (m, 2H, Ar*H*), 7.31-7.41 (m, 6H, Ar*H*); ^{13}C NMR ($CDCl_3$, 100 MHz) δ ppm 23.9 (CH_2), 30.0 (CH_2), 31.9 (CH_3), 42.7 (CH_2), 52.4 (CH_2), 61.5 (CH), 127.4 (CH), 129.0 (2CH), 129.2 (CH), 129.3 (CH), 129.7 (2CH), 130.6 (CH), 131.6 (C), 133.0 (C), 133.8 (C), 134.2 (C), 175.9 (C), 177.4 (C); LC-MS (APCI$^+$) m/z: 391.1 (MH^+),

tr 3.70 min; IR ν (cm^{-1}): 3299, 2948, 1700, 1658, 1557, 1445, 1397, 1397, 1332, 1282, 1043, 829; Anal. Calcd for $C_{20}H_{20}Cl_2N_2O_2$: C, 61.39; H, 5.15; N, 7.16. Found: C, 61.06; H, 5.42; N, 6.83%.

*(S)-1-benzyl-5-oxo-N-(2-phenylethyl)pyrrolidine-2-carboxamide (**37**)*. Amide **37** was synthesized from **27a** following the procedure described for **1c**, and crystalized in CH_3CN. Yield 43.4%. White solid. mp 113-119°C (CH_3CN); Rf (CH_2Cl_2:MeOH = 95:5) = 0.5; ^{1}H NMR (DMSO-d_6, 400 MHz) δ ppm 1.67-1.77 (m, 1H, CH_2CH_2CH), 2.04-2.16 (m, 1H, CH_2CH_2CH), 2.20-2.38 (m, 2H, CH_2CH_2CH), 2.72 (t, *J* = 6.7 Hz, 2H, $NHCH_2CH_2$), 3.23-3.41 (m, 2H, $NHCH_2$), 3.57 (d, *J* = 14.6 Hz, 1H, NCH_2), 3.82 (dd, *J* = 8.8, 3.5 Hz, 1H, CH_2CH_2CH), 4.80 (d, *J* = 15.3 Hz, 1H, NCH_2), 7.11 (d, *J* = 7.3 Hz, 2H, Ar*H*), 7.17-7.23 (m, 3H, Ar*H*), 7.23-7.37 (m, 5H, Ar*H*), 8.17 (s, 1H, N*H*); ^{13}C NMR (DMSO-d_6, 100 MHz) δ ppm 22.7 (CH_2), 29.1 (CH_2), 34.7 (CH_2), 40.1 (CH_2), 44.2 (CH_2), 59.0 (CH), 126.0 (CH), 127.1 (CH), 127.5 (2CH), 128.1 (2CH), 128.4 (2CH), 128.6 (2CH), 136.5 (C), 139.1 (C), 170.6 (C), 174.5 (C); IR ν (cm^{-1}): 3278, 3062, 2926, 1685, 1644, 1545, 1241, 697; Anal. Calcd for $C_{20}H_{22}N_2O_2$: C, 74.51; H, 6.88; N, 8.69. Found: C, 74.46; H, 6.65; N, 8.63%.

*(S)-1-(4-chlorobenzyl)-5-oxo-N-(2-phenylethyl)pyrrolidine-2-carboxamide (**38**)*. Amide **38** was synthesized from **27d** following the procedure described for **1c**, and crystalized in CH_3CN. Yield 28.1%. White solid. mp 114-117°C (CH_3CN); Rf (CH_2Cl_2:MeOH = 95:5) = 0.5; ^{1}H NMR ($CDCl_3$, 400 MHz) δ ppm 1.78-1.98 (m, 1H, CH_2CH_2CH), 2.14-2.26 (m, 1H, CH_2CH_2CH), 2.29-2.38 (m, 1H, CH_2CH_2CH), 2.40-2.51 (m, 1H, CH_2CH_2CH), 2.81 (t, *J* = 7.2 Hz, 2H, $NHCH_2CH_2$), 3.43-3.61 (m, 2H, $NHCH_2$), 3.66 (d, *J* = 15.4 Hz, 1H, NCH_2), 3.71 (dd, *J* = 8.7, 3.5 Hz, 1H, CH_2CH_2CH), 4.78 (d, *J* = 15.3 Hz, 1H, NCH_2), 5.78 (br t, *J* = 5.6 Hz, 1H, N*H*), 7.04 (d, *J* = 8.4 Hz, 2H, Ar*H*), 7.15-7.19 (m, 2H, Ar*H*), 7.24-7.28 (m, 2H, Ar*H*), 7.34 (d, *J* = 8.4 Hz, 2H, Ar*H*); ^{13}C NMR ($CDCl_3$, 100 MHz) δ ppm 23.6 (CH_2), 29.5 (CH_2), 35.2 (CH_2), 40.2 (CH_2), 44.9 (CH_2), 60.5 (CH), 126.8 (CH), 128.7 (2CH), 128.8 (2CH), 129.0 (2CH), 129.8 (2CH), 133.8 (C), 134.3 (C), 138.2 (C), 170.9

(C), 175.7 (C); IR ν (cm^{-1}): 3296, 3068, 2936, 1682, 1652, 1545, 1246, 696; Anal. Calcd for $C_{20}H_{21}ClN_2O_2$: C, 67.32; H, 5.93; N, 7.85. Found: C, 67.16; H, 5.99; N, 8.10%.

*(S)-1-(4-bromobenzyl)-5-oxo-N-(2-phenylethyl)pyrrolidine-2-carboxamide (**39**)*. Amide **39** was synthesized from **27e** following the procedure described for **1c**, and crystalized in CH_3CN. Yield 10.7%. White solid. mp 120-124°C (CH_3CN); Rf (CH_2Cl_2:MeOH = 9:1) = 0.4; ^{1}H NMR (DMSO-d_6, 400 MHz) δ ppm 1.81-1.91 (m, 1H, CH_2CH_2CH), 2.03-2.15 (m, 1H, CH_2CH_2CH), 2.18-2.29 (m, 1H, CH_2CH_2CH), 2.31-2.45 (m, 1H, CH_2CH_2CH), 2.77 (t, *J* = 7.5 Hz, 2H, $NHCH_2CH_2$), 3.37-3.52 (m, 2H, $NHCH_2$), 3.57 (d, *J* = 15.3 Hz, 1H, NCH_2), 3.69 (dd, *J* = 9.3, 3.8 Hz, 1H, CH_2CH_2CH), 4.81 (d, *J* = 14.9 Hz, 1H, NCH_2), 6.55 (br t, *J* = 5.7 Hz, 1H, NH), 6.92 (d, *J* = 8.2 Hz, 2H, ArH), 7.14 (d, *J* = 7.4 Hz, 2H, ArH), 7.15-7.20 (m, 1H, ArH), 7.22-7.26 (m, 2H, ArH), 7.37 (d, *J* = 7.8 Hz, 2H, ArH); ^{13}C NMR (DMSO-d_6, 100 MHz) δ ppm 22.7 (CH_2), 29.1 (CH_2), 34.7 (CH_2), 40.1 (CH_2), 43.7 (CH_2), 59.0 (CH), 120.2 (C), 126.0 (CH), 128.2 (2CH), 128.6 (2CH), 129.8 (2CH), 131.2 (2CH), 136.0 (C), 139.1 (C), 170.6 (C), 174.7 (C); IR ν (cm^{-1}): 3292, 3064, 2935, 1682, 1653, 1545, 697; Anal. Calcd for $C_{20}H_{21}BrN_2O_2$: C, 59.86; H, 5.27; N, 6.98. Found: C, 59.70; H, 5.27; N, 7.15%.

*(S)-1-(4-methylbenzyl)-5-oxo-N-(2-phenylethyl)pyrrolidine-2-carboxamide (**40**)*. Amide **40** was synthesized from **27f** following the procedure described for **1c**, and crystalized in CH_3CN. Yield 41.6%. White solid. mp 108-112°C (CH_3CN); Rf (CH_2Cl_2:MeOH = 95:5) = 0.5; ^{1}H NMR ($CDCl_3$, 400 MHz) δ ppm 1.88-1.99 (m, 1H, CH_2CH_2CH), 2.13-2.28 (m, 1H, CH_2CH_2CH), 2.32 (s, 3H, $ArCH_3$), 2.34-2.40 (m, 1H, CH_2CH_2CH), 2.41-2.51 (m, 1H, CH_2CH_2CH), 2.79 (t, *J* = 6.8 Hz, 2H, $NHCH_2CH_2$), 3.41-3.61 (m, 2H, $NHCH_2CH_2$), 3.70 (d, *J* = 15.6 Hz, 1H, NCH_2), 3.74 (dd, *J* = 9.4, 3.9 Hz, 1H, CH_2CH_2CH), 4.89 (d, *J* = 14.8 Hz, 1H, NCH_2), 5.53 (br t, *J* = 5.5 Hz, 1H, $NHCH_2$), 6.99-7.04 (m, 2H, ArH), 7.07-7.12 (m, 2H, ArH), 7.14-7.18 (m, 2H, ArH), 7.21-7.25 (m, 1H, ArH),

7.29-7.35 (m, 2H, Ar*H*); ^{13}C NMR ($CDCl_3$, 100 MHz) δ ppm 21.1 (CH_3), 23.6 (CH_2), 29.6 (CH_2), 35.2 (CH_2), 40.3 (CH_2), 45.4 (CH_2), 60.6 (CH), 126.8 (CH), 128.4 (2CH), 128.7 (2CH), 128.8 (2CH), 129.5 (2CH), 132.7 (C), 137.7 (C), 138.2 (C), 171.1 (C), 175.7 (C); IR ν (cm^{-1}): 3281, 3063, 2929, 1682, 1652, 1542, 1241, 697; Anal. Calcd for $C_{21}H_{24}N_2O_2$: C, 74.97; H, 7.19; N, 8.33. Found: C, 74.84; H, 7.15; N, 8.25%.

*(S)-1-(4-methoxybenzyl)-5-oxo-N-(2-phenylethyl)pyrrolidine-2-carboxamide (**41**)*. Amide **41** was synthesized from **27g** following the procedure described for **1c**, and crystalized in CH_3CN. Yield 31.0%. Yellow solid. mp 0146-149°C (CH_3CN); Rf (CH_2Cl_2:MeOH = 95:5) = 0.7; ^{1}H NMR ($CDCl_3$, 400 MHz) δ ppm 1.85-1.95 (m, 1H, CH_2CH_2CH), 2.12-2.22 (m, 1H, CH_2CH_2CH), 2.27-2.37 (m, 1H, CH_2CH_2CH), 2.39-2.49 (m, 1H, CH_2CH_2CH), 2.78 (t, *J* = 7.0 Hz, 2H, $NHCH_2CH_2$), 3.41-3.62 (m, 2H, $NHCH_2CH_2$), 3.65 (d, *J* = 14 Hz, 1H, NCH_2), 3.72 (dd, *J* = 9.3, 3.7 Hz, 1H, CH_2CH_2CH), 3.76 (s, 3H, OCH_3), 4.84 (d, *J* = 14.8 Hz, 1H, NCH_2), 5.57 (br t, *J* = 5.6 Hz, 1H, $NHCH_2$), 6.79 (d, *J* = 8.7 Hz, 2H, Ar*H*), 7.03 (d, *J* = 8.7 Hz, 2H, Ar*H*), 7.15 (d, *J* = 8.7 Hz, 2H, Ar*H*), 7.20-7.25 (m, 1H, Ar*H*), 7.26-7.33 (m, 2H, Ar*H*); ^{13}C NMR ($CDCl_3$, 100 MHz) δ ppm 23.7 (CH_2), 29.7 (CH_2), 35.3 (CH_2), 40.3 (CH_2), 45.2 (CH_2), 55.3 (CH_3), 60.6 (CH), 114.2 (2CH), 126.8 (CH), 127.8 (C), 128.7 (2CH), 128.8 (2CH), 129.8 (2CH), 138.2 (C), 159.3 (C), 171.1 (C), 175.7 (C); IR ν (cm^{-1}): 3272, 3028, 2938, 1686, 1650, 1514, 1250, 695; Anal. Calcd for $C_{21}H_{24}N_2O_3$: C, 71.57; H, 6.86; N, 7.95. Found: C, 71.40; H, 6.92; N, 7.95%.

*(S)-1-(2,4-dichlorobenzyl)-5-oxo-N-(2-phenylethyl)pyrrolidine-2-carboxamide (**42**)*. Amide **42** was synthesized from **27c** following the procedure described for **1c**, and crystalized in CH_3CN. Yield 54.2%. Yellow solid. mp 149-151°C (CH_3CN); Rf (CH_2Cl_2:MeOH = 97:3) = 0.3; ^{1}H NMR ($CDCl_3$, 400 MHz) δ ppm 1.92-2.05 (m, 1H, CH_2CH_2CH), 2.13-2.29 (m, 1H, CH_2CH_2CH), 2.30-2.40 (m, 1H, CH_2CH_2CH), 2.43-2.56 (m, 1H, CH_2CH_2CH), 2.81 (t, *J* = 6.8 Hz, 2H, $NHCH_2CH_2$),

3.53 (td, *J* = 6.8, 5.5 Hz, 2H, NHC*H*$_2$CH$_2$), 3.74-3.81 (m, 1H, CH$_2$CH$_2$C*H*), 4.08 (d, *J* = 15.3 Hz, 1H, NC*H*$_2$), 4.88 (d, *J* = 15.3 Hz, 1H, NC*H*$_2$), 5.76 (br s, 1H, N*H*CH$_2$), 7.04-7.42 (m, 8H, Ar*H*); ^{13}C NMR ($CDCl_3$, 100 MHz) δ ppm 23.7 (CH_2), 29.3 (CH_2), 38.3 (CH_2), 40.4 (CH_2), 42.7 (CH_2), 60.8 (CH), 126.7 (CH), 127.6 (CH), 128.7 (2CH), 128.8 (2CH), 129.4 (CH), 131.4 (CH), 132.0 (C), 134.4 (C), 134.5 (C), 138.3 (C), 170.9 (C), 175.8 (C); LC-MS (APCI$^+$) m/z: 92.3 (MH^+), tr 3.66 min; IR ν (cm^{-1}): 3280, 1691, 1650, 1558, 1243, 1099, 698; Anal. Calcd for $C_{20}H_{20}Cl_2N_2O_2$: C, 61.39; H, 5.15; N, 7.16. Found: C, 61.25; H, 5.41; N, 7.03%.

*(S)-1-(4-nitrobenzyl)-5-oxo-N-(2-phenylethyl)pyrrolidine-2-carboxamide (**43**)*. Amide **43** was synthesized from **26** following the procedure described for **1c**, and crystalized in CH_3CN. Yield 65.6%. White solid. mp 150-151°C (CH_3CN); Rf (CH_2Cl_2:MeOH = 95:5) = 0.4; ^{1}H NMR ($CDCl_3$, 400 MHz) δ ppm 1.91-2.03 (m, 1H, CH$_2$C*H*$_2$CH), 2.14-2.27 (m, 1H, C*H*$_2$CH$_2$CH), 2.32-2.42 (m, 1H, C*H*$_2$CH$_2$CH), 2.45-2.56 (m, 1H, CH$_2$C*H*$_2$CH), 2.82 (t, *J* = 6.7 Hz, 2H, NHCH$_2$C*H*$_2$), 3.48-3.63 (m, 2H, NHC*H*$_2$CH$_2$), 3.69 (dd, *J* = 9.18, 3.7 Hz, 1H, CH$_2$CH$_2$C*H*), 3.75 (d, *J* = 15 Hz, 1H, NC*H*$_2$), 4.99 (d, *J* = 15 Hz, 1H, NC*H*$_2$), 5.50 (br t, *J* = 5.6 Hz, 1H, N*H*CH$_2$), 7.13-7.17 (m, 2H, Ar*H*), 7.23-7.27 (m, 3H, Ar*H*), 7.29-7.34 (m, 2H, Ar*H*), 8.11 (d, *J* = 8.6 Hz, 2H, ArH); ^{13}C NMR ($CDCl_3$, 100 MHz) δ ppm 23.6 (CH_2), 29.3 (CH_2), 35.2 (CH_2), 40.2 (CH_2), 44.9 (CH_2), 60.6 (CH), 124.0 (2CH), 127.0 (2CH), 128.7 (2CH), 128.9 (2CH), 129.0 (2CH), 138.1 (C), 143.3 (C), 147.6 (C), 170.5 (C), 175.7 (C); IR ν (cm^{-1}): 3294, 3072, 2935, 1686, 1652, 1522, 1343, 697; Anal. Calcd for $C_{20}H_{21}N_3O_4$: C, 65.38; H, 5.76; N, 11.44. Found: C, 65.08; H, 5.77; N, 11.39%.

*(S)-N-(2,4-Dichlorobenzyl)-4-(hydroxyimino)-5-oxo-1-(thiophen-2-yl)pyrrolidine-2-carboxamide (**45**)*. A stirred mixture of (*S*)-*N*-(2,4-dichlorobenzyl)-5-oxo-1-(thiophen-2-yl)pyrrolidine-2-carboxamide **44** (2.00 g, 5.0 mmol), $NaNO_2$ (0.98 g, 14.0 mmol), 50 mL of THF, 100 mL of DMF, 50 mL of acetic acid and a few drops of HCl was cooled down to 0°C for 3 hours.

The solvents were evaporated and 500 mL CH_2Cl_2 were added. The mixture was washed 3 times with 200 mL H_2O and dried using $MgSO_4$. The resulting solution was purified by column chromatography (EtOAc:*n*-heptane = 0:1 to 1:0). Solvents were evaporated and Et_2O was added to crystalize the desired product as a white powder in 1% yield (20 mg, 0.05 mmol). mp 191-192°C (Et_2O); Rf (EtOAc:*n*-Heptane = 8:2) = 0.6; ^{1}H NMR (DMSO-d_6, 400 MHz) δ ppm 2.71 (dd, J = 1.4, 18.4 Hz, 1H, CCH_2CH), 3.18 (dd, J = 9.0, 18.4 Hz, 1H, CCH_2CH), 4.35 (dd, J = 4.2, 5.5 Hz, 2H, NHCH_2), 4.95 (ddd, J = 0.8, 1.9, 8.7 Hz, 1H, CCH$_2$CH), 6.69 (d, J = 3.7 Hz, 1H, ArH), 6.95 (dd, J = 3.9, 5.6 Hz, 1H, ArH), 7.20 (d, J = 5.8 Hz, 1H, ArH), 7.29 (d, J = 8.4 Hz, 1H, ArH), 7.38 (dd, J = 0.6, 1.5 Hz, 1H, ArH), 7.61 (d, J = 2.3 Hz, 1H, ArH), 9.18 (t, J = 5.6 Hz, 1H, NHCH$_2$), 12.29 (s, 1H, NOH); ^{13}C NMR (DMSO-d_6, 100 MHz) δ ppm 26.6 (CH_2), 40.0 (CH_2), 57.4 (CH), 111.6 (CH), 119.4 (CH), 123.9 (CH), 127.2 (CH), 128.6 (CH), 130.6 (CH), 132.5 (C), 133.1 (C), 134.7 (C), 138.9 (C), 149.2 (C), 160.6 (C), 169.6 (C); IR ν (cm^{-1}): 3235, 3076, 1712, 1665, 1554, 1446, 686; Anal. Calcd for $C_{16}H_{13}Cl_2N_3O_3S$: C, 48.25; H, 3.29; N, 10.55; S, 8.05. Found: C, 48.28; H, 3.25; N, 10.58; S, 8.32%.

*(S)-Methyl 4-[(dichlorobenzylamino)methylidene]-5-oxopyrrolidine-1,2-dicarboxylate (**47**)*. A stirred mixture of (*S*)-dimethyl 4-[(dimethylamino)methylidene]-5-oxopyrrolidine-1,2-dicarboxylate **46** (4.00 g, 15.6 mmol), 2,4-dichlorobenzylamine (2.75 g, 15.6 mmol) and $ZrCl_4$ (0.18 g, 0.8 mmol) was heated at 60°C for 48 hours. Water (50 ml) and CH_2Cl_2 (50 ml) were added. A solid remained and was filtered. The organic layer was collected and the aqueous layer was washed two times with CH_2Cl_2. The organic layers were mixed and then dried on $MgSO_4$. The solid was solved in MeOH and added to the organic layers. A second silica column was used (CH_2Cl_2:MeOH = 1:0 to 9:1). The recovered solid was washed with EtOH to afford 0.92 g of white solid (compound **48**, yield 12.4%, with the same characteristics as described in the literature[21j]). Evaporation of the

filtered EtOH, and recrystallization in EtOH gave the desired white solid in 11 % yield (0.60 g, 1.5 mmol). mp 184-190°C (EtOH); Rf (CH_2Cl_2:MeOH = 95:5) = 0.5; ^{1}H NMR (DMSO-d_6, 400 MHz) δ ppm 2.39 (dd, *J* = 16.3, 2.8 Hz, 1H, CCH_2CH), 2.86 (dd, *J* = 15.3, 11.3 Hz, 1H, CCH_2CH), 3.65 (s, 3H, OCH_3), 3.66 (s, 3H, OCH_3), 4.43 (d, *J* = 5.1 Hz, 2H, NHCH_2), 4.64 (dd, *J* = 10.6, 4.8 Hz, 1H, CCH_2CH), 7.20-7.34 (m, 2H, N*H*CH_2 and CC*H*NH), 7.38 (d, *J* = 8.4 Hz, 1H, Ar*H*), 7.48 (dd, *J* = 8.4, 2.3 Hz, 1H, Ar*H*), 7.64 (d, *J* = 2.3 Hz, 1H, Ar*H*); ^{13}C NMR (DMSO-d_6, 100 MHz) δ ppm 25.7 (CH_2), 41.1 (CH_2), 53.3 (CH_3), 53.7 (CH_3), 56.0 (CH), 93.9 (C), 128.5 (CH), 129.8 (CH), 131.7 (C), 133.7 (C), 134.0 (C), 136.9 (CH), 153.3 (CH), 167.6 (C), 173.2 (2C); IR ν (cm^{-1}): 3326, 1762, 1621, 1318, 1182, 1081, 992; Anal. Calcd for $C_{16}H_{16}Cl_2N_2O_5$: C, 49.63; H, 4.16; N, 7.23. Found: C, 49.62; H, 4.13; N, 7.19%.

*(S)-N-(2,4-dichlorobenzyl)-2-oxo-3-(thiophen-2-yl)-1,3-oxazolidine-4-carboxamide (**60**)*. Amide **60** was synthesized from **59** following the procedure described for **16i** and purified on a silica column (silica gel, CH_2Cl_2:MeOH = 95:5). Yield 29.3%. White solid. mp 188-189°C (Et_2O); Rf (CH_2Cl_2:MeOH = 95:5) = 0.6; ^{1}H NMR (DMSO-d_6, 400 MHz) δ ppm 4.34 (dd, *J* = 8.8, 3.7 Hz, 1H, OCH_2CH), 4.36 (dd, *J* = 5.6, 2.2 Hz, 2H, NHCH_2), 4.70 (t, *J* = 8.9 Hz, 1H, OCH_2CH), 4.96 (dd, *J* = 9.2, 3.7 Hz, 1H, OCH_2CH), 6.53 (dd, *J* = 3.8, 1.4 Hz, 1H, Ar*H*), 6.89 (dd, *J* = 5.5, 3.8 Hz, 1H, Ar*H*), 7.13 (dd, *J* = 5.5, 1.4 Hz, 1H, Ar*H*), 7.28 (d, *J* = 8.2 Hz, 1H, Ar*H*) , 7.38 (dd, *J* = 8.2, 2.1 Hz, 1H, Ar*H*), 7.62 (d, *J* = 2.1 Hz, 1H, Ar*H*), 9.08 (brt, *J* = 5.6 Hz, 1H, N*H*CH_2); ^{13}C NMR (DMSO-d_6, 100 MHz) δ ppm 40.1 (CH_2), 58.8 (CH), 66.0 (CH_2), 112.0 (CH), 118.7 (CH), 124.5 (CH), 127.2 (CH), 128.6 (CH), 130.5 (CH), 132.5 (C), 133.1 (C), 134.5 (C), 139.1 (C), 154.3 (C), 168.4 (C); IR ν (cm^{-1}): 3332, 1748, 1667, 1548, 1466, 1222, 1053, 679; Anal. Calcd for $C_{15}H_{12}Cl_2N_2O_3S$: C, 48.53; H, 3.26; N, 7.55; S, 8.64. Found: C, 48.42; H, 3.25; N, 7.58; S, 8.32%.

*N-(2,4-Dichlorobenzyl)-5-oxopyrrolidine-3-carboxamide (**64**)*. Amide **64** was synthesized from **63** following the procedure described for **1c**, and purified on a silica column (silica gel, CH_2Cl_2:MeOH = 99:1). Yield 77.0%. White solid. Rf (CH_2Cl_2:MeOH= 95:5) = 0.1; mp 186-192 °C (CH_2Cl_2/MeOH); ^{1}H NMR ($CDCl_3$, 400 MHz) δ (ppm) 2.50 (dd, *J* = 26.5, 9.6 Hz, 1H, C*H*$_2$), 2.62 (dd, *J* = 25.5, 8.6 Hz, 1H, C*H*$_2$), 3.10-3.21 (m, 1H, C*H*), 3.50-3.56 (m, 1H, C*H*$_2$), 3.58-3.66 (m, 1H, C*H*$_2$), 4.49 (d, *J* = 6.2 Hz, 1H, C*H*$_2$), 5.42 (br s, 1H, N*H*), 5.94 (br s, 1H, N*H*), 7.29-7.32 (m, 1H, Ar*H*), 7.32 (dd, *J* = 8.2, 2.0 Hz, 1H, C*H*), 7.38 (d, *J* = 2.0 Hz, 1H, Ar*H*); ^{13}C NMR ($CDCl_3$, 100 MHz) δ (ppm) 33.6 (CH_2), 40.6 (CH), 41.5 (CH_2), 44.5 (CH_2), 127.6 (CH), 129.5 (CH), 131.5 (CH), 133.8 (C), 134.4 (C), 134.5 (C), 171.7 (C), 175.8 (C); IR ν (cm^{-1}): 3270, 3196, 1690, 1637, 1556; Anal. Calcd for $C_{12}H_{12}Cl_2N_2O_2$: C, 50.20; H, 4.21; N, 9.76. Found: C, 50.18; H, 4.23; N, 9.76%.

*N-(2,4-Dichlorobenzyl)-5-oxo-1-thien-2-ylpyrrolidine-3-carboxamide (**65**)*. Amide **65** was synthesized from **64** following the procedure described for **16i**, and purified on a silica column (silica gel, CH_2Cl_2:MeOH = 99:1). Yield 85.0%. White solid. mp 183-186°C (CH_2Cl_2/MeOH); Rf (CH_2Cl_2:MeOH= 95:5) = 0.8; ^{1}H NMR ($CDCl_3$, 400 MHz) δ (ppm) 2.81 (dd, *J* = 16.8, 9.5 Hz, 1H, C*H*$_2$CHCH$_2$), 2.91 (dd, *J* = 17.2, 8.6 Hz, 1H, C*H*$_2$CHCH$_2$), 3.17-3.28 (m, 1H, CH$_2$C*H*CH$_2$), 4.00 (dd, *J* = 9.7, 9.0 Hz, 1H, CH$_2$CHC*H*$_2$), 4.11 (dd, *J* = 10.1, 7.4 Hz, 1H, CH$_2$CHC*H*$_2$), 4.52 (d, *J* = 6.2 Hz, 2H, NHC*H*$_2$), 6.03 (br s, 1H, N*H*CH$_2$), 6.50-6.52 (m, 1H, Ar*H*), 6.84-6.88 (m, 1H, Ar*H*), 6.91-6.94 (m, 1H, Ar*H*), 7.21-7.24 (m, 1H, Ar*H*), 7.33 (d, *J* = 8.2 Hz, 1H, Ar*H*), 7.40 (s, 1H, Ar*H*); ^{13}C NMR ($CDCl_3$, 100 MHz) δ (ppm) 35.1 (CH_2), 37.6 (CH_2), 41.6 (CH_2), 50.8 (CH), 110.0 (C), 111.1 (CH), 118.4 (CH), 123.9 (CH), 127.6 (CH), 129.6 (CH), 131.7 (CH), 133.6 (C), 134.4 (C), 134.6 (C), 169.2 (C), 171.1 (C); IR ν (cm^{-1}): 3286, 3091, 1681, 1646, 677; Anal. Calcd for $C_{16}H_{14}Cl_2N_2O_2S$: C, 52.04; H, 3.82; N, 7.59. Found: C, 52.05; H, 3.83; N, 7.59%.

*N-(2,4-Dichlorobenzyl)pyridine-2-carboxamide (**67**)*. Amide **67** was synthesized from **66** following the procedure described for **1c**, and purified on a silica column (silica gel, CH_2Cl_2:MeOH = 99:1). Yield 80.0%. White solid. mp 61-65°C (Et_2O); Rf (CH_2Cl_2:MeOH = 95:5) = 0.6; ^{1}H NMR (DMSO-d_6, 400 MHz) δ ppm 4.56 (d, J = 6.4 Hz, 2H, NHCH_2), 7.33 (d, J = 8.5 Hz, 1H, ArH), 7.41 (dd, J = 8.5, 2.4 Hz, 1H, ArH), 7.61 (d, J = 2.2 Hz, 1H, ArH), 7.64 (ddd, J = 7.5, 4.7, 1.6 Hz, 1H, ArH), 8.01 (dd, J = 7.7, 1.6 Hz, 1H, ArH), 8.04-8.08 (m, 1H, ArH), 8.68-8.70 (m, 1H, ArH), 9.40 (br t, J = 6.4 Hz, 1H, NHCH$_2$); ^{13}C NMR (DMSO-d_6, 100 MHz) δ ppm 40.6 (CH_2), 122.5 (CH), 127.2 (CH), 127.7 (CH), 128.9 (CH), 130.2 (CH), 132.5 (C), 133.1 (C), 136.0 (CH), 138.3 (CH), 149.0 (C), 150.0 (C), 164.7 (C); IR ν (cm^{-1}): 3383, 3058, 1668, 1514, 1464; Anal. Calcd for $C_{13}H_{10}Cl_2N_2O$: C, 55.54; H, 3.59; N, 9.96. Found: C, 55.55; H, 3.58; N, 9.97%.

*2-{[(2,4-Dichlorobenzyl)amino]carbonyl}-1-methylpyridinium iodide (**68**)*. A mixture of *N*-(2,4-dichlorobenzyl)pyridine-2-carboxamide **67** (7.49 g, 26.6 mmol) and methyl iodide (6.90 g, 48.6 mmol) was heated at reflux of methyl iodide for 24 h. CH_3CN was added and the desired product crystalized overnight. It was filtered to give a yellow solid in 28% yield (3.20 g, 7.6 mmol). mp 162-166°C (CH_3CN); ^{1}H NMR (DMSO-d_6, 400 MHz) δ ppm 4.31 (s, 3H, NCH_3), 4.62 (d, J = 5.6 Hz, 2H, NHCH_2), 7.48 (dd, J = 8.2, 2.3 Hz, 1H, ArH), 7.59 (d, J = 8.2 Hz, 1H, ArH), 7.70 (d, J = 2.3 Hz, 1H, ArH), 8.21-8.29 (m, 2H, ArH), 8.73 (td, J = 7.8, 1.2 Hz, 1H, ArH), 9.12 (d, J = 6.0 Hz, 1H, ArH), 9.79 (br t, J = 5.6 Hz, 1H, NHCH$_2$); ^{13}C NMR (DMSO-d_6, 100 MHz) δ ppm 41.2 (CH_2), 47.0 (CH_3), 127.6 (CH), 128.0 (CH), 129.0 (CH), 129.3 (CH), 131.7 (CH), 133.5 (CH), 133.9 (C), 134.2 (CH), 146.9 (C), 148.0 (C), 148.1 (C), 160.7 (C); IR ν (cm^{-1}): 3186, 3010, 1668, 1548, 1285, 783; Anal. Calcd for $C_{14}H_{13}Cl_2IN_2O$: C, 39.75; H, 3.10; N, 6.62. Found: C, 39.76; H, 3.12; N, 6.62%.

*(S,E)-2-cyano-1-(1-phenylethyl)-3-(quinolin-5-yl)guanidine (**74a**)*. A mixture of 5-isothiocyanatoquinoline **73** (0.93 g, 5 mmol) and (S)-1-phenylethanamine (1 g, 5 mmol) in anhydrous tetrahydrofuran was stirred at r.t. for 1 h. Mercuric acetate (1.6 g, 5 mmol) followed by sodium cyanamide (0.96 g, 15 mmol) was added to this mixture. This mixture was stirred at R.T. for 12 h. The precipitated black mercuric sulfide was filtered through celite and the filtrate was concentrated under reduced pressure. The residue was washed with EtOH and CH_2Cl_2 to yield 1.10 g (70% yield) of a white solid. mp 189-191°C (EtOH); Rf (CH_2Cl_2:MeOH = 95:5) = 0.3; ^{1}H NMR (DMSO-d_6, 400 MHz) δ ppm 1.36 (d, J = 6.7 Hz, 3H, CH_3), 5.02-5.12 (m, 1H, CHCH$_3$), 7.22-7.37 (m, 5H, ArH), 7.40-7.56 (m, 3H, ArH), 7.75 (t, J = 8.3 Hz, 1H, ArH), 7.96 (d, J = 8.4 Hz, 1H, ArH), 8.10 (br s, 1H, NH), 8.90-8.94 (m, 1H, ArH) , 9.34 (br s, 1H, NH); ^{13}C NMR (DMSO-d_6, 100 MHz) δ ppm 22.5 (CH_3), 51.3 (CH), 117.3 (CN), 121.8 (CH), 125.1 (C), 125.5 (C), 126.5 (2CH), 127.3 (C), 128.3 (C), 128.7 (2CH), 129.6 (CH), 131.8 (CH), 133.9 (C), 144.3 (CH), 148.9 (CH), 151.0 (CH), 158.8 (CH); IR ν (cm^{-1}): 3174, 3103, 2976, 2168, 1557, 1373, 1353, 799, 699; Anal. Calcd for $C_{19}H_{17}N_5$: C, 72.36; H, 5.43; N, 22.21. Found: C, 72.38; H, 5.44; N, 22.20%.

Material and Methods for Chiral Supercritical Fluid Chromatography

Stationary phases: The chiral analytical column used for this study was a Chiralpak AD-H, purchased from Chiral Technologies Europe (Illkirch, France). This column had dimensions 250 mm x 4.6 mm i.d. with 5 µm particle size and was coated on a silica-gel support.

Chromatographic system and conditions: The chromatographic system used was an SFC-PICLAB hybrid 10-20 apparatus (PIC Solution, Avignon, France) equipped with an autosampler comprised a 48-vial plate and a 24-vial plate (model Alias, Emmen, Netherlands), three model 40P pumps: two for CO_2 and a third for the modifier (Knauer, Berlin, Germany), a column oven with a Valco ten-position column selection valve, and a Valco six-position solvent switching valve. The

proportion of the modifier in the mobile phase was adjusted by a piston pump. It was then directly added in the CO_2 feeding, and the mixture of the both (modifier and CO_2) was pumped by another piston pump at the total flow rate. The pump head used for pumping the CO_2 was cooled to – 8°C by a cryostat (model Minichiller, Huber, Offenburg, Germany). The injection valve was supplied with 50 or 100 µL sample loops. The system was also composed of a Smartline 2600 diode array detector (DAD) (Knauer, Berlin, Germany). Detection wavelength was set at 210 nm. After the detector, the outlet pressure was controlled by a back-pressure regulator (BPR). The outlet regulator tube was heated to 55°C to avoid ice formation during the CO_2 depressurization. The system was controlled, and the data were acquired with the SFC PicLab Analytic Online v.3.1.2 software and the data were processed with the Analytic Offline v.3.2.0 software (PIC Solution, Avignon, France). During the separation optimization, the mobile phase was CO_2-modifier mixtures with the proportion of methanol of 20 %, flow rate was 4 mL/min. All analyses were run in isocratic mode. The column oven temperature was 40°C and the outlet pressure was maintained at 120 bar for all experiments.

Result: One enantiomer of compound **16i** was identified (retention time, t_R, of 11.55 min; see Supporting Information for chromatogram).

Biological Assays. Measurement of TO-PRO-3 Accumulation in human P2RX7-Expressing HEK293 Cells.

HEK-293 cells overexpressing human P2RX7 were stained with the calcium indicator Fluo-3 AM and then incubated with the non-permeant DNA intercalatants TO-PRO-3 (large pore opening) and propidium iodide (cell viability) in presence of different molecules at 10^{-5}M concentration for 15 min before addition of the P2RX7 agonist BzATP (100 µM). Compound **1a** was used as a reference antagonist for human P2RX7. Cells were then analyzed after 1 hour by flow cytometry using Cyan

cytometer (Beckman). Percentages of cells displaying P2RX7 activation (Fluo-3/TO-PRO-3 double positive cells) in presence of the molecules were calculated.

Radioligand binding studies. Measurement of [^{3}H]A-804598 Displacement by P2RX7 Antagonists.

Ki values were determined for compounds giving a displacement of the reference antagonist ([^{3}H]-A804598) greater than 50%. The binding of [^{3}H]-A804598 to membranes of HEK293 cells expressing human P2X7 receptors was performed by saturation binding experiments and characterized by a K_D value of 11.08 ± 2.6 nM. This value is in good agreement with the literature.

Stock solutions of the compounds were prepared in DMSO and further diluted with the binding buffer to the desired concentration. Final DMSO concentrations in the assay were less than 0.1%. Briefly [^{3}H]-A804598 (80 nM final) as radioligand for the *h*P2X7 receptor, was added to 25 µg of membranes resuspended in 300 µL (final volume) binding buffer (50 mM Tris-HCl, 0,1% BSA, pH 7.4). After 1 h at room temperature, the incubation was stopped and the solutions were rapidly filtered over Unifilter-96 GF/C glass fiber, presoaked in PEI (0.5%), on a Filtermate Unifilter 96-Harvester (PerkinElmer) and washed 10 times with an ice-cold binding buffer. The radioactivity on the filters was measured using TopCount NXT™ Microplate Scintillation Counter (PerkinElmer) using 30 µL of MicroScint™ 40 (PerkinElmer) after 30 min resting. Assays were performed at least in three independent experiments in duplicate or triplicate. The nonspecific binding was determined in the presence of 5 mM A-804598.

ELISA of Human IL1β in Differentiated THP-1 Cells.

Cell cultures: THP-1 cells were cultured in RPMI 1640 medium (Gibco by LifeTechnologies™, France) supplemented with 10% FCS. THP-1 cells were differentiated in the presence of phorbol-12-myristate 13-acetate (100nM).

ELISA analyses: Macrophages (10^6 cells) were plated 1mL in 24-well plates, pretreated with antagonist P2RX7 molecules at concentration 10^{-5} or 10^{-6} mol/L and exposed to 10 µmol/L of LPS (Sigma-Aldrich, France), and 70 µmol/L BzATP (Sigma-Aldrich, France) at 37 °C and 5% CO_2 in 0.2 mL RPMI 1640 medium supplemented with 10% fetal bovine serum. 0.2 mL of the supernatant was collected at various times (0, 2, 4 and 6 hours). IL1β content in supernatants was quantified by ELISA (Human IL1β, BioLegend, ELISA MAX™) as described previously.[34]

Statistical analysis: Statistical analysis was performed with Prism 4.0 from GraphPad. Data were analyzed using the Mann-Whitney U test to compare pairs of groups. The results are expressed as the mean ± SD of individual experimental groups. Differences were considered significant when the P value was <0.05.

ROS Assay. Macrophages (105 cells) were plated in 96-well plates, pretreated with antagonist P2X7 molecules at concentration 10^{-5} or 10^{-6} mol/L and exposed to 10 µmol/L of LPS recruiting a signaling pathways through TLR4 to induce ROS (Sigma-Aldrich, France), and 70 µmol/L BzATP-mediated ROS production (Sigma-Aldrich, France)[35] at 37 °C and 5% CO_2 in 100µL RPMI 1640 medium supplemented with 10% fetal bovine serum. A volume of 50µL of a mixture of 50 µg/mL horseradish peroxidase and 50 µM luminol were added to each well. The chemiluminescence was measured in a FLUOstar Omega Fluorometer (BMG Labtech). H_2O_2 alone without macrophages at a low concentration 1.7 mol/L was used as a positive control.

***In vitro* incubation with human liver microsomes**

Briefly, once thawed, HLMs (2 mg protein/mL for a final volume of 100 µL) were pre-activated by alamethicin on ice in an intermediate volume of 50 µL in 0.1 M Tris-HCl-$MgCl_2$ (10 mM $MgCl_2$ and 100 mM Tris-HCl solution) at pH 7.4. This mixture was added to a 50 µL-dried residue of a methanol-DMSO (9/1) solution of compound **16i** at a concentration of 0.2 mg/mL. Fifty µL of a

cofactor mixture (5 mM UDPGA, 1.3 mM NADPH, 3.3 mM G6P and 0.5 U/mL G6PD) in 0.1 M Tris-HCl were then added. The enzymatic reaction was performed at 37 °C for 60 min, and stopped by the addition of 100 µL of methanol-containing methyl-clonazepam at 1.25 mg/L and β-OH-ethyltheophyllin at 16 mg/L, used as internal standards for the chromatographic analysis. Samples were centrifuged at 4 °C for 14 min at 32 000 g and supernatants were diluted in 400 µL of 3 % 5-sulfosalicylic acid before injection of 75 µL into the chromatographic system.

Liquid chromatography with quadrupole-time of flight mass spectrometry detection

The Waters ultra-performance liquid chromatography system consisted of two binary solvent manager LC pumps, a sample manager autosampler and a column manager oven Acquity™. Mass spectrometry data were acquired using an XEVO G2-XS QTOF (Waters, Milford, MA, USA) instrument controlled with MassLynx™ 4.1 software. For mass accuracy, a LockSpray™ interface was used with a Leucine Enkephalin ($[M + H]^+$ *m/z* 556.2771) solution (200 pg/µL) infused at 10 µL/min as the lock mass, providing exact mass measurement within 1 ppm RMS mass accuracy.

Extractions of the sample (75 µL of diluted supernatants) were performed using an OASIS HLB on-line column (30 x 2.1 mm, 20 µm) (Waters, Milford, MA, USA). The mobile phases consisted in 0.2 % ammonia solution (A1) and 100 % methanol (B1) and the elution profile was as follows: 0.5 min, 0% B1, flow rate 2.0 mL/min; 1.0 min, 0% B1, flow rate 0.2 mL/min; 15 min, 100% B1, flow rate 0.2 mL/min; 30 min, 100% B1, flow rate 2.0 mL/min. The chromatographic separation was performed using an Acquity HSS C18 column (150 x 2 mm, 1.8 µm) (Waters, Milford, MA, USA) in an oven temperature of 50 °C, and mobile phases including ammonium formate buffer 5 mM, pH 3 (A2) and acetonitrile in 1% formic acid (B2); flow rate of 0.4 mL/min was used. Initial concentration of mobile phase B2 (3%) held until 0.5 min, increased to 40 % at 25 min, then to 100% at 26 min, and finally held until 30 min.

For detection, mass spectrometric conditions were as follows: positive electrospray ionization interface (ESI+), 20 V as ion spray voltage, source temperature at 140 °C and desolvatation temperature at 500 °C with a desolvation gas flow rate of 900 L/h, nitrogen as desolvation gas and argon as collision gas. Conditions for the time of flight mass spectrometer (TOF MS^e)scan mode were as follows: scan range 100–1000 *m/z* for function 1 and 50–1000 *m/z*, with a collision energy ramp from 10–40 eV, for function 2.

Data processing and evaluation of compound **16i** metabolites were performed using the Metabolynx^{TM} 4.1 software (Waters, Milford, MA, USA). Theoretically possible biotransformations of compound **16i** were simulated, including possible hydroxylation, *N*-dealkylation, deamination and glucuronidation transformations. The automated metabolite profiling process was completed using the fragmentation interpretation software tool MassFragment^{TM} 4.1 (Waters, Milford, MA, USA), to allow software driven assignment of metabolite structures from fragmentation patterns.

As previously reported, a control sample containing propafenone was analyzed using the incubation and chromatographic conditions as for the metizolam in order to assess the efficacy of the enzymatic system.[32] The efficacy was considered to be correct if the production of both main CYP- and UGT-derived metabolites of propafenone (i.e., hydroxypropafenone and hydroxypropafenone glucuronide) was observed.

***In vivo* Assay.**

Acute inflammation was induced as followed: Mice received 3.8% dextran sulfate (DSS) treatment from day 1 to 5 and then returned to normal tap water for 10 days. Treatment was given daily by intraperitoneal injection of compounds (2.5 mg/kg) dissolved in 10% DMSO/PBS. We used the following semi quantitative clinical score: 0, no weight loss; 1, loss < 5%; 2, loss < 10%;

3, loss < 20%; 4, loss < 30% and 5, > 30%. The scores for stool consistency were measured as 0, normal; 1, loose stools; 2, watery diarrhea; or 3, severe watery diarrhea. Rectal bleeding was scored as 0, no blood; 1, presence of petechia; 2, stools with a trace of blood; or 3, bleeding. Inflammation score was performed by trained pathologists. Briefly, the severity of inflammation (none, mild, moderate, severe), extent of inflammation (none, mucosa, mucosa, and submucosa, transmural), crypt damage (none, basal to 1/3, basal to 2/3, crypt loss, crypts, and epithelium loss), and percentage of tissue affected by inflammation were scored. The unpaired Mann – Whitney t test was used to evaluate the statistical significance between groups.

Computational methods

Pharmacophore perception of P2RX7 antagonists

Common pharmacophore features were generated from 9 reference P2RX7 ligands (see Supporting Information for structures) using Align-It program,[36] onto a linux workstation. From ChemAxon suite (http://www.chemaxon.com), MarvinSketch was used for drawing and 3D conversion of chemical structures whereas Calculator Plugins were used for conformation generation. The reference compound A1 was selected as the most rigid molecule onto which other compound conformations were matched. Pharmacophore models were computed from the 4 most diverse conformations of A1 iteratively matching 1696 conformations sampled from the 8 other molecules. The best pharmacophore models were selected as the ones that maximize the fitting value between pharmacophore feature centers and corresponding atoms in molecules.

Molecular docking of P2RX7 antagonists

Pd-P2RX7 was used as structural template for docking studies as sequence is totally conserved into region corresponding to allosteric binding site. Among the 6 experimental structures of *pd*-P2RX7 co-crystallized with different reference allosteric antagonists,[23] we chose the 5U1X PDB entry co-

crystallized with JNJ-47965567 exhibiting the highest structural similarity with the studied chemical series as low-weighted and coiled structures. Molecular docking jobs were performed with AutodockVina 1.1.2,[37] using the 5U1X homotrimeric P2RX7 structure with 2 of 3 allosteric binding sites occupied and centering a large searching box that includes the whole extracellular trimeric region in order to assess the specificity for allosteric binding site. Receptor-ligand interaction was derived from a pKd calculated from the Vina score, a standard free energy of binding (ΔG^0_{bind}) associated to each binding docking pose, and according to the following thermodynamic relationship:

$$\Delta G^0_{bind} = -RTlnK_{eq} = -2{,}303.RTlog_{10}K_{eq}$$

$$pK_d = \frac{\Delta G^0_{bind}}{-2{,}303.RT}$$

ASSOCIATED CONTENT

Supporting Information (references for previously described compounds; ^{1}H, ^{13}C and ^{19}F NMR spectra of unprecedented compounds described in this report; supercritical fluid chromatograms of compound **16i**; flow cytometry results for series **I-VI**; and cell-proliferation assay results for compounds selected by the NCI) associated with this article can be found in the online version. The following file "Supporting_information.pdf" is available free of charge.

AUTHOR INFORMATION

Corresponding Author

*E-mail: alina.ghinet@yncrea.fr

Author Contributions

The manuscript was written through contributions of all authors. All authors have given approval to the final version of the manuscript.

Funding Sources

The authors gratefully acknowledge the "Métropole Européenne de Lille" (MEL) for G.H.'s PhD scholarship, the DigestScience Foundation (Foundation on digestive tract diseases and nutrition) and the Institut National du Cancer, France (INCa, project P2RX7 2015-137) for financial support.

Notes

The authors declare no competing financial interest.

ACKNOWLEDGMENT

The authors also acknowledge the National Cancer Institute (NCI) for biological evaluation of compounds on their 60-cell panel: the testing was performed by the Developmental Therapeutics Program, Division of Cancer Treatment and Diagnosis (the URL to the Program's website: http://dtp.cancer.gov). We thank Thierry Juhel (IRCAN) for assistance with animals.

ABBREVIATIONS

ATP, adenosine 5'-triphosphate; BR, Bredereck's reagent; BzATP, (4-benzoyl)benzoyl-adenosine-5'-triphosphate; Da, dalton; IL, interleukine; Glu, glutamate; *h*-, human; HEK, human embryonic kidney; IL, interleukin; IBD, inflammatory bowel diseases; LPS; lipopolysaccharides; MDR, multi-drug resistant; NADPH, nicotinamide adenine dinucleotide phosphate; NCI, National Cancer Institute; NMR, nuclear magnetic resonance; P2RX7, P2RX7 receptor; P2XR, P2X receptors; *pd*-, panda; PGA, pyroglutamic acid; PGAm, pyroglutamide; PGM, methyl pyroglutamate; PK, pharmacokinetic; PTSA, *para*-toluene sulfonic acid; ROS, reactive oxygen

species; Ser, serine; TLC, thin layer chromatography; TMS, tetramethylsilane; TNF, tumor necrosis factor.

REFERENCES

[1] North, R. A. Molecular physiology of P2X receptors. *Physiol. Rev.*, **2002**, *82*, 1013-1067.

[2] Jiang, L. H.; Baldwin, J. M.; Roger, S.; Baldwin, S. A. Insights into the Molecular Mechanisms Underlying Mammalian P2RX7 Receptor Functions and Contributions in Diseases, Revealed by Structural Modeling and Single Nucleotide Polymorphisms. *Front. Pharmacol.*, **2013**, *4*, 55.

[3] Ralevic, V.; Burnstock, G. Receptors for purines and pyrimidines. *Pharmacol. Rev.*, **1998**, *50*, 413-492.

[4] Di Virgilio, F. The P2Z purinoceptor: an intriguing role in immunity, inflammation and cell death. *Immunol. Today*, **1995**, *16*, 524-528.

[5] (a) Mehta, N.; Kaur, M.; Singh, M.; Chand, S.; Vyas, B.; Silakari, P.; Bahia, M. S.; Silakari, O. Purinergic receptor $P2X_7$: a novel target for anti-inflammatory therapy. *Bioorg. Med. Chem.*, **2014**, *22*, 54-88. (b) Ferrari, D.; Pizzirani, C.; Adinolfi, E.; Lemoli, R. M.; Curti, A.; Idzko, M.; Panther, E.; Di Virgilio, F. The P2RX7 receptor: a key player in IL1 processing and release. *J. Immunol.* **2006**, *176*, 3877-3883.

[6] Chessel, I. P.; Hatcher, J. P.; Bountra, C.; Michel, A. D.; Hugues, J. P.; Green, P.; Egerton, J.; Murfin, M.; Richardson, J.; Peck, W. L.; Grahames, C. B.; Casula, M. A.; Yiangou, Y.; Birch, R.; Anand, P.; Buell, G. N. Disruption of the P2RX7 purinoceptor gene abolishes chronic inflammatory and neuropathic pain. *Pain*, **2005**, *114*, 386-396.

[7] (a) Li, H.; Jin, Z., Li, X.; Wu, L.; Jin, J. Associations between single-nucleotide polymorphisms and inflammatory bowel disease-associated colorectal cancers in inflammatory bowel disease patients: a meta-analysis. *Clin. Trans. Oncol.*, **2017**, *19*, 1018-1027. (b) Garcia-Marcos, M.; Perez-Andres, E.; Tandel, S.; Fontanils, U.; Kumps, A.; Kabre, E.; Gomez-Munoz, A.; Marino, A.; Dehaye, J. P.; Pochet, S. Coupling of two pools of P2RX7 receptors to distinct intracellular signaling pathways in rat submandibular gland. *J. Lipid Res.*, **2006**, *47*, 705-714. (c) Lister, M. F.; Sharkey, J.; Sawatzky, D. A.; Hodgkiss, J. P.; Davidson, D. J.; Rossi, A. G.; Finlayson, K. The role of the purinergic P2RX7 receptor in inflammation. *J. Inflamm.*, **2007**, *4*, 5.

[8] Perl, A.; Gergely, P. Jr.; Puskas, F.; Banki, K. Metabolic switches of T-cell activation and apoptosis. *Antioxid. Redox Signal.* **2002**, *4*, 427-443.

[9] Lemaire, I.; Falzoni, S.; Leduc, N.; Zhang, B.; Pellegatti, P.; Adinolfi, E.; Chiozzi, P.; Di Virgilio, F. Involvement of the purinergic P2RX7 receptor in the formation of multinucleated giant cells. *J. Immunol.*, **2006**, *177*, 7257-7265.

[10] Jantaratnotai, N.; Choi, H. B.; McLarnon, J. G. ATP stimulates chemokine production via a store-operated calcium entry pathway in C6 glioma cells. *BMC Cancer*, **2009**, *9*, 442.

[11] (a) Sun, C.; Heid, M. E.; Keyel, P. A.; Salter, R. S. The Second Transmembrane Domain of P2RX7 Contributes to Dilated Pore Formation *PLOS ONE*, **2013**, *8*, e61886. (b) Dubyak, G. R. P2RX7 receptor regulation of non-classical secretion from immune effector cells. *Cell. Microbiol.*, **2012**, *14*, 1697-1706. (c) Ferrari, D.; Pizzirani, C.; Gulinelli, S.; Callegari, G.; Chiozzi, P.; Idzko, M.; Panther, E.; Di Virgilio, F. Modulation of P2RX7 receptor functions by polymyxin B: crucial role of the hydrophobic tail of the antibiotic molecule. *Br. J. Pharmacol.*, **2007**, *150*, 445-454. (d)

Volonté, C.; Apolloni, S.; Skaper, S. D.; Burnstock, G. P2RX7 receptors: channels, pores and more. *CNS Neurol. Disord. Drug. Targets*, **2012**, *11*, 705-721.

[12] (a) Surprenant, A.; Rassendren, F.; Kawashima, E.; North, R. A.; Buell, G. The cytolytic P2Z receptor for extracellular ATP identified as a P2X receptor (P2RX7). *Science*, **1996**, *272*, 735-738. (b) North, R. A.; Jarvis, M. F. P2X receptors as drug targets. *Mol. Pharmacol.*, **2013**, *83*, 759-769.

[13] Yan, Z.; Li, S.; Liang, Z.; Tomic, M.; Stojilkovic, S. S. The P2RX7 Receptor Channel Pore Dilates under Physiological Ion Conditions *J. Gen. Physiol.*, **2008**, *132*, 563-573.

[14] (a) Steinberg, T. H.; Silverstein, S. C. Extracellular ATP^{4-} promotes cation fluxes in the J774 mouse macrophage cell line. *J. Biol. Chem.*, **1987**, *262*, 3118-3122. (b) Baricordi, O. R.; Melchiorri, L.; Adinolfi, E.; Falzoni, S.; Chiozzi, P.; Buell, G.; Di Virgilio, F. Increased proliferation rate of lymphoid cells transfected with the P2X, receptor. *J. Biol. Chem.*, **1999**, *274*, 33206-33208. (c) Bianco, F.; Ceruti, S.; Colombo, A.; Fumagalli, M.; Ferrari, D.; Pizzirani, C.; Matteoli, M.; Di Virgilio, F.; Abbracchio, M. P.; Verderio, C. A role for P2RX7 in microglial proliferation. *J. Neurol. Chem.*, **2006**, *99*, 745-758.

[15] (a) Guile, S. D.; Alcaraz, L.; Birkinshaw, T. N.; Bowers, K. C.; Ebden, M. R.; Furber, M.; Stocks, M. J. Antagonists of the P2RX7 Receptor. From Lead Identification to Drug Development. *J. Med. Chem.*, **2009**, *52*, 3123-3141. (b) Longhi, M. S.; Moss, A.; Jiang, Z. G.; Robson, S. C. Purinergic signaling during intestinal inflammation *J. Mol. Med.*, **2017**, *95*, 915-925. (c) Burnstock, G. P2X ion channel receptors and inflammation. *Purinergic Signal.*, **2016**, *15*, 59-67.

[16] Ferrari, D.; Pizzirani, C.; Adinolfi, E.; Lemoli, R. M.; Curti, A.; Idzko, M.; Panther, E.; Di Virgilio, F. The P2RX7 receptor: a key player in IL1 processing and release. *J. Immunol.*, **2006**, *176*, 3877-3883.

[17] Stagg, J.; Smyth, J. M. Extracellular adenosine triphosphate and adenosine in cancer. *Oncogene*, **2010**, *29*, 5346-5358.

[18] (a) Barlett, R.; Stokes, L.; Sluyter, L. The P2RX7 receptor channel: recent development and the use of P2RX7 antagonists in models of disease. *Pharmacol. Rev.*, **2014**, *66*, 638-675. (b) Hofman, P.; Cherfils-Vicini, J.; Bazin, M.; Ilie, M.; Juhel, T.; Hébuterne, X.; Gilson, E.; Schmid-Alliana, A.; Boyer, O.; Adriouch, S.; Vouret-Craviari V. Genetic and pharmacological inactivation of the purinergic P2RX7 receptor dampens inflammation but increases tumor incidence in a mouse model of colitis-associated cancer. *Cancer Res.*, **2015**, *75*, 835-845.

[19] For selected reviews, see: (a) Nimmo, A. J.; Vink, R. Recent patents in CNS drug discovery: the management of inflammation in the central nervous system. *Recent Pat. CNS Drug. Discov.*, **2010**, *5*, 35. (b) Baudelet, D.; Lipka, E.; Millet, R.; Ghinet, A. Involvement of the P2RX7 purinergic receptor in inflammation: an update of antagonists series since 2009 and their promising therapeutic potential. *Curr. Med. Chem.*, **2015**, *22*, 713-729. (c) Chrovian, C. C.; Rech, J. C.; Bhattacharya, A.; Letavic, M. A. P2RX7 antagonists as potential therapeutic agents for the treatment of CNS disorders. *Prog. Med. Chem.*, **2014**, *53*, 65-100.

[20] Burnstock, G. Purinergic signaling: therapeutic developments. *Front. Pharmacol.*, **2017**, *8*, 661.

[21] Our previous work in the field of pyroglutamic acid derivatives shown in this study: (a) Caulier, P.; Rigo, B.; Fasseur, D.; Couturier, D. Studies on pyrrolidones. Convenient syntheses of methyl, methyl *N*-methyl- and methyl *N*-methoxymethylpyroglutamate. *J. Heterocycl. Chem.* **1991**, *28*, 1143-1146. (b) Fasseur, D.; Rigo, B.; Leduc, C.; Caulier, P.; Couturier, D. Studies on pyrrolidones. Synthesis and *N*-alkylation of β-enaminoesters derived from pyroglutamic acid. *J. Heterocycl. Chem.* **1992**, *29*, 1285-1291. (c) Baudelet, D.; Daïch, A.; Rigo, B.; Lipka, E.; Gautret, P.; Homerin,

G.; Claverie, C.; Rousseau, J.; Abuhaie, C.-M.; Ghinet, A. Impact of functional groups on the copper initiated N-arylation of 5-functionalized pyrrolidin-2-ones and their vinylogues. *Synthesis*, **2016**, *48*, 2226-2244. (d) Homerin, G.; Baudelet, D.; Dufrénoy, P.; Rigo, B.; Lipka, L.; Dezitter, D.; Furman, C.; Millet, R.; Ghinet, A. $ZrCl_4$ as a new catalyst for ester amidation: an efficient synthesis of *h*-P2RX7R antagonists. *Tetrahedron Lett.*, **2016**, *57*, 1165-1170. (e) Caulier, P.; Fasseur, D.; Couturier, D.; Rigo, B.; Kolocouris, A. Studies on pyrrolidones. On the carbamoylation of some pyroglutamic derivatives. *J. Heterocycl. Chem.*, **1996**, *33*, 1233-1237. (f) Rigo, B.; Couturier, D. Studies on pyrrolidones. Synthesis of methyl *N*-(4-nitrobenzyl)pyroglutamate. *J. Heterocycl. Chem.*, **1985**, *22*, 207-208. (g) Rigo, B.; Gautret, P.; Legrand, A.; Hénichart, J.-P.; Couturier, D. Reaction of trimethylsilyl benzhydryl ethers with methyl N-(trimethylsilyl)pyroglutamate: an easy and rapid N-alkylation. *Synlett*, **1997**, 998-1000. (h) Bourry, A.; Akué-Gédu, R.; Rigo, B.; Hénichart, J.-P.; Sanz, G.; Couturier, D. Studies on pyrrolidones. An improved Synthesis of *N*-arylmethyl pyroglutamic acids. *J. Heterocycl. Chem.*, **2003**, *40*, 989-993. (i) Kolocouris, N. M.; Rigo, B. Etude dans la série des pyrrolidinones. Synthèse des acides N-(aryl methyl) oxo-5 pyrrolidine carboxyliques-2. *Chim. Chron.*, **1982**, *11*, 309-317. (j) Homerin, G.; Lipka, E.; Rigo, B.; Millet, R.; Dezitter, D.; Furman, C.; Ghinet, A. Discovery of highly functionalized scaffolds: Pyrroloimidazolediones as P2RX7 receptor antagonists. *Tetrahedron* **2017**, *73*, 5327-5336. (k) Homerin, G.; Lipka, E.; Rigo, B.; Farce, A.; Dubois, J.; Ghinet, A. On the discovery of new potent human farnesyltransferase inhibitors: emerging pyroglutamic derivatives. *Org. Biomol. Chem.*, **2017**, *15*, 8110-8118.

[22] (a) Chambers, L. J.; Gleave, R.; Senger, S.; Walter, D. S. Substituted n-phenylmethyl -5-oxo-proline-2-amides as P2RX7-receptor antagonists and their methods of use. WO 2008003697A1 *Chem. Abstr.* **2008**, *148*, 145026. (b) Abdi, M. H.; Beswick, P. J.; Billinton, A.; Chambers, L. J.;

Charlton, A.; Collins, S. D.; Collis, K. L.; Dean, D. K.; Fonfria, E.; Gleave, R. J.; Lejeune, C. L.; Livermore, D. G.; Medhurst, S. J.; Michel, A. D.; Moses, A. P.; Page, L.; Patel, S.; Roman, S. A.; Senger, S.; Slingsby, B.; Steadman, J. G.; Stevens, A. J.; Walter, D. S. Discovery and structure–activity relationships of a series of pyroglutamic acid amide antagonists of the P2RX7 receptor. *Bioorg. Med. Chem. Lett*. **2010**, *20*, 5080-5084. (c) Abberley, L.; Bebius, A.; Beswick, P. J.; Billinton, A.; Collis, K. L.; Dean, D. K.; Fonfria, E.; Gleave, R. J.; Medhurst, S. J.; Michel, A. D.; Moses, A. P.; Patel, S.; Roman, S. A.; Scoccitti, T.; Smith, B.; Steadman, J. G. A.; Walter, D. S. Identification of 2-oxo-N-(phenylmethyl)-4-imidazolidinecarboxamide antagonists of the P2RX7 receptor. *Bioorg. Med. Chem. Lett.* **2010**, *20*, 6370-6374.

[23] Karasawa, A.; Kawate, T. Structural basis for subtype-specific inhibition of the P2RX7 receptor. *eLife*, **2016**, *5*, e22153.

[24] (a) Baxter, A.; Bent, J.; Bowers, K.; Braddock, M.; Brough, S.; Fagura, M.; Lawson, M.; Tom, M.; Mortimore, M.; Robertson, M.; Weaver, R.; Webborn, P. Hit-to-Lead studies: the discovery of potent adamantane amide P2RX7 receptor antagonists. *Bioorg. Med. Chem. Lett.*, **2003**, *13*, 4047-4050. (b) Florjancic, A. S.; Peddi, S.; Perez-Medrano, A.; Biqin, L.; Namovic, M. T.; Grayson, G.; Donnelly-Roberts, D. L.; Jarvis, M. F.; Carroll W. A. Synthesis and in vitro activity of 1-(2,3-dichlorophenyl)-*N*-(pyridin-3-ylmethyl)-1*H*-1,2,4-triazol-5-amine and 4-(2,3-dichlorophenyl)-*N*-(pyridin-3-ylmethyl)-4*H*-1,2,4-triazol-3-amine P2RX7 antagonists *Bioorg. Med. Chem. Lett.*, **2008**, *18*, 2089-2092. (c) Beswick, P. J.; Billinton, A.; Chambers, L. J.; Dean, D. K.; Fonfria, E.; Gleave, R. J.; Medhurst, S. J.; Michel, A. D.; Moses, A. P.; Patel, S.; Roman, S. A.; Roomans, S.; Senger, S.; Stevens, A. J.; Walter D. S. Structure-activity relationships and in vivo activity of (1H-pyrazol-4-yl)acetamide antagonists of the P2X(7) receptor. *Bioorg. Med. Chem. Lett.*, **2010**, *20*, 4653-4556. (d) Abdi, M. H.; Beswick, P. J.; Billinton, A.; Chambers, L. J.; Charlton, A.; Collins, S. D.; Collis, K. L.; Dean, D. K.; Fonfria, E.; Gleave, R. J.; Lejeune, C. L.; Livermore, D. G.; Medhurst, S. J.;

Michel, A. D.; Moses, A. P.; Page, L.; Patel, S.; Roman, S. A.; Senger, S.; Slingsby, B.; Steadman, J. G. A.; Stevens, A. J.; Walter D. S. Discovery and structure-activity relationships of a series of pyroglutamic acid amide antagonists of the P2RX7 receptor. *Bioorg. Med. Chem. Lett.*, **2010**, *20*, 5080-5084.

[25] Stanovnik, B.; Svete, J. Synthesis of Heterocycles from Alkyl 3-(Dimethylamino)propenoates and Related Enaminones. *Chem. Rev.* **2004**, *104*, 2433-2480.

[26] Seki, M.; Hatsuda, M.; Mori, Y.; Yoshida, S.-I.; Yamada, S.-I.; Shimizu, T. A practical synthesis of (+)-biotin from L-cysteine. *Chem. Eur. J.*, **2004**, *10*, 6102-6110.

[27] Paytash, P. L.; Sparrow, E.; Gathe, J. C. The Reaction of Itaconic Acid with Primary Amines, *J. Am. Chem. Soc.*, **1950**, *72*, 1415-1416.

[28] Donnelly-Roberts, D. L.; Namovic, M. T.; Surber, B.; Vaidyanathan, S. X.; Perez-Medrano, A.; Wang, Y.; Carroll, W. A.; Jarvis, M. F. [(3)H]A-804598 ([(3)H]2-cyano-1-[(1S)-1-phenylethyl]-3-quinolin-5-ylguanidine) is a novel, potent, and selective antagonist radioligand for P2RX7 receptors. *Neuropharmacol.*, **2008**, *56*, 223-229.

[29] Compound **74b** was tritiated by Pharmaron UK Ltd. - The Old Glassworks, Nettlefold Road, Cardiff, CF24 5JQ, United Kingdom.

[30] Letavic, M. A.; Lord, B.; Bischoff, F.; Hawryluk, N. A.; Pieters, S.; Rech, J. C.; Sales, Z.; Velter, A. I.; Ao, H.; Bonaventure, P.; Contreras, V.; Jiang, X.; Morton, K. L.; Scott, B.; Wang, Q.; Wickenden, A. D.; Carruthers, N. I.; Bhattacharya A. Synthesis and Pharmacological Characterization of Two Novel, Brain Penetrating $P2X_7$ Antagonists. *ACS Med. Chem. Lett.*, **2013**, *4*, 419-422.

[31] logP were calculated using ACD/ChemSketch Version 12.0 for Microsoft Windows (Advanced Chemistry Development, Inc.)

[32] (a) Kintz, P.; Richeval, C.; Jamey, C.; Ameline, A.; Allorge, D.; Gaulier, J.-M.; Raul, J.-S. Detection of the designer benzodiazepine metizolam in urine and preliminary data on its metabolism. *Drug Test. Anal.*, **2017**, *9*, 1026-1033. (b) Vacek, J.; Papoušková, B.; Vrba, J.; Zatloukalová, M.; Křen, V.; Ulrichová, J. LC/MS metabolic study on quercetin and taxifolin galloyl esters using human hepatocytes as toxicity and biotransformation in vitro cell model. *J. Pharm. Biomed. Anal.*, **2013**, *86*, 135-142.

[33] Cao, D.; Liu, Y.; Yan, W.; Wang, C.; Bai, P.; Wang, T.; Tang, M.; Wang, X.; Yang, Z.; Ma, B.; Ma, L.; Lei, L.; Wang, F.; Xu, B.; Zhou, Y.; Yang, T.; Chen, L. Design, synthesis and evaluation of in vitro and in vivo anticancer activity of 4-substituted coumarins: A novel class of potent tubulin polymerization inhibitors. *J. Med. Chem.*, **2016**, *59*, 5721-5739.

[34] Choteau, L., Vancraeyneste, H.; Dubuquoy, L.; Jouault, T.; Poulain, D.; Sendid, B.; Jawhara, S.; Le Roy, D.; Calandra, T.; Roger, T.; Romani, L. Role of TLR1, TLR2 and TLR6 in the modulation of intestinal inflammation and Candida albicans elimination. *Gut Pathog.*, **2017**, *9*, 9.

[35] Munoz, M. F.; Gao, R.; Tian, Y.; Henstenburg, B. A.; Barret, J. E.; Hu, H. Neuronal P2X7 receptor-induced reactive oxygen species production contributes to nociceptive behavior in mice. *Sci. Rep.*, **2017**, *7*, 3539.

[36] Taminau, J.; Thijs, G.; De Winter, H. Pharao: pharmacophore alignment and optimization. *J. Mol. Graph. Model.*, **2008**, *27*, 161-169.

[37] Trot, O.; Olson, A. J. AutoDock Vina: improving the speed and accuracy of docking with a new scoring function, efficient optimization, and multithreading. *J. Comput. Chem.*, **2010**, *31,* 455-461.